Stromal Gene Signatures as Source of Targets for Drug-Repositioning and Prognostic Biomarkers in Prostate Cancer

Thesis

The Open University
Milton Keynes, United Kingdom

Affiliated Research Centre:
IRCCS Istituto Nazionale dei Tumori
Milano, Italy

Stromal Gene Signatures as Source of Targets for Drug-Repositioning and Prognostic Biomarkers in Prostate Cancer

Thesis presented for the Degree of Doctor of Philosophy
The Open University, Milton Keynes (UK)
School of Life, Health and Chemical Sciences

Valentina Doldi
M.Sc. in Medical Biotechnology and Molecular Medicine
Personal identifier: F5767073

July-2020

Abstract

The interplay between cancer cells and adjacent stroma is fundamental for the development and progression of tumours. In fact, this crosstalk sustains carcinogenesis and promotes the acquisition of additional malignant features. In prostate cancer (PCa), cancer-associated fibroblasts (CAFs) have been shown to fuel tumour development and metastasis by mutually interacting with tumour cells. In this regard, defining stromal gene signatures relevant for cancer progression could be a successful strategy to identify novel therapeutic targets and prognostic biomarkers for PCa. Recently, we have performed a gene expression profiling analysis comparing CAFs and fibroblasts stimulated with IL-6 or TGF-β, to examine the molecular signatures involved in fibroblast activation. The gene set enriched analysis revealed that CAFs are characterized by positive enrichment of genes coding for calcium, sodium, and potassium cation channels and genes related to extracellular matrix (ECM)-remodelling. This evidence suggests a crucial role of characteristic stromal-related pathways in fibroblast conversion to a phenotype able to sustain PCa progression. In addition, the definition of reactive stroma players that are crucial for cancer progression could be a strategy to identify novel therapeutic targets and biomarkers for the early detection of aggressive PCa.

To better understand the involvement of cation channels in CAFs activation and potentially revert such activated phenotype, in this work we treated CAFs with specific cation channel inhibitors, such as antiarrhythmics. Interestingly, we found that antiarrhythmics are able to interfere with crucial features of prostate CAFs, as indicated by the modulation of specific activation markers and reduction of contraction and migration capabilities. Moreover, co-culture experiments indicate that antiarrhythmics

are able to impair CAF-induced proliferative spur and EMT in PCa cells, and ultimately induce tumour growth delay in vivo.

Given the ability of a reactive stroma to support cancer progression, the prognostic relevance of selected genes found up-regulated in activated fibroblasts was tested in relation to clinical-pathological characteristics and patient outcome.

Among crucial factors found up-regulated in prostate CAFs compared to normal fibroblasts we identified a set o ECM-remodelling protein, including periostin. Interestingly, the immunostaining analysis we performed in a series of prostatectomies from PCa patients confirmed that periostin is mainly expressed in the stroma components surrounding tumour foci, and that its staining correlates with tumour grade and cribriform gland morphology, which is indicative of adverse outcome. Most importantly, high levels of stromal periostin expression were associated with a significantly increased probability to experience biochemical recurrence after prostatectomy. In light of the positive correlation observed between periostin stromal staining and aggressive disease, we also investigated the prognostic potential of circulating periostin in patients with potentially indolent tumours followed in the context of an active surveillance protocol. However, results from the study indicated that baseline plasma levels of periostin displayed a moderate capability to identify patients with aggressive disease.

Overall these studies may open new opportunities for the translation of drugs already used in different fields into the targeting of tumour-associated fibroblasts with the aim to interrupt their tumour-supportive spur. Finally, the characterisation of relevant stromal gene signatures may improve diagnostic tools for an early identification of high-risk PCa.

This study was conducted under the supervision of Dr. Nadia Zaffaroni and Dr. Paolo Gandellini at the Molecular Pharmacology Unit, headed by Dr. Nadia Zaffaroni, at the Department of Applied Research & Technological Development, Fondazione IRCCS Istituto Nazionale dei Tumori, Milano, Italy.

Table of Contents

List of Figures and Tables

Abbreviations

ADT: androgen deprivation therapy luteinizing hormone-realising hormone (LH-RH)

AR: androgen receptor

AS: Active surveillance

ATCC: American Type Tissue Culture Collection

ATRA: retinoic acid

AUC: Areas under the curves

aWPMY: activated-WPMY-1

BCR: biochemical recurrence

CAFs: cancer-associated fibroblasts

CAR: chimerical antigen reception

CM: conditioned medium

CRPC: castration resistant PCa

CTCs: circulating tumour cells

ECM: extracellular matrix

EGF: epidermal growth factor

ELISA: enzyme-linked immunosorbent assays

EMT: epithelial to mesenchymal transition

EPE: extraprostatic extension

FAP: fibroblasts activation protein

FBS: fetal bovine serum

FC: fold change

FDR: False Discovery Rate

FGF2: fibroblast growth factor

fPSA: free-PSA

GnRH: goserelin acetate

GS: Gleason Pattern Score

HGF: hepatocyte growth factors

HPFs: human prostate fibroblasts

HR: Hazard Ratio

ICAM1: intercellular adhesion molecules

IGF: insulin-like growth factors

IHC: immunohistochemistry

IL-6: interleukin-6

IMPACT: identification of men with genetic predisposition of prostate cancer

IND: indolent

ISUP: International Society of Urological Pathology

LH: luteinizing hormone

MMPs: metalloproteases

NES: normalized enrichment score

NGF: nerve growth factors

OR: Odds Ratio

PCA: principal component analysis

PCA3: prostate cancer antigen 3

PDAC: pancreatic ductal adenocarcinoma preclinical

PDGF: platelet-derived growth factor

PHI: Prostate Health Index

PIN prostatic intraepithelial neoplasia

PSA: prostate-specific antigen

ROC: Receiver Operating Characteristics

SDF-1: stroma cell-derived factor 1

SDS: sodium dodecyl sulphate

SHH: sonic hedgehog

SMO: smoothened

ssGSEA: single-sample gene set enriched analysis

SST1: somatostatin

TFG-β: transforming growth factor β

TNM: tumour-node-metastasis

tPSA: total PSA

UP: upgrading

Introduction

1. INTRODUCTION

1.1. Prostate Cancer

1.1.1. *Epidemiology*

According to global cancer statistics 2018, prostate cancer (PCa) represents the second worldwide diagnosed solid tumour, and the fifth cause of cancer death in males (Figure. 1.1) [1].

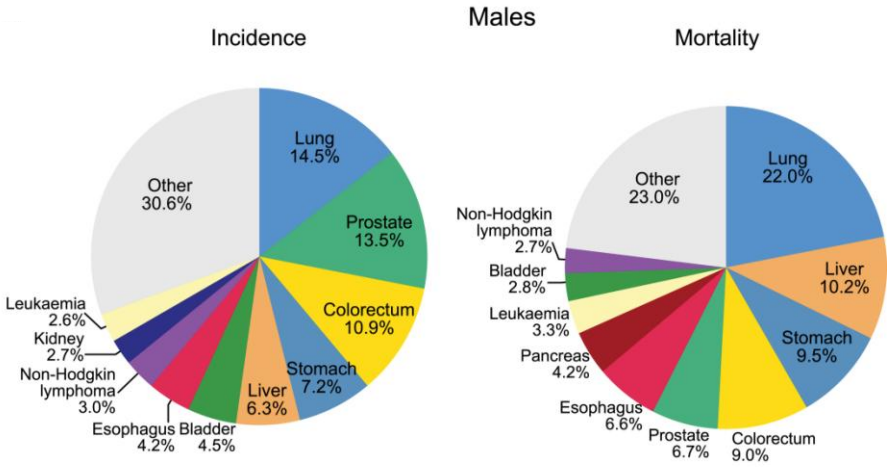

Figure 1.1. Pie charts present the distribution of cases and deaths for the 10 Most common cancers in 2018 for males. The area of the pie chart reflects the proportion of the total number of cases or deaths; nonmelanoma skin cancers are included in the "other" category. (Adapted from GLOBOCAN 2018 [1]).

The development of advanced diagnostic procedures and the increased aging of population, has led to a higher incidence of PCa diagnosis in Western countries. Although the risk factors related to PCa development are not fully understood, increasing evidence strongly links PCa and patient age [2]. The age–adjusted PCa incidence is 0.0005% in men younger than 39 years, and increases to 13.7% for those aged 60-79 years [3]. Moreover, PCa seems to be associated with family history. In fact, the link between hereditary factors and PCa was described in a case-control study, which highlighted that the risk of developing PCa was twice higher in men who had an affected brother or father with respect to those not having any tumour case in their family [2].

In the era of genomics, the presence of mutations in specific genes, such as *BRCA1* and *BRCA2,* has been implicated in increasing the risk of PCa [4]. In this regard, the identification of men with genetic predisposition of prostate cancer (IMPACT) study showed that *BRCA2* mutation is associated with an increased frequency of intermediate or high-risk PCa [4].

Finally, increasing evidence has established a correlation between PCa development and recurrent prostate gland inflammations. At the present, the role of chronic inflammation in PCa is not clear yet. However, several studies have reported that viruses, bacteria or toxic agents can cause prostatitis or severe infections, which lead to create a permissive environment for PCa development [5].

1.1.2. *Diagnosis*

In the 1979, the discovery of prostate-specific antigen (PSA) had completely changed PCa diagnosis and replaced the previously used prostatic acid phosphatase test [6]. The PSA is a glycoprotein produced by the normal as well as malignant cells of the prostate gland. In the early 1990s, the FDA established a novel clinical practice which combines PSA test and the digital rectal exam for asymptomatic PCa diagnosis [7]. Specifically, the PSA test is based on the detection of PSA levels in the blood. PSA levels ≤ 4.0 ng/ml are considered normal, higher than 4.0 are supposedly indicative of PCa [8]. However, also benign prostate hyperplasia, prostatitis and urinary infections are disease conditions associated with high serum PSA levels. In this context, despite the widespread use, the PSA test displays a low specificity for clinically relevant disease, in fact a great amount of patients carrying high-grade tumours display low levels of PSA in the blood [9,10]. On this basis, PSA screening has fallen under controversy, especially regarding the limited specificity of this test in properly detecting PCa. However, approximately 25% of the men that exhibit elevated PSA levels in the blood will receive a diagnosis of PCa [11].

PCa diagnosis is based on the examination of histopathological specimens obtained by trans-rectal or trans-perineal ultrasound guided core biopsies. Recently, the fusion of the magnetic resonance imaging with real time ultrasonography, thus allowing the visualisation of suspicious lesions, has been developed for targeted biopsy [12].

PCa is classified according to the Gleason Pattern Score (GS). Donald Gleason developed this grading system for prostatic adenocarcinoma in the 1966 [13]. The

system is based on histological appearance of tumour cells, and it consists of the description of the glandular differentiation extent and growth within the prostate stroma. In details, the GS is the sum of two scores, ranging from 1 (well-differentiated) to 5 (undifferentiated), representative of the most dominant and the second most prevalent differentiation grade within the tumour, respectively (Figure 1.2) [13].

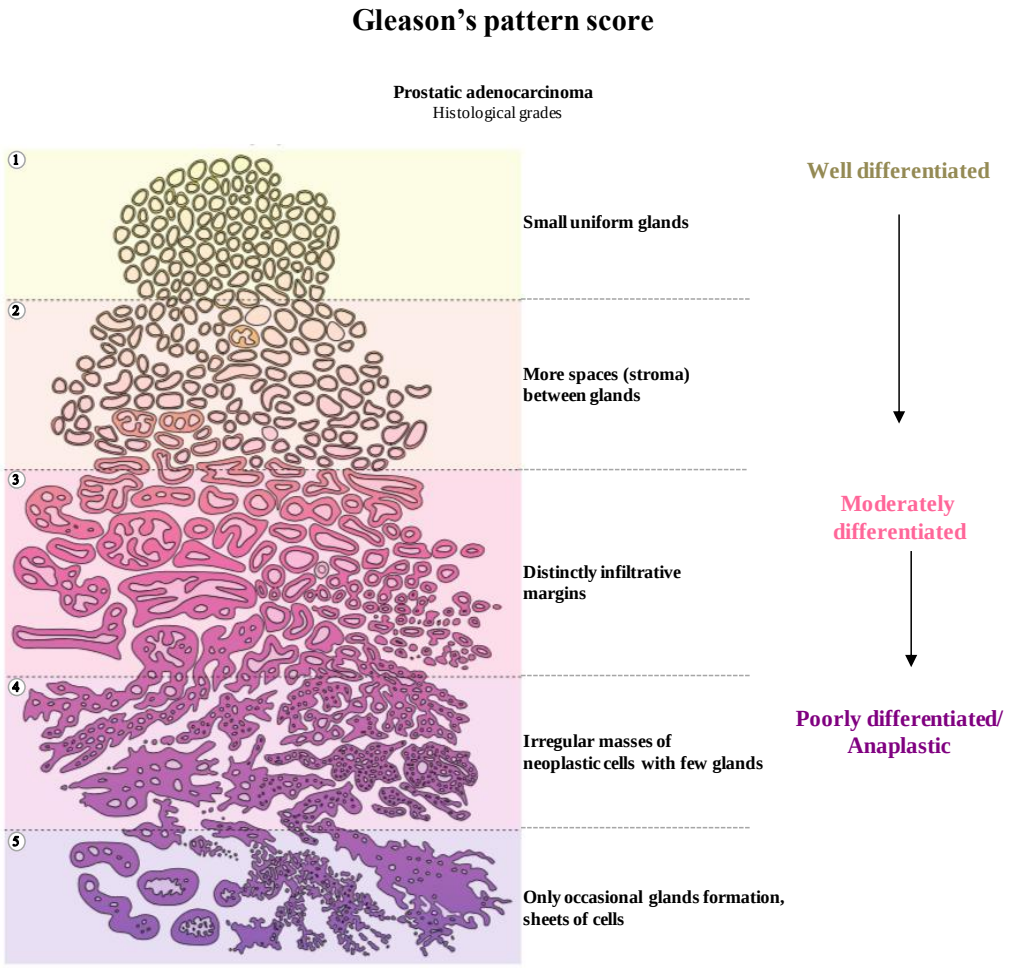

Figure 1.2. Schematic representation of the grading system developed by Gleason. (Adapted from N. J. Sathianathen Nature Reviews Urology [14])

In the 2005, the International Society of Urological Pathology (ISUP) modified the original GS during a consensus conference [15]. Substantial modifications were

recommended, including the morphologic criteria to interpret cribriform pattern 4 with respect to cribriform pattern 3. In the 2014, the original scheme proposed by Gleason has been dramatically modified, resulting in the total elimination of 1 and 2 score from diagnosis. According to the new grading system, a grade shift was introduced. Specifically, certain GS 6 tumours are now considered 7, thus improving the concordance between needle biopsy and prostatectomy pathology. Concomitantly, a subgroup of GS 6 tumours was reported to display a better prognosis than the historic one [16]. Subsequently, Epstein and collaborators introduced a Modified Gleason Scoring Classification in the 2016. This last change includes five grading groups: grade group 1 (GS ≤ 6), grade group 2 (GS 3+4 = 7), grade group 3 (GS 4+3 = 7), grade group 4 (GS 4+4 = 8), and grade group 5 (GS 9–10) (Table 1.1). Mainly, this innovative grading system established the identification of two different subgroups associated with GS 7 tumours. Specifically, therapeutic decision-making based on the previous single GS 7 tumours failed to recognize that 3+4=7 and 4+3=7 are very different from a prognostic point of view. The establishment of the Epstein grading system, distinguishes between these two groups separating them into grade group 3 and 4, respectively [17] .

New grading system	Gleason score	Histologic definition
Grade group 1	≤ 3+3=6	• Only individual discrete well-formed glands
Grade group 2	3+4=7	• Predominantly well-formed glands with lesser component of poorly formed/ fused/cribriform glands
Grade group 3	4+3=7	• Predominantly poorly formed/fused/ cribriform glands with lesser component of poorly formed glands
Grade group 4	8	• Only poorly formed/fused/cribriform glands • Predominantly well-formed glands and a lesser component lacking glands
Grade group 5	9-10	• Lack of gland formation (or with necrosis) with or without poorly formed/ fused/cribriform glands

Table 1.4. New Epstein grading system. (Adapted from Epstein et al, Eur Urol 2015)

Finally, the PCa staging is still based on the tumour-node-metastasis (TNM) system. This classification is used to stage different types of cancer an it is based on the size and anatomical extent of the tumour (T), the number of lymph nodes that present cancer cell invasion (N) and the presence of distant metastasis (M).

1.2. Prostate Cancer Management

As various malignancies, the treatment of PCa depends of the staging, defined by the anatomical extension and aggressiveness of the disease. Since PCa is a disease mostly frequent in elderly men, the life expectancy of the patient and the presence of comorbidities may complicate the therapeutic decision-making process [18]. Moreover, the quality of life, together with the oncological outcome, is also relevant in PCa management.

In this setting, the PCa management includes conservative approaches, such as active surveillance or watchful waiting, and curative treatments, such as radical prostatectomy or radiotherapy, hormone therapy and chemotherapy.

However, the survival benefits of these treatments and their efficacy remain controversial.

1.2.1. *Clinically insignificant PCa*

Active surveillance (AS) and watchful waiting are conservative protocols for clinically insignificant PCa. Truly indolent PCa display a very low metastatic potential, which allows the disease monitoring in order to avoid or temporally delay treatment-induced adverse effects in patients [19]. The main purpose of AS and watchful waiting is to prevent over-treatment and potentially enhance quality of life in patients who received the diagnosis of indolent PCa. Watchful waiting strategy is based on the monitoring of symptoms of local or distant PCa progression and is recommended for those patients with a limited life expectation (< 5 years) [19].

AS was adapted from watchful waiting, and it is an active and extensive way for monitoring localised and early stage PCa, characterised by a very slow potential progression. This monitoring approach is exclusively proposed to patients with a low risk and clinically insignificant disease. Robust evidence indicated that most patients enrolled in AS likely never develop PCa-related symptoms [19]. However, at the first sign of a major risk, radical treatments will be addressed in order to cure the tumour, while still maintaining high chances of healing.

The crucial event in AS strategy is the correct and univocal identification of patients truly suitable for the protocol, who are those that harbour an "insignificant tumour". This subgroup of men who received a diagnosis of insignificant PCa manly carry a "pseudo-disease" that could be part of the ageing process and does not pose a significant threat to their lives [20]. In accordance with the Epstein and D'Amico risk-classification, "insignificant tumours" include very-low and low-risk PCa, which are characterised by stage T2a or lower, Gleason 6 tumour or less on biopsy cores, no more than two positive cores, no involvement of more than 50% of a positive core, PSA levels < 10 ng/ml and PSA density less than 0.15 ng/ml/ml (Table 1.2).

Category	Criteria
Very low risk	• Stage T1c, • Gleason ≤ 6, and • PSA < 10 ng7ml • PSA density < 0.15 ng/ml/ml, • ≤ 2 cores positive • ≤ 50% cancer in each core
Low-risk	• Stage T2a or lower, • Gleason ≤ 6, and • PSA < 10 ng7ml

Table 1.5. Risk classification of very low, low risk PCa, according to D'Amico [21] and Epstein [22].

During AS, the evolution of the tumour is observed, and the schedule of monitoring includes: the dosage of PSA levels in the blood every 3 months (possibly always performed by the same laboratory); an urological visit with rectal exploration to evaluate the prostate (shape, size, texture) at least every 6 months and a prostate biopsy after 1 year of inclusion (and then after 4 and 7 years). In case of positivity to the examinations patients are immediately redirected to radical treatment.

Ideally, the AS programme should monitor patients characterised by a very slow tumour progression. However, multiple studies reported that, at the first re-biopsy, about 25% of enrolled patients harbour a clinical relevant PCa and drop out from the protocol, indicating that this minority might have been incorrectly classified as carriers of <insignificant disease [23]. Therefore, the critical aspect for successful AS is the best possible selection of patients with truly "insignificant tumours". In this regard, recent evidence indicated that the incorporation of multi-parametric

magnetic resonance imaging into AS selection criteria might improve the detection of high-grade tumours, thus excluding those men that actually need radical treatments [24].

Overall, the AS patient treatment rates at 10 and 15 years is about 36% and 45%, respectively. Moreover, about the 90% of patients enrolled in AS can be expected to have organ-confined disease, without compromising the oncological outcome. In light of this evidence, AS might be considerate the ideal options for men with very-low risk disease, and a recommendable approach for low-risk disease [23].

1.2.2. *Clinically relevant PCa*

Radical treatments, which are surgery and radiotherapy, represent the main therapeutic options for clinically localized PCa, providing the highest efficacy in terms of healing from the disease. Surgery consists of the entire removal of the prostate, seminal vesicles and pelvic lymph nodes. The main criticisms related to radical prostatectomy procedures are urinary incontinence and rectal dysfunction events. As for urinary incontinence, it is a disorder that manifests itself in the vast majority of patients immediately after surgery, but often regresses within three months. Current understanding of prostate anatomy and retro prostatic neurovascular bundles has led to develop a conservative nerve-sparing prostatectomy. This surgical approach represents the modern standard radical prostatectomy procedure able to significant reduce the occurrence of postoperative erectile dysfunction. At the present, the “open-air” radical prostatectomy has been almost completely replaced by a mini invasive approach that allows operating by 5 small incisions on the abdomen, minimizing invasiveness. Moreover, the advent of

robot-assisted laparoscopy and 3D stereoscopic visualization has led to develop a mini-invasive radical prostatectomy surgery, which it is comparable with open procedure in terms of oncological and functional outcomes.

Similar to radical prostatectomy, radiotherapy is a first line treatment for clinically localized PCa. The therapeutic outcomes provided by radiotherapy are comparable with those of prostatectomy, and therefore the choice between prostatectomy and radiotherapy is concerted between the patient and the clinicians. At present, the main types of radiation techniques used for PCa treatment are external beam radiotherapy and brachytherapy. The main goal of external beam radiotherapy is to reach the maximum radiation dose at the target organ with the least adjacent tissue damage. Differently from external radiotherapy, brachytherapy is a type of irradiation modality where tiny radioactive seeds are placed into the prostate. This approach improves the efficacy of the treatment since the radiation is directly delivered within the prostate. Recently, the advent of 3D conformal radiotherapy and intensity-modulated radiotherapy have further improved the delivery of the treatment and substantially reduced side effects, which are related to the tissue toxicity induced by radiation on prostate surrounding tissues and local organs. Finally, it is also worth mentioning of the role of adjuvant radiotherapy in patients with adverse pathological features after prostatectomy. When the tumour extends beyond the prostatic capsule thus increasing the risk of local relapse, radiotherapy is delivered immediately post-operation. It is a treatment option highly recommended for patients with an early-stage localised disease, being a minimally invasive treatment that is performed in day-surgery, characterized by a low rate of complications and guaranteeing a high preservation of life quality [25].

The first line of treatment against advanced prostate cancer is represented by androgen deprivation therapy (ADT). The basis for ADT in PCa has been established by the Noble prize-winning finding that highlighted the relevance of androgen hormones in PCa cell growth [26,27]. Androgens can be surgically depleted using orchiectomy. However, this surgical castration procedure has been largely replaced by pharmacological suppression. Pharmacological methods are based on the use of luteinizing hormone-realising hormone (LH-RH) or goserelin acetate (GnRH) agonists and androgen antagonists. The LH-RH or GnRH agonist acts by blocking the luteinizing hormone (LH) production, thus resulting in the suppression of the androgen hormone production by the testicles. As for androgen antagonists, these drugs are used to compete with androgen hormones for binding to its receptor on cell surfaces and block prostate cell stimulation induced by the hormones. Differently from LH-RH agonists, androgen antagonists cause less erectile dysfunction but more side effects on breast tissue. Ciproterone acetate, cicalutamide, futamide, enzalutamide are common androgen antagonists used in the clinical practice. Among the androgen antagonists, abiraterone acetate is an oral anti-androgen able to target the biosynthesis of androgen hormones, manly used in the management of castration-resistant PCa and recently approved in the pre-chemotherapy setting [28]. At present, hormone therapy may be used before, during or after surgery or radiotherapy. However, the timing and the schedule of ADT administration in PCa patients have several controversial aspects. In this regard, recent data demonstrate that immediate administration of ADT in men with biochemical relapse following radical treatments improves overall survival of patients and reduces the risk of recurrence. Moreover, data regarding the potential of prescribing intermittent or continuous ADT highlighted that intermittent

administration of hormone therapy substantially reduces the adverse effects induced by ADT.

In order to enhance the quality of life and substantially improve overall survival for men with castration resistant PCa (CRPC), chemotherapy is used. Taxane-based chemotherapy in association with prednisone represents a valid treatment used in this PCa patient setting. The first agent that showed an improvement of both quality of life and progression free-survival in CRPC patients was docetaxel [29]. Subsequently, also cabazitaxel has been demonstrated to improve survival in CRPC patients [30]. Currently, data derived form several clinical trials indicated that the standard therapy for CRPC is represented by the combination of docetaxel and ADT (168-172).

In advanced PCa, bone metastasis occurrence is the predominant event. In this setting, differently from palliative radiotherapy, radium-223 α-particle emitter is the only approved therapy used to target bone metastasis in PCa patients (187). Concerning the immunotherapy approaches, the Sipuleucel-T vaccine has been recently approved in the USA. The use of this autologous active cellular immune treatment improved overall survival in men with metastatic-CRPC [31] .

1.3. Diagnostic and prognostic biomarkers to guide the early detection of PCa

1.3.1. *Diagnostic Biomarkers*

At present, PSA is the only approved biomarker able to aid the early detection of PCa, indicate disease recurrence after radical treatments and determine the efficacy of drug therapies. However, the advent of PSA screening has led to PCa overdiagnosis and overtreatment, pointing out the low specificity of this test for clinically relevant PCa [32]. The moderate capability of PSA screening to identify indolent from aggressive tumours was confirmed by multiple studies, which highlighted that PSA-based screening provide only 25% of PCa specific-mortality reduction in face of elevated cost of overdiagnosis [33,34].

In order to aid clinicians in the early detection and categorisation of PCa, PSA-related markers were combined in promising diagnostic and prognostic models. An improvement of specificity in PCa diagnosis has been observed by using free-PSA (fPSA) ratio. Although the total PSA (tPSA) is mainly complexed with serum proteins, a correlation between fPSA fraction and PCa has been observed. Specifically, a lower % fPSA was associated with the presence PCa in those patients who displayed modest levels of tPSA (4-10 ng/ml) with respect to PCa-free men [35,36]. In addition, Prostate Health Index (PHI) was developed by combining tPSA, fPSA and (-2)proPSA, which is a fPSA isoform showing an elevated specificity for PCa [37]. Multicentre studies indicated that the specificity of PHI model for the detection of clinically relevant PCa was about 38% [38]. Hence, the PHI model displays a higher specificity for PCa than tPSA, and a significant association with higher GS tumours. Moreover, PHI displayed the capability to predict

biochemical recurrence following radical prostatectomy, thus indicating a possible use of PHI as prognostic biomarker [39]. In light of these findings, the % fPSA and the PHI model were approved for men with 4-10 ng/ml tPSA levels before initial or repeat biopsy.

Interestingly, the innovative Progensa is a test to measure the urine levels of prostate cancer antigen 3 (PCA3) non-long-coding RNA, which is unexpressed in normal and hyperplast prostate [40]. The function of PCA3 is currently unknown, however its levels in the first-void or post digital-rectal examination urine were able to predict PCa with a specificity of the 79% in a cohort of men with elevated PSA levels and prior negative biopsy [41]. Several studies highlighted the greater accuracy of PCA3 for PCa detection with respect to tPSA, especially when it is used as a score. However, further investigations indicated that PCA3 score is not associated with progression in AS or after radical treatments. Moreover, discrepancies emerged regarding the establishment a univocal cut-off value of PCA3 score for PCa detection [42,43]. To date, PCA3 test with a cut-off score of 25 was approved by FDA for men age > 50 with a previous negative biopsy.

The limitations of the current clinical examination tests and the advances in understanding the molecular biology of PCa have led to the development of more sensitive biomarkers. In the genomic era, the mutational landscape of organ-confined PCa has been investigated, highlighting significant genomic alterations that could potentially guide the early detection of PCa. For instance, recurrent somatic *TMPRSS2-ERG* gene fusion was described in over 50% of all PCa and was associated with PCa-specific mortality [44] . Moreover TMPRSS2-ERG gene product was found to be detectable in the urine, and displayed a specificity up to 93% for

PCa but at the cost of a low sensitivity (about to 37%) [45]. In light of this, the molecular assay "Mi Prostate score" based on combining TMPRSS2-ERG RNA and PCA3 detection in the urine samples and serum PSA levels has displayed a 95% of sensitivity and 38% of specificity for aggressive PCa [46].

Other genomic alterations were commonly observed in early-stage PCa, including *SPOP*, *TP53*, *FOXA1* and *IDH1* mutations, and also *PTEN* loss, *MYC* amplification and PI3K signalling activation [47,48]. These findings substantially improved the knowledge of PCa carcinogenesis, however an association between PCa different molecular subtypes and progression or lethality has not been clarified yet. In this regard, further efforts are needed to develop an accurate molecular screening for the early detection of PCa.

Since DNA hyper-methylation occurs very frequently in many cancers, its potential as a biomarker for early detection of PCa was investigated. In this regard, the ConfirmMDx assay has been developed to assess the methylation state of *GSTP1*, *APC* and *RASSF1*, which were previously found to be associated with PCa. Notably, the ConfirmMDx epigenetic assay could be potentially used for the identification of a "cancerization field" effect in negative core biopsies, thus indicating the presence of occult PCa or predicating its development [49]. However, the diagnostic accuracy for clinically relevant PCa was not confirmed yet (Table 1.3.).

1.3.2. *Prognostic biomarkers*

The Gleason score is the most used clinical prognostic marker for PCa, displaying a significant association with PCa specific mortality. In addition, the recent PCa

grading modifications introduced by Epstein have further improved its prognostic potential to predict biochemical recurrence after radical treatments when tested in a cohort of 20,000 patients [22]. Moreover, D'Amico risk stratification model, which combines clinical factors, such as Gleason score, stage and PSA, is actually the most robust and widely-used tool to define disease recurrence and guide decision-making regarding additional or adjuvant therapy upon radical treatments [21]. However, limited tools are available for reducing the risk of under-sampling during prostate biopsy and clearly predict unfavourable disease. In this regard, several promising potential tools are currently in different stages of development or under investigation. Among these, the OncotypeDX™ score is a genomic assay based on the detection of 17 genes related to androgen signalling, stroma response, cell organization and proliferation. This tool has demonstrated a good performance for predicting aggressive disease in very-low, low and intermediate PCa settings. Notably, this assay could be potentially used as a valid tool in the post-biopsy setting for reducing the risk of PCa under-sampling and guide decision-making in AS protocol [50]. In addition, the RNA-based Prolaris™ molecular assay has shown a good prognostic potential in terms of biochemical recurrence after radical treatments. This assay has been retrospectively tested in a large cohort of paraffin-embedded specimens and it was able to predict biochemical relapse, by providing a mathematical score derived from the combination of 31-gene expression levels. Another RNA-based genomic assay is the Decipher™, a 22-gene assay that was able to predict development or early metastasis after treatment [51]. Currently, Decipher™ and Prolaris™ assays are under prospective validation. Finally, the Promark™ in-situ proteomic multi-marker assay has been tested on Gleason 3+3 and 3+4 core biopsy, providing a robust capability to predict aggressive disease

despite biopsy under-sampling [52]. This proteomic test is mentioned in the NCCP PCa guidelines as a promising tool for risk assessment in the post-biopsy setting for who men that are considering AS protocol (Table 1.3.).

Biomarker	Type	Specimen type	Application
PSA	Protein	Blood	Diagnostic
%fPSA	Protein	Blood	Diagnostic
PCA3	non-long coding RNA	Urine	Diagnostic
TMPRSS2-ERG	RNA fusion transcript	Urine	Diagnostic
ConfirmMDX	Epigenetic DNA	Prostate tissue	Diagnostic
OncotypeDX™	DNA	Prostate tissue	Prognostic
Prolaris™	RNA	Prostate tissue	Prognostic
Decipher™	RNA	Prostate tissue	Prognostic
Promark™	Protein	Prostate tissue	Prognostic

Table 1.6. Summary of current organ-confined PCa biomarkers and tools.

1.4. Tumour microenvironment

1.4.1. *Cancer-associated fibroblasts in cancer progression*

Tumour growth into a full malignancy is not just determined by cancer cells themselves, but also by several non-cancer cells within the tumour microenvironment. Immune cells, endothelial cells, structural components and cancer-associated fibroblasts (CAFs) are actively involved in cancer development. Among the key components of the tumour microenvironment, it is becoming clear that CAFs are prominent modifiers of several carcinogenesis steps, including cancer initiation, development and progression [53]. In fact, CAFs orchestrate the synthesis and modulation of extracellular matrix (ECM) and the release of pro-tumourigenic factors. Moreover, CAFs can induce angiogenesis, create an immunosuppressive environment and regulate cancer therapy responses.

In the last decade, a great expansion into CAF-related research has enhanced our knowledge of this subpopulation and brought out novel potential therapeutic strategies against cancer aimed at targeting CAFs. However, their origins, features and functions within the tumour microenvironment are still not fully established. Emerging evidence indicates that CAFs are involved in complex interactions with cancer cells, having both tumour-promoting and suppressing functions [54–56].

In normal tissues, fibroblasts are elongated cells embedded in the connective tissue, and negative for epithelial, endothelial and leukocyte markers. They are involved in ECM deposition, epithelial cell differentiation induction, inflammation and wound healing control [57,58]. In the physiological context, during wound repair, fibroblasts become activated with an increased ECM deposition and contraction force

development in order to heal the injury. Once the wound is repaired, they undergo apoptosis or revert to a quiescent phenotype. In contrast, in the tumour reactive stroma, fibroblasts remain permanently activated as observed in fibrotic tissues, thus leading to a overproduction of ECM and pro-tumourigenic factors [58]. In this setting, the number of activated fibroblasts, that usually express higher levels of α-SMA, fibroblasts activation protein (FAP), vimentin, and exhibit increased ECM production, is substantially increased with respect to normal tissues. Although the molecular mechanisms that underline fibroblast recruitment at tumoural site are still being unravelled, it is well known that fibroblast activation is guided by several factors released from cancer calls. For example, it has been reported that transforming growth factor β (TFG-β), platelet-derived growth factor (PDGF) and fibroblast growth factor (FGF2) are key modulators of fibroblast activation, thus inducing of a desmoplastic stroma deposition [59–61]. Actually, these factors are able to cause dramatic changes in CAFs, including an enhancement of their migratory potential and secretory phenotype. Among the molecules released by CAFs, stroma cell-derived factor (SDF-1) fosters tumour growth by promoting angiogenesis and recruiting bone marrow-derived endothelial cells [62]. Moreover, CAFs release ECM degradation proteases such as MMPs, which promote motility and invasion of cancer cells. For instance, epithelial to mesenchymal transition (EMT) and invasiveness of cancer cells was found to be actively influenced by CAF-secreted MMP3, which directly cleaves E-cadherin [63]. In addition, by remodelling ECM within the tumour microenvironment, CAFs are involved in the generation and maintenance of the cancer stem cell niche. In this regard, increasing evidence highlighted that the activation of WNT-signalling in cancer cells could be regulated by proximal CAFs within the stem niche [64].

CAFs are also crucial mediator of secondary tumour growth at metastatic sites, by releasing growth factors and cytokines into the circulation. In this regard, it has been reported that CAFs are able to foster breast cancer metastasis to the lung by expressing VEGFA and tenascin C [65]. Moreover, CAF-released IL-11 was found to promote distant organ colonization in colorectal cancer setting [66].

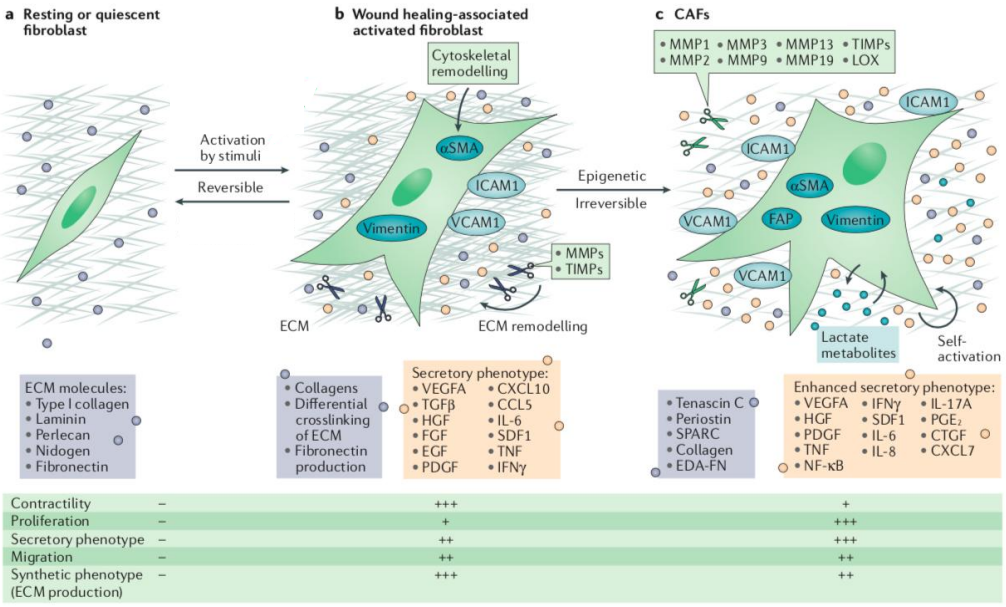

Figure 1.3. The multi-step activation of fibroblasts. Schematic representation of fibroblass activation from quiescent or resting fibroblast to wound healing-associated fibroblasts or CAFs (adapted from Kalluri R. Nature Reviews 2016).

In order to sustain their activated state, characterised by high proliferative rate, motility and intense secretion activity, CAFs undergo important metabolic reprogramming. Interestingly, this metabolic conversion of CAFs is able to sustain cancer cell metabolism to overcome the hypoxic environment within the tumoural mass. Specifically, tumour-derived stimuli, including TFG-β and PDGF, were able

to promote aerobic glycolysis in CAFs, thus increasing the production of lactate, fatty acid and ketone body that may support cancer cell metabolism [67,68]. Moreover, this reciprocal metabolic symbiosis between cancer cells and CAFs was found to be associated with increased invasive and therapeutic resistance properties [69].

In addition to promote tumour growth, induce EMT, foster cancer metastasis and provide a metabolic support to cancer cell, the secretory phenotype of activated CAFs exhibits immunomodulatory functions. Secretome analysis have highlighted that CAFs dynamically interact with several components of the tumour microenvironment by the secretion of chemokines, cytokines and angiogenic factors, including IL-4, IL-6, IL-8, IL-10 and CCL2. In this regard, CAF-secreted IL-4, IL-6, IL-8 are able to induce immunosuppressive myeloid differentiation. Moreover, in vitro evidence indicated that CAF-released CCL2 may contribute to create an immunosuppressive tumour microenvironment by recruiting and polarizing macrophages. Finally, CAFs can indirectly modulate cancer immunity through the promotion of angiogenesis and regulation of immune cell trans-endothelia migration. In fact, increased levels of intercellular adhesion molecules (ICAM1), which acts as a docking for attraction, activation and polarization of immune cells, were found on the surface of activated fibroblasts.

The CAF functions described so far highlight the great heterogeneity of this cell population and suggest that CAFs could co-exist in different and specific phenotypes, which reflect their functions. Based on increasing literature evidence it has been recently proposed to classify CAFs into subtypes with respect to their role within the tumour microenvironment, as for macrophage polarization or other immune cells. Hence, currently four interchanging classes of activated fibroblasts have been identified, such as tumour-restraining CAFs (F1 subtype), tumour-

promoting CAFs (F2 subtype), secretory CAFs (F3 subtype) which influence tumour immunity and angiogenesis and ECM-producing CAFs (F4 subtype). However, due to the pleiotropic functions and plasticity of CAFs, it cannot be excluded that further studies might lead to define novel functional CAF subpopulations within the tumour microenvironment (Figure 1.4.).

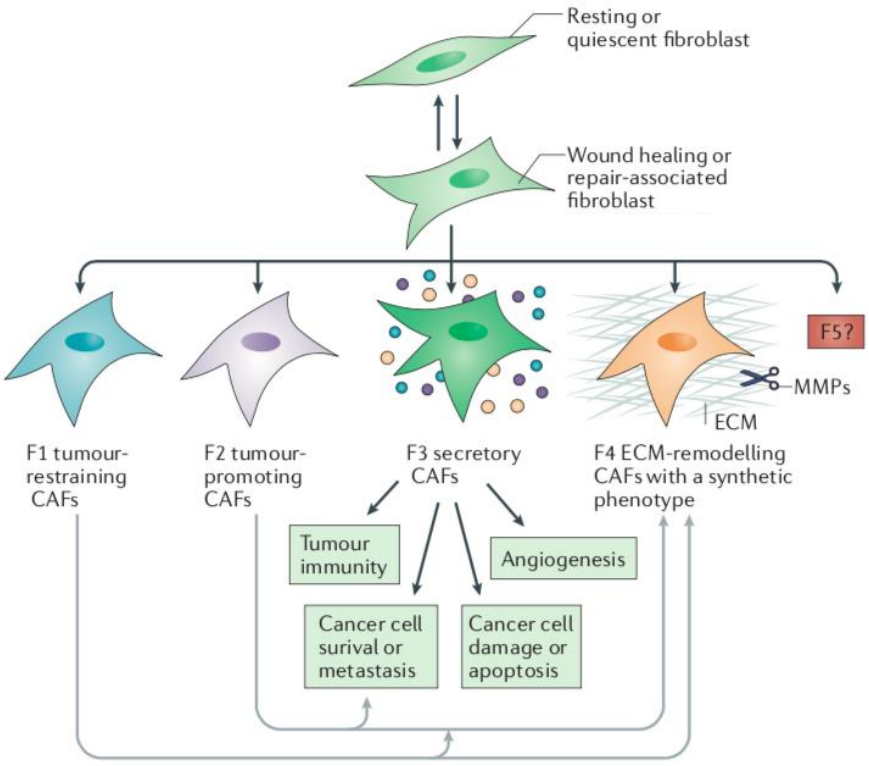

Figure 1.4. A proposed classification of CAFs on the basis of their functions. (Adapted from Kalluri R. Nature Reviews 2016).

1.4.2. *Role of CAFs in PCa*

The prostate stroma is a complex environment characterized by fibroblasts, smooth muscle cells (SMC), endothelial cells, immune cell types, nerves and ECM structures. Reciprocal interactions between prostate stromal constituents and its epithelium are fundamental to organogenesis. In physiological conditions, prostate tissue homeostasis is generally maintained by fibroblasts and SMCs, which regulate the proliferation of epithelial cells, the synthesis and remodelling of ECM structures, and are actively involved in tissue repair [70]. Similarly, interactions between tumour cells and stroma components are crucial aspects of tumour mass formation, progression, dissemination and growth at distant sites. In PCa, as well as in early precancerous lesions, the stroma resembles that of wound repair, with massive reactive stroma formation, characterized by reduced levels of laminin and elevated deposition of tenascin C [71,72]. These changes in ECM composition are instrumental for PCa development. Indeed, it has been experimentally proved that ECM isolated from PCa reactive stroma was able to improve proliferation and motility of LNCaP cells [73]. Moreover, the volume of reactive stroma observed in Gleason 4 tumours is significantly higher than the storma of the less aggressive Gleason 3 [72], and its extent correlates with cancer recurrence after radical treatments [74].

PCa reactive stroma largely consists of CAFs, which are functionally and structurally different from normal fibroblasts, and are generally characterized by the expression of fibroblast activation markers such as α-SMA, tenascin C, fibronectin and FAP, and as well common markers, such as vimentin and FSP-1 [75].

During prostate carcinogenesis, the number of SMCs is dramatically decreased within the reactive stroma, with a concomitant enhancement of CAFs [72].

At present, the cell origin of CAFs is elusive. Several groups have identified different possible cells of origin, including resident fibroblasts, SMCs, circulating bone marrow-derived progenitor cells and trans-differentiation from endothelial or epithelial to mesenchymal cells [76,77]. Regardless their cellular origin, several experimental and pathological observations have widely established their functional involvement in each step of PCa development, progression and dissemination [78]. For instance, experimental evidence has been shown that CAFs are able to enhance in vitro and in vivo PCa cell proliferation, and also promote EMT, resulting in cancer cell invasion enhancement [79,80]. Moreover, the massive reactive stroma observed in PCa is indicative of an increased ECM production and remodelling, caused by CAF-secreted ECM protein and proteases, such as metalloproteases MMPs (e.g. MMP2 and MMP9) and urokynase-type plasminogen activator, which induce tissue remodelling [72].

In the 1999, Olumi and collaborators, described that prostate CAFs were able to transform non-tumourigenic prostate epithelial cells, thus providing the first experimental evidence of CAF involvement in PCa progression [81]. Subsequently, advances in prostate CAF understanding highlighted that hepatocyte growth factors (HGF), insulin-like growth factors (IGF), nerve growth factors (NGF), Wnt1, epidermal growth factor (EGF) and fibroblasts growth factors 2 (FGF2) are key growth factor realised by CAFs and able to provide PCa cell growth [78]. In addition, CAFs have been shown to substantially contribute to PCa progression by supporting both ECM deposition and turnover, and by influencing tumour cell plasticity. Recent data have demonstrated that PCa cells are susceptible to undergo

EMT by CAF-released paracrine factors, including MMPs. In this regard, experimental models have shown that both tumour growth and spontaneous metastases are increased in mice subcutaneously co-injected with PCa cells and CAFs [80]. More specifically, Giannoni and collaborators have recently investigated the mechanisms underlying CAF-mediated EMT in PCa cells, showing that CAFs were able to mediate the NF-Band HIF1 activation in cancer cells through the release of reactive oxygen species [82]. Subsequently, HIF1 activation in cancer cells lead to repress miR-205 transcription [83], which is in turn an indirect regulator of E-cadherin expression [84]. As result, miR-205 repression in PCa cells was able to induce E-cadherin down-regulation, thus promoting EMT and cell dissemination.

As for many tumours, CAFs were able to support cancer cell proliferation through a mutual metabolic reprogramming. Specifically, the limited nutrients and oxygen availability within the tumour microenvironment foster cancer cells to perturb CAF metabolism. Indeed in PCa, CAFs are forced to undergo an anaerobic glycolysis programme in order to produce lactate, which is extruded by CAFs through the monocarboxylate transporter-4 [69]. On the over hand, cancer cells increased monocarboxylate transporter-1 expression levels in order to improve the uptake of lactate [69], thus becoming the main proliferative boosts for cancer cell growth.

Aging has been largely linked to the development of PCa [85], and it is possible that aging stromal components could actively contribute to PCa progression, by releasing tumour-promoting factors. In this regard, it has been recently shown that senescent prostate fibroblasts stimulate the growth of neoplastic prostate epithelium thought the secretion of specific factors [86]. Moreover, in line with these observations, in vivo studies established that stromal regions infiltrating tumoural foci are enriched in senescent stromal cells [87]. Recently, Taddei ML and

collaborators have reported an interesting link between senescence and CAFs. Indeed, the hypoxia-induced miR-210 up-modulation in prostate fibroblasts was sufficient to induce senescence features in fibroblasts, and also a simultaneous conversion of them into activated one, with a phenotype that resembling CAFs [88]. Surprisingly, activated fibroblasts overexpressing miR-210 were able to promote cancer cell EMT, support angiogenesis and to recruit endothelial precursor cells and monocytes/macrophages [88].

Given the relevance of aging and inflammation response, which could in part influence stroma reprogramming and also drive prostate carcinogenesis, emerging evidence highlighted a possible role of IL-6, as a key factor in the interconnection between fibroblast activation, senescence features and inflammation. Indeed, both senescent prostate epithelial cells and fibroblasts may potentially release IL-6 in the tumour microenvironment, thus contributing to establish or maintain a senescent reactive milieu able to stimulate PCa initiation and progression. In this regard, we recently found a substantial overlap between the transcriptomes of normal prostate fibroblast stimulated in vitro with IL-6 and CAFs isolated from radical prostatectomy samples[89]. Specifically, in order elucidated the biology and signalling mechanisms involved in reactive stroma formation, the gene expression profile of patient derived CAF and normal fibroblasts (HPF) activated in vitro with IL-6 or TGF-β were compared to HPF using a gene set enrichment analysis (GSEA). Overall, we found in all activated fibroblasts (CAFs and in vitro activated fibroblasts) a positive enrichment of terms related to actin cytoskeleton remodelling, muscle contractility and glycolysis/gluconeogenesis pathways, all common features of activated fibroblasts thus supporting the well-known similarity between CAFs and myofibroblasts [89]. Interestingly, among positively enriched gene

sets there were also the "voltage gated cation channel activity" gene set, containing genes that code for calcium, sodium and potassium channels probably involved in the acquisition of a contractile phenotype, and the "interferon-alpha-beta signalling" gene set, which contains genes that are likely modulated upon cytokine stimulation (including IL-6, i.e. Interferon-β) (Figure 1.5- upper panel). In addition, genes related to ECM regulation were positively enriched in both CAFs and IL6-activated fibroblasts but showed an opposite trend in TGF-β-HPFs (Figure 1.5- lower panel). However, we experimentally observed that patient derived CAF and in vitro activated fibroblasts with IL-6 and TGF-β were characterized by enhanced collagen synthesis and α-SMA expression, which are typical features of myofibroblasts (Figure 1.5- lower panel).

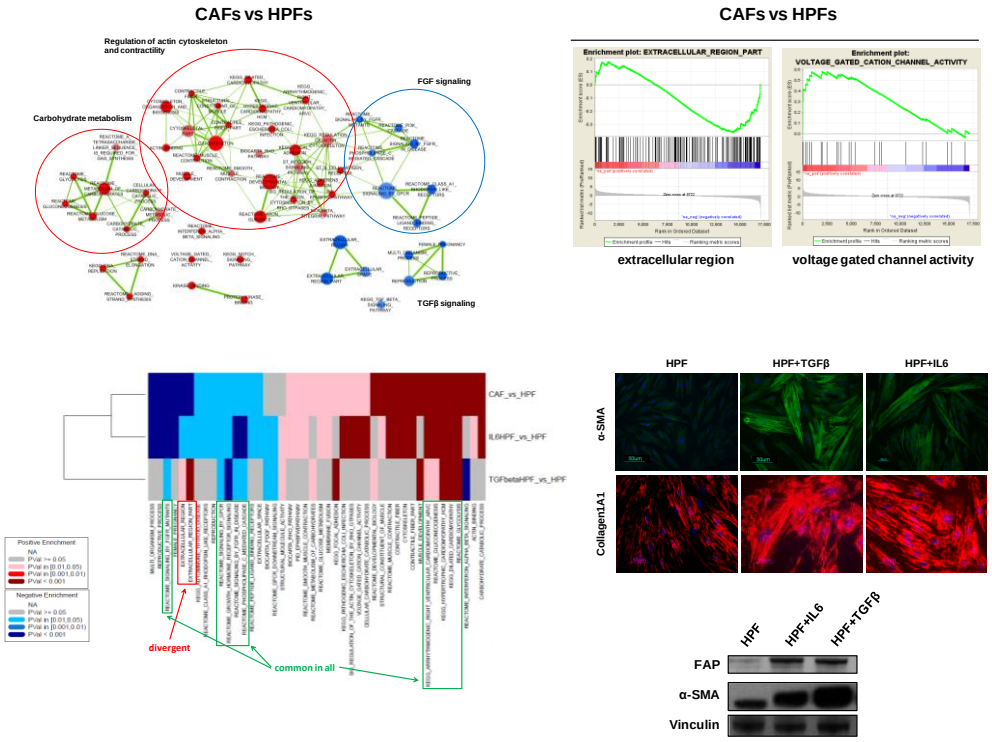

Figure 1.5. Gene expression profiling and phenotype characterization of patient derived CAFs, in vitro activated fibroblasts with IL-6 and TGF- β compared to normal fibroblasts. (*Upper left panel*) Graphical representation of selected gene

sets positively (*red*) or negatively (*blue*) enriched gene sets in CAFs (n = 3) compared with HPFs (n = 3). (*Upper right panel*) Selected gene sets positively enriched in CAFs compared with HPFs. (*Lower left panel*) Heatmap summarizing significantly enriched gene sets in at least two of the evaluated comparisons (CAF vs HPF, IL-6-HPF vs HPF, TGF-β-HPF vs HPF, n = 3 for each group. (*Lower right panel*) Representative immunofluorescence images and immunoblotting of specific fibroblasts activation markers in HPFS exposed to IL-6 or TGF- β. (Adapted from Doldi V.et al. Oncotarget 2015).

The pro-tumourigenic effect of CAFs goes beyond the direct stimulation of cancer cells. Actually CAFs have been shown to influence other cell types within the tumour microenvironment and also contribute to determine tumour resistance to treatments. In this regard, the ECM over-production of CAFs results in a matrix stiffening, which can physically impair the delivery of chemotherapeutics at the tumour site. In addition, it has been shown that fibronectin-rich matrix, which is generally produced by CAFs within the tumoural stroma, displays an anti-apoptotic effect in vitro on prostate cancer cell lines, promoting cell survival upon exposure to conventional anticancer agents and radiation [90]. Moreover, it has been experimentally shown that the co-injection of CAFs and LNCaP cells in a xenograft model of PCa induced early angiogenesis [91]. Finally, CAF-derived growth factors, such as FGF, HGF and TGF-β, and CAF-mediated ECM deregulation can create a tumour permissive microenvironment and potentially modulate immune infiltration promoting a immune suppressive milieu [92,93]. Collectively, this evidence suggests a possible crucial role of CAFs in shaping the prostate tumour immunosuppressive microenvironment, however such involvement has not been fully described.

1.4.3. *Strategies for targeting cancer associated fibroblasts*

The ability of CAFs to promote cancer progression makes them promising therapeutic targets for anti-cancer strategies. Indeed, advances in understanding CAF role in cancer have increased the number of CAF-targeting preclinical studies, and a few of them have moved into clinical investigation.

The main problem concerning CAF-targeting strategies is the lack of specific CAF cell surface markers, which limits the possibility to perform a direct and specific depletion of CAFs from the tumour microenvironment. However, multiple studies were focused on targeting FAP, which is a cell surface protein generally expressed by activated fibroblasts and actively involved in the recruitment of myofibroblasts at the tumoural site. In this regard, it has been recently demonstrated that either genetic deletion of FAP or its pharmacology inhibition, with PT630 peptide, lead to a robust reduction of stromagenesis, which is associated with tumour growth delayed in lung and colon cancer in vivo models [94] Moreover, a FAP-targeting immonotoxin has been developed for the depletion of FAP-expressing CAFs in the tumour microenvironment, and has been shown to induce a strong tumour inhibition effect in a metastatic breast cancer models [95].

The potential of innovative FAP-targeting approaches have been also investigated in the preclinical and clinical settings. Indeed, sibrotuzumab, a humanised monoclonal antibody against FAP protein resulted clinically safe and able to reduce tumour progression [96,97]. However, it failed in phase II clinical trial due to limited clinical response.

Notably, a DNA vaccine targeting FAP displayed a moderate capability to promote $CD8^+$ cytotoxic response against FAP-expressing CAFs, improving the uptake of anticancer drugs in preclinical models of colon and breast cancer [98]. An innovative FAP-specific chimeric antigen receptor (CAR) T cells approach has been also developed and provided a specific immune response against FAP^+ CAFs, resulting in moderate antitumour efficacy in mesothelioma and lung cancer preclinical models [99,100]. However, severe side effects are associated to FAP-specific CARs approach, including lethal toxicity and cachexia, due to massive depletion of bone marrow stroma cells expressing FAP protein [101,102].

Of note, a phase III clinical trial is currently ongoing to target CAF precursor infiltration in the tumour site by using bevacizumab. Specifically, bevecizumab acts by reducing VEGF-mediated recruitment of endothelial cells, which are a considerable source of CAFs within the tumour [103].

Another interesting CAF-targeting strategy is aimed at reverting the CAF pro-tumourigenic phenotype into a more tumour suppressive or quiescent state. These approaches are identified as "CAF normalization". In this regard, recent studies performed in pancreatic ductal adenocarcinoma preclinical (PDAC) models highlighted that retinoic acid (ATRA) could revert fibroblast activated state and sequentially suppress WNT-β-catenin signaling in cancer cells or enhance the number of $CD8^+$ T cells infiltrating the tumour site [104,105]. Again, in PDAC models the treatment with calcipotriol, a vitamin D receptor ligand, induced a strong stromal reprogramming, thus reducing the reactive stroma deposition and concomitantly improving chemotherapeutic delivery into the tumour [106].

Targeting activation signalling or effectors of CAFs could be a useful strategy aimed at abolishing the CAF-mediated pro-tumourigenic effects. In this regard,

several molecules have been identified as CAF activators, which are involved in fibroblast recruitment and activation, or CAF effectors that actively support tumour formation and progression. Among them, IL-6 and JAK1-STAT3 signalling has been largely reported to be involved in fibroblast activation [69,107]. Recently, an interesting preclinical study showed that IL-6-mediated JAK1 activation in CAFs results in a robust ECM remodelling that promotes cancer cell invasion and migration. Starting from this, a novel anti-IL6 monoclonal antibody and a specific JAK1 inhibitor, named ruxolitinib, have entered preclinical and clinical testing in the cancer setting [108,109]. In addition, in a cervical cancer preclinical model, it has been shown that imatinib (a clinically approved PDGFR inhibitor) was able to reduce tumour angiogenesis and cancer cell proliferation, by suppressing FGF2 and FGF7 production in CAFs [110]. Another crucial CAF effector potentially targetable is SDF1, which is massively produced by FAP^+ CAFs. SDF1 acts through the stimulation of CXCR4 receptor, thus causing local immunosuppression by reducing $CD8^+$ T cell infiltration within the tumour site. In this context, the pharmacological inhibition of SDF1-CXCR4 axis, with AMD3001, reversed FAP^+ CAF-mediated immunosuppression.

It is known that CAFs are characterised by high secretion of several stromal components, growth factors and cytokines, which actively influence tumoural cell behaviour. In this regard, it has been reported that the pharmacological inhibition of mTOR-4E-BP1 pathway with somatostatine analogue (Pasireotide) in αSMA^+ CAFs, which overexpress somatostatin receptor (SST1), lead to the downergulation of CAF-secreted factors in a pancreatic preclinical model, including the key regulator of reactive stroma IL-6 [111].

Finally, targeting CAF-derived ECM production and relative associated signalling represents another promising strategy that could potentially reduce ECM stiffness and favour drug delivery at tumour site. In this regard, it has been reported that losartan, an angiotensin inhibitor, is able to reduce CAF collagen production, thus improving vascular perfusion and drug delivery in pancreatic and breast tumours [112].

Interestingly, the stimulation of the transmembrane smoothened (SMO) receptor by tumour-derived sonic hedgehog (SHH) on CAF surface leads to the activation of Hedgehog signalling, resulting in a increased deposition of reactive stroma. In this context, the treatment with IPI-929, a selective SMO inhibitor, resulted in a substantial reduction of CAF number within the tumour microenvironment and a simultaneous increase of vasculature pressure, that ultimately led to improve gemcitabine uptake at the tumoural site and sensitivity to VEGF inhibition [113,114] (Figure 1.5).

Collectively, the mentioned studies successfully reported that CAF depletion from the tumour microenvironment or their inactivation could substantially foster anti-cancer agent delivery at the tumour site. Specifically, among the approaches described above, SMO and JAK1 inhibitors have emerged as a promising potential complement to cancer therapies and are currently tested in a considerable number of clinical trials [114,115]. However, no anti-CAF therapy has been yet translated into the clinic. In this regard, further advances in the knowledge of CAF biology, and a clear understanding of intercellular interaction involving CAFs are needed to improve and develop efficacious therapeutic approaches based on targeting of the stromal components.

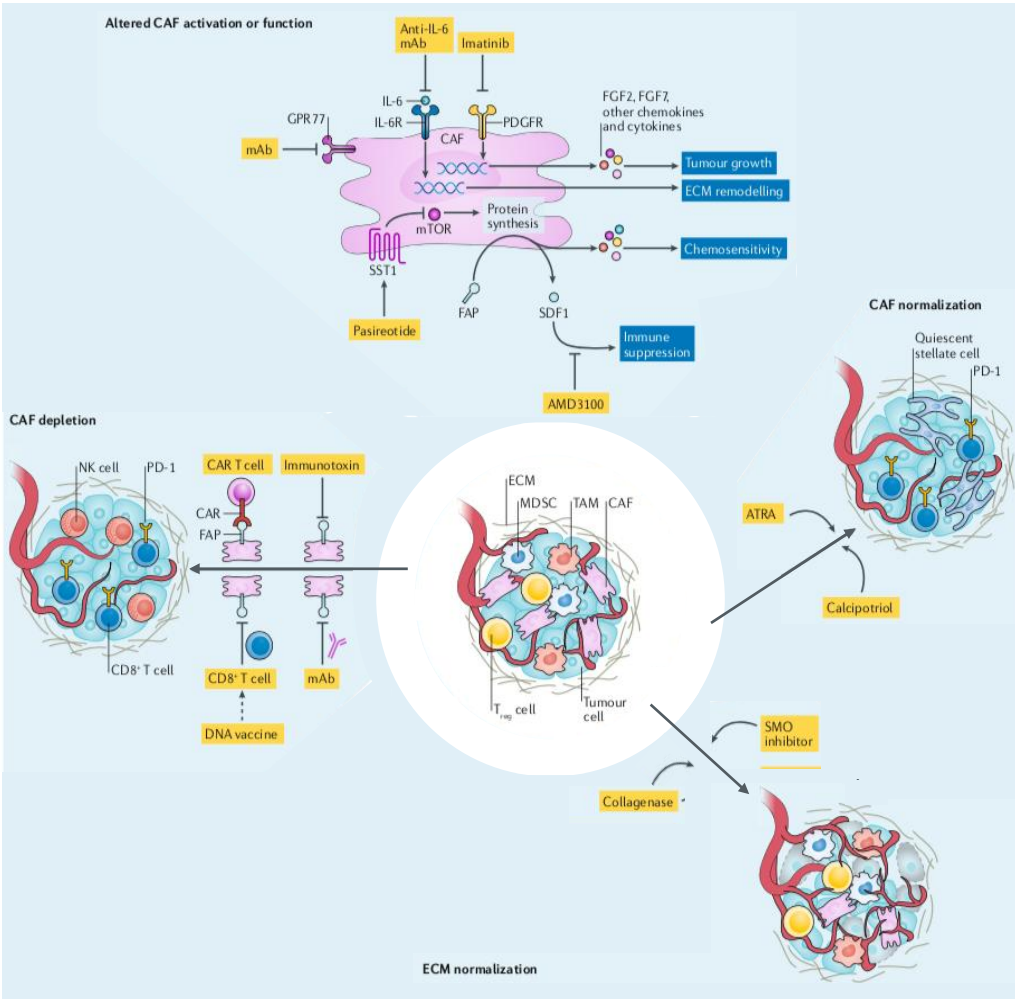

Figure 1.6. Principal strategies for CAF-directed anticancer therapy. Four approaches for targeting CAFs within the tumour microenvironment. (Adapted from Chen X, Nature Reviews 2019).

Study Aims

2. STUDY AIMS

Tumour microenvironment is an ensemble of different cellular and structural factors, including vasculature and immune-related cells, fibroblasts and the extracellular matrix (ECM), which sustains cancer progression in an intricate network of signals hard to dissect and to characterize experimentally. In the prostate cancer context (PCa), cancer associated fibroblasts (CAF) have been shown to fuel tumour development and metastasis by mutually interacting with tumour cells. Recently, by comparatively analysing gene expression profiles of prostate CAFs, in viro activated fibroblast with IL-6 or TGF-β and normal fibroblasts, we found that tumour reactive fibroblasts are characterized by positive enrichment of gene sets related to muscle contraction, including voltage gated cation channel genes and ECM-remodeling proteins involved in cancer progression (Figure 2.1) (87).

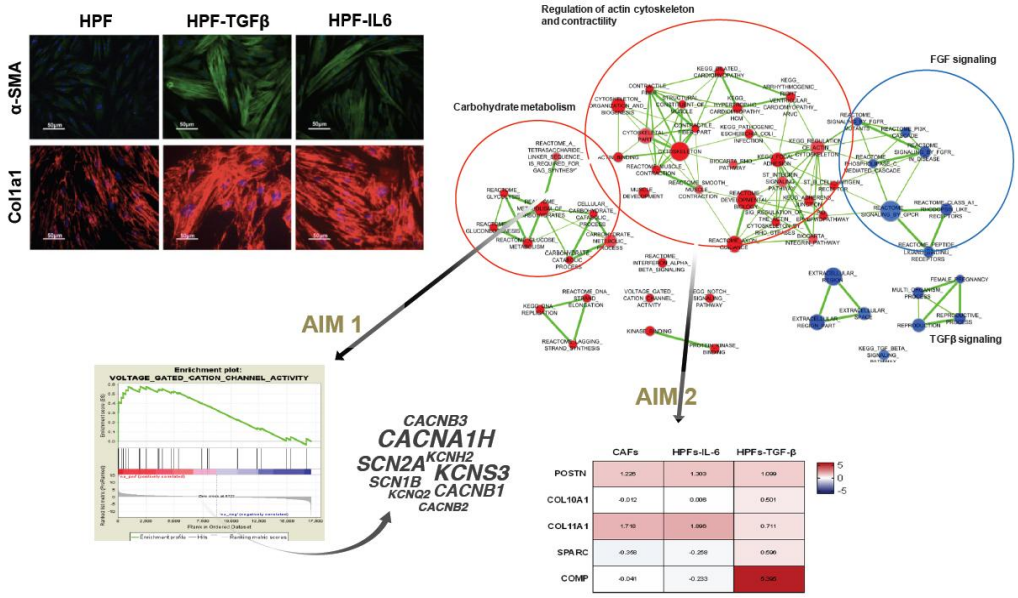

Figure 2. 1. Graphical overview of study rationale

Ths preliminary evidence suggests a crucial role of characteristic stromal-related pathways involved in fibroblast conversion to a phenotype able to sustain PCa progression.

On the basis of these observations, this study is aimed to test whether specific stromal gene signatures found to be characteristic of prostate CAFs may 1) help to develop novel therapeutic strategies against PCa, based on targeting the activated stroma (rather than tumour cells) through the use of drug repositioning and repurposing approaches, 2) have clinical potential as novel prognostic biomarkers in PCa.

To achieve the specific aims of the thesis project:

1) antiarrhythmic drugs, which are able to block the activity of voltage gate cation protein found up-modulated in CAFs, have been used in a drug-repositioning approach in order to counteract the myocardiocyte-like phenotype of prostate CAFs

2) select ECM related genes found to be up-regulated in reactive fibroblasts were assessed as novel potential stromal biomarkers for risk assessment in PCa.

This thesis work is expected to help undestainding the involvement of tumour adjacent stroma in PCa progression, generating useful information to rationally design innovative therapeutics strategies, and identify novel biomarkers for risk assessment in PCa.

Materials and Methods

3. MATERIALS AND METHODS

3.1. Cells and culture conditions

3.1.1. *Isolation and culture conditions of primary fibroblasts*

Primary cancer-associated fibroblasts (CAFs) and human prostate fibroblasts (HPFs) were isolated from prostate specimens of five PCa-bearing patients (Gleason score 4+5) who underwent radical prostatectomy upon informed consent, in accord with the ethics committee of IRCCS Istituto Nazionale dei Tumori of Milano. Intra-tumoural areas or non-tumoural regions of radical prostatectomy specimens were identified by an expert uro-pathologist of our institute, selected and cut in small pieces (3mm x 3mm) and digested overnight at 37°C and 5% CO_2 in DMEM medium (Lonza, Basel, Switzerland) supplemented with 5% fetal bovine serum (FBS) (Gibco, Thermo Fisher Scientific, Waltham, MA, USA), 300 units/ml collagenase and 100 units/ml hyaluronidase solution (Stemcell Technologies Vancouver, Canada), and 1% penicillin-streptomycin (Lonza, Basel, Switzerland). The cell suspension was centrifuged at 1,500 g for 5 minutes. The resulting fibroblast-rich pellet was suspended and plated in DMEM medium (Lonza) containing 15% FBS (Gibco, Thermo Fisher Scientific), 4 mM L-glutamine and 1% penicillin-streptomycin (Lonza). CAFs or HPFs were maintained in culture for 3 passages and the absence of epithelial marker expression was verified before being used in the experiments. All established primary cultures were used until the 15 passages and maintained in DMEM medium (Lonza) containing

10% FBS (Gibco, Thermo Fisher Scientific) and 4 mM L-glutamine (Lonza). Cells were grown as a monolayer, at 37°C in a 5% CO_2 atmosphere.

3.1.2. *Cell lines*

In the study the following human prostate cell lines were used: DU145, PC3 and WPMY-1. All cell lines were purchased from American Type Tissue Culture Collection (ATCC, VA, USA). DU145 cell line derives from a brain metastasis of a Caucasian 69-year-old PCa patient and displays an epithelial morphology. DU145 cell line is not hormone sensitive and does express neither androgen receptor (AR) nor the prostate specific antigen (PSA). PC-3 cell line derives from a bone metastasis of a 62-year-old Caucasian PCa patient. As for DU145 cell line, it is hormone insensitive and presents no AR or PSA. Both DU145 and PC-3 cells are able to form adenocarcinoma when injected into nude mice. These PCa cell lines were maintained in RPMI-1640 medium (Lonza) supplemented with 10% FBS (Gibco, Thermo Fisher Scientific), at 37°C and 5% CO_2.

The prostate myofibroblast stromal cell line WPMY-1 was derived from stromal cells of the peripheral zone of the histologically normal adult prostate. WPMY-1 cell line was immortalized with SV40-large-T antigen gene, using a pRSTV plasmid construct. WPMY-1 cells were maintained in DMEM (Lonza) supplemented with 10% FBS (Gibco, Thermo Fisher Scientific). WPMY-1 cells are not able to grow when injected into nude mice.

Cell lines were grown as a monolayer, at 37°C in a 5% CO_2 atmosphere and routinely checked for mycoplasma contamination (MycoAlert Mycoplasma Detection Kit, Lonza). Cell lines were authenticated and periodically monitored by genetic profiling

using short tandem repeat analysis (AmpFISTR Identifiler PCR amplification kit, Thermo Fisher Scientific).

3.2. *In vitro* experiments

3.2.1. *Conditioned medium*

For indirect co-culture and in vivo experiments, conditioned medium (CM) was collected from HPFs, CAFs and WPMY-1 treated or not with antiarrhythmic drugs and from DU145 cells. To obtain CM, a total of 7×10^5 cells were seeded in T-75 cm^3 culture flask, treated with 1 μM of amiodarone (Hikma Pharmaceuticals, London, UK), 1 μM verapamil (Abbott Laboratories, Chicago, USA) 1 μM nifedipine (Meda AB, Solna, Sweden) or flecainide (Meda AB) for 24 hours. Upon treatment, the culturing medium was removed, cells were washed 2 times with PBS (Lonza) and 6 ml of serum-free medium was added. Twenty-four hours later, the CM was collected, clarified for 5 minutes at 1,500 g and used freshly to treat PCa cells (DU145 or PC-3), to activate WPMY-1 or concentrated for western blotting analysis.

3.2.2. *Cell growth curves*

PCa cells (DU145 and PC-3) were seeded in 12-well plates (2×10^4 cell/well) and after 24 hours, cells were exposed to CM of HPFs, CM of CAFs or CM of CAF-treated with 1 μM of amiodarone (Hikma Pharmaceuticals, London, UK), 1 μM verapamil (Abbott Laboratories, Chicago, USA) 1 μM nifedipine (Meda AB, Solna, Sweden) or flecainide (Meda AB). Upon starvation with appropriate CM, cells were harvested with Trypsin-EDTA (Lonza) and counted at 24, 48 and 72 hours with an automated cell counter (Beckman, Coulter, Brea, CA, USA). All cell growth experiments were performed at least 3 times.

3.2.3. *Migration assay*

For migration assessment cells were seeded at 4×10^4 cells/well into a 12-well culture plate. After 2 days, the monolayer of cells was wounded by manual scratching with a pipet tip, washed with PBS (Lonza), photographed (t0 point) and media were replaced with serum-free DMEM containing 1 μM of amiodarone (Hikma Pharmaceuticals), 1 μM of verapamil (Abbott Laboratories), 1 μM nifedipine (Meda AB), or 1 μM flecainide (Meda AB) for CAFs experiments or, with CM of CAFs treated or not with 1 μM of amiodarone (Hikma Pharmaceuticals), 1 μM of verapamil (Abbott Laboratories), 1 μM nifedipine (Meda AB), or 1 μM flecainide (Meda AB) for DU145 cell migration experiments. Images of cell movement were captured at regular time intervals until 48 hours by using a microscope equipped with digital camera. The rate of cell migration was determined by using ImageJ software that measures the distance travelled by cells during the desired time frame.

3.2.4. *3D gel collagen contraction assays*

Type I collagen from rat-tail (Sigma-Aldrich) was dissolved at 2 mg/ml in 0.1% acetic acid to create a stock solution. The collagen matrix was quickly prepared on ice by adding 6 ml of collagen stock solution to 3.6 ml of 0.1% acetic acid, 1.2 ml of 10× concentrated DMEM, and 1.2 ml of sodium bicarbonate solution (11.76 mg/ml) for a final concentration of 1 mg/ml collagen. The pH was adjusted to 7.2–7.4 by adding 0.1 mol/l NaOH. CAFs or HPFs cells were then added to achieve a final concentration of 5×10^5 cells/ml; 500 μl of this suspension was aliquoted into each well of a 24-well culture plate. After 30 minutes of incubation at 37°C with 5% CO_2 for polymerisation, the matrix in each well was overlayed with 500 μl of complete growth medium. After

24 hours from incubation, CAFs were treated with 1 μM amiodarone (Hikma Pharmaceuticals), 1 μM verapamil (Abbott Laboratories), 1 μM nifedipine (Meda AB) or 1 μM flecainide (Meda AB), in serum free medium. Serum-free medium served as control. Then, the gels were mechanically released from the wall and bottom of the wells with a sterile spatula. Gel contraction was monitored for 48 hours and scanned by standardized photography at time 0 and at sequential time points (6, 24 and 48 hours) (Figure 3.1).

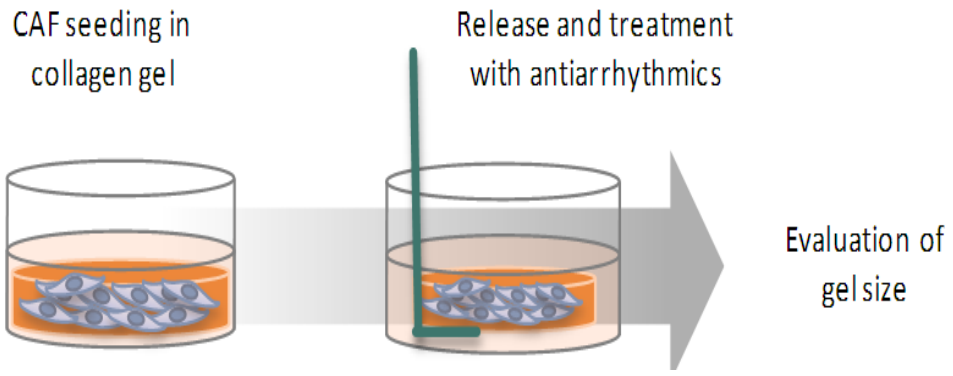

Figure 3. 1. Schematic representation of a 3D collagen assays

3.3. Molecular biology analyses

3.3.1. *RNA isolation*

To perform gene expression analysis, total RNA was isolated using miRNeasy mini kit (Qiagen, Hilden, Germany), which combines phenol/guanidine-based lysis of cells and silica-membrane–based purification of total RNA. Cell pellets were homogenised within 700µl of QIAzol Lysis Reagent (Qiagen), a monophasic solution of phenol and guanidine thiocyanate, designed to facilitate cell lysis, inhibit RNases and also to remove most of the cellular DNA and proteins from the lysate by organic extraction. Tissue specimens in a deep-cold state were homogenised by using a micro-dismembrator. Subsequently, samples were incubated at room temperature for 5 minutes. Then, 140 µl of chloroform were added and the homogenate was separated into aqueous and organic phases by centrifugation (15 minutes at 12,000 g at 4°C). The upper aqueous phase (enriched in RNA) was transferred to a new collection tube avoiding the transfer of any interphase. 1.5 volumes of 100% ethanol were added and mixed thoroughly by pipetting in order to precipitate RNA from the aqueous phase. Then, 700 µl of each sample, including any precipitate, was transferred into an RNeasy Mini column in a 1.5 ml collection tube, and then centrifuged at ≥ 8000 g at room temperature for 15 seconds. The flow-through was discarded and 700 µl of Buffer RWT (Qiagen) were added to the columns and centrifuged for 15 seconds at ≥ 8000 g at room temperature. Then the columns were washed with 500 µl of Buffer RPE (Qiagen) by two centrifugation steps. Finally, columns were transferred to a new 1.5 ml

tube and 30 µl of RNase-free water were pipetted directly into the column membrane and centrifuged for 1 minute at ≥ 8000 g to elute RNA.

The total amount of RNA was quantified through the NanoDrop 2000c (NanoDrop, Thermo Fisher Scientific) spectrophotometer. The determination of nucleic acid concentrations is based on the absorbance at 260 nm, corrected for the extinction coefficient specific for RNA (=40 ng-cm/µL). Moreover, purity ratios were verified for each sample, by considering as "pure" a value of ~ 2.0 for 260/280 ratio (indicative of the presence of protein, phenol or other contaminants that absorb strongly at or near 280 nm) and 1.8-2.0 for 260/230 ratio (the presence of residual phenol, guanidine, magnetic beads, carbohydrates or proteins). Quantified RNA samples were stored at -20° C until use.

3.3.2. *Reverse transcription*

Reverse transcription was performed using High Capacity cDNA Reverse Transcription Kit (Applied Biosystems, Thermo Fisher Scientific). For each sample, the reaction was carried out by using 1.25 µg of total RNA in a reverse-transcription master mix containing 5 µl of 10x High Capacity buffer, 2 µl of dNTPs mix, 2.5 µl of Reverse Transcriptase, 2.5 µl of RNase Inhibitor, 5 µl of random primers and RNase-free water to a final volume of 50 µl (volumes for 1 reaction). A thermal cycler was used to perform the retrotranscription reaction as following: 60 minutes at 37°C followed by 5 minutes at 95°C to inactivate Reverse Transcriptase. cDNA was stored ad -20°C until use. Detection of mRNAs was performed using appropriate assays.

3.3.3. *mRNA expression analysis*

mRNA quantifications were assessed by using the specific following TaqMan gene expression assays (Applied Biosystems, Thermo Fisher Scientific): CACNA1H Hs01103527_m1, CACNB1 Hs00609503_m1, CACNB2 Hs01100744_m1, CACNB3 Hs0016787_m1, SCN2A Hs01109871_m1, SCN1B Hs00962350_m1, KCNS3 Hs04234270_m1, ACTA2 Hs00909449_m1 (α-SMA), FAP Hs00990806_m1, COL1A1 Hs00164004_m1, FSP Hs002433202_m1, CDH1 Hs00170423_m1, CTNNB1 Hs00355045_m1, VIMENTIN Hs05024057_m1, SNAI1 Hs00195591_m1, PERIOSTIN Hs01566750_m1, GAPDH Hs02786624_g1.

GAPDH was used as endogenous control. For each sample, a mix was prepared using: 17.5 µl of TaqMan Fast universal master mix (Applied Biosystems, Thermo Fisher Scientific), 1.75 µl of specific primer, 3.5 µl of diluted cDNA and RNase-free water to a final volume of 35 µl (volumes for 1 reaction). The amplification reaction was performed as following: 95°C for 15 minutes, 40 cycles of denaturation at 95°C for 15 seconds and annealing at 55°C for 30 seconds, and a final step of extension at 72°C for 30 seconds. Amplifications were run on the 7900HT FastReal-Time PCR System equipped with Sequence Detection Systems 2.4 software. Data analysis was performed by using RQ manager software (Applied Biosystems, Thermo Fisher Scientific) and reported as relative quantity with respect to a calibrator sample using the $2^{-\Delta\Delta Ct}$ method. The $2^{-\Delta\Delta Ct}$ method is a comparative method that relies on comparing the differences in Ct (threshold cycles) values obtained with normal (reference) versus experimental (target) samples. Specifically, the Ct for each sample was determined. Next, the ΔCt value was calculated as the difference between the Ct value of the target gene and the Ct value of the endogenous control: ΔCt = Ct (target gene) - Ct (reference gene). In the

next steps, the ΔΔCt value and the normalized target expression were calculated: ΔΔCt = ΔCt (target sample) - ΔCt (reference sample). The relative quantification (RQ), which allows analyse changes in gene expression in the sample of interest relative to the reference sample, is calculated as $2^{-\Delta\Delta Ct}$.

For gene expression analysis, 150 ng of total RNA was labelled using a reverse transcription priming method to prime the entire length of each RNA transcript, including both polyA and non-polyA mRNA to provide complete and un-biased transcriptome coverage. This protocol efficiently generated amplified and biotinylated sense-stranded DNA targets, avoiding loss of specificity due to antisense strand interference. Data was checked for quality before being assessed on the Affymetrix Clariom S Human MicroArray.. On this array expression for each mRNA was assessed by approximately 11 probes, which were tiled throughout the transcript. The array provides basic gene level coverage of known genes.

3.4. Biochemical analyses

3.4.1. *Cell viability*

The cytotoxic effect of amiodarone (Hikma Pharmaceuticals, London, UK), verapamil (Abbott Laboratories), nifedipine (Meda AB) or flecainide (Meda AB, Solna) was determined by the CellTiter96® AQueous One Solution Cell Proliferation Assay (MTS) (Promega Corporation, Madison Wisconsin, USA). The MTS assay is a colorimetric assay that allows assessing the cell viability. MTS is chemically reduced by cells into formazan which is soluble in tissue culture medium. The conversion of MTS into aqueous soluble formazan is accomplished by dehydrogenase enzymes found in metabolically active cells. The measurement of the absorbance of the formazan, which is proportional to the number of living cells, is a good indication of the viability of the cells and therefore of the cytotoxicity as well. The absorbance is measured at 490 nm. Cells were plated for 24 hours in 96-well flat-bottomed microtiter plates at a density of 1.5×10^3/50 µl, and then treated with increasing concentrations amiodarone (Hikma Pharmaceuticals, London, UK), verapamil (Abbott Laboratories), nifedipine (Meda AB) or flecainide (Meda AB, Solna) (0-5 µM) for 72 hours. At the end of the treatment, 20 µl of the MTS solution was added to each well and the plate was incubated for 3 hours in a 5% CO_2 incubator at 37°C. The absorbance at 490nm was recorded using the POLARstar optima plate-reader (VWR International, Radnor, Pennsylvania, USA). The percentage of cell viability was calculated using the following formula:

Viability (%) = [Abs490 treated cells/Abs490 control] x 100.

3.4.2. *Western blotting*

Protein lysates were prepared using a lysis buffer composed of 0.5 M Tris HCl pH 6.81 (Trizma hydrochloride, Sigma-Aldrich, Merck, MA, USA), 10% sodium dodecyl sulphate (SDS) (Lonza) and protease/phosphatase inhibitors (25 mM sodium fluoride, 10 µg/ml pepstatin A, 1 mM PMSF, 10 µg/ml leupeptin 30 µg/ml aprotinin, 1 mM sodium orthovanadate and 1 mM sodium molibdate), all purchased from Sigma-Aldrich.

At the appropriate time point, cells were harvested and pellets were washed in iced PBS (Lonza), and then homogenized for 30 minutes on ice in 100 µl of lysis buffer. In order to perform *ex vivo* evaluations, frozen-tumour specimens were homogenised by using a micro-dismembrator and lysed for 30 minutes on ice in 800 µl of lysis buffer. Lysates were clarified by centrifugation at 14,000 g for 15 minutes, cooled in ice and stored at -20°C.

Protein concentration was determined using spectrophotometer POLARstar OPTIMA (VWR International) at a wavelength of 562 nm using Pierce BCA Protein Assay Kit (Invitrogen, Thermo Fisher Scientifics) as colorimetric assay. To perform protein quantification, the Bovine Serum Albumin according to scale of dilutions from 0.01 µg/µl to 0.05 µg/µl was used as a standard reference.

For the assessment of secreted-proteins, CM of HPFs and CAFs treated or not with antiarrhythmics was clarified for 10 minutes at 1500 g and 6× concentrated by using Concentrator spin 5K MVCO column (Agilent Technologies, Santa Clara, CA) for 20 minutes at 1200 g and used for protein detection.

Cell lysates, concentrated-CM, tissue-homogenised or plasma samples were fractionated by SDS-polyacrylamide gel electrophoresis and then transferred into

nitrocellulose membranes (Amersham, Pittsburgh, PA). 20 μg of protein for toral lysis protein and 5 μl for CM or plasma samples were loaded into gradient NuPAGE gels (4-12%) following manufacturer's instructions. Running buffer was prepared using: Tris-glycine 100 ml, SDS 10% 10 ml and water to a final volume of 1 L. The electrophoretic run was performed at 110 V for the time necessary to allow the separation of proteins. Then, the gel was transferred to the nitrocellulose filter using transfer buffer composed of: Tris-glycine 100 ml, methanol (96%) 200 ml and water to a final volume of 1 L. Transfer efficacy was evaluated by Ponceau S staining (Sigma-Aldrich). Filters were blocked in PBS-Tween/0.5% skim milk (Sigma-Aldrich) and probed overnight with the appropriate primary antibodies: CACNH1 (1:500 ab128251; Abcam), CACNB1 (1:500 ab155179; Abcam) KSCNS3 (1:500 ab34710; Abcam), SCN2A (1:500 ab65163; Abcam), SCN1B (1:500 ab107370; Abcam), α-SMA (1:3000, A2547 Sigma-Aldrich), Collagen I (1:1000 ab34710; Abcam), phospho-FAK (1:500 Y397 ab4803; Abcam), FAK (1:1000 ab131435; Abcam), E-cadherin (1:1000 sc-7870 H-108, Santa Cruz), β-catenin (1:500 ab223075; Abcam), Vimentin (1:2000 ab92547; Abcam), Snail (1:500 C15D3 #3879, Cell signalling Technology), MMP2 (1:200 ab92536; Abcam) Periostin (1:500 ab14041, Abcam), Sparc (1:1000 ON1-1 33-5500, Invitrogen), COL11A1 (1:500 NBP1-55803; Novus Biologicals), COL11A1 (1:500 LS-B14811; Biocompare), Comp (1:200 NB100-2478, Novus Biologicals), β-actin (1:5000, ab8227; Abcam) or β-tubulin (1:3000 ab6046, Abcam).

The filters were then incubated with the respective secondary peroxidase-linked whole antibodies (GE healthcare, UK) 1 h at room temperature. Bound antibodies were detected using the Novex ECL, HRP Chemiluminescent substrate Reagent Kit (Life Technologies, Thermo Fisher Scientific) and filters were auto-radiographed.

Band quantification was performed taking advantage of the ImageJ software. For the preparation of figures, the original western blots were cropped to generate the figure panels with the relevant lanes. Cropped images were then subjected to uniform image enhancement of contrast and brightness. Molecular weights were determined using the colorimetric SeeBlue Plus Protein Standard (Life Technologies, Thermo Fisher Scientific) and standard protein bands were removed from the chemoluminescent blot image.

3.4.3. *Immunofluorescence*

To perform immunofluorescence analysis, CAFs were seeded at 6×10^4 cell/well in a 6-well plate containing a coverslips suitable for microscopy. After 24 hours, CAFs were treated with 1 μM amiodarone (Hikma Pharmaceuticals), 1 μM verapamil (Abbott Laboratories), 1 μM nifedipine (Meda AB) or 1 μM flecainide (Meda AB), in serum free medium. Forty-eight hours later cells were rinsed in PBS (Lonza) and fixed in 4% formaldehyde dissolved in PBS for 10 minutes. After washing with PBS, cells were permeabilised with 1:1 Acetone / Methanol solution. After 2 washes in PBS, cells were probed with primary antibodies for phospho-FAK (1:200 Y397 ab4803; Abcam) diluted in antibody diluent (Dako Ab Diluent from Agilent Technologies) for 1 hour at room temperature. After washing with PBS, an Alexa Fluor594-labeled secondary antibody Thermo Fisher Scientific) was used to incubate cells for 1 hour at room temperature. Actin filaments were stained using phalloidin-conjugated-Fluor488 dye and nuclei were stained with DAPI (Invitrogen, Thermo Fisher Scientific) and images were acquired by Nikon Eclipse E600 microscope using ACT-1 software (Nikon).

3.4.4. *Cell cycle analysis*

For cell cycle evaluation, DU145 were seeded in 6 well plates (6× 10^4 cell/well) and after 24 hours, cells were exposed to CM of HPFs, CM of CAFs or CM of CAF-treated with 1 μM of amiodarone (Hikma Pharmaceuticals, London, UK), 1 μM verapamil (Abbott Laboratories, Chicago, USA) 1 μM nifedipine (Meda AB, Solna, Sweden) or flecainide (Meda AB). 72-hours upon starvation with appropriate CM, cells were harvested with Trypsin-EDTA (Lonza) and fixed in cold 70% ethanol solution for 30 minutes on ice. Cells were washed in PBS 1X (Lonza) and resuspended in the staining solution composed of PBS with 100 ng/μl of RNase A (Sigma-Aldrich) and 50 μg/mL Propidium Iodide (Sigma-Aldrich). Stained cells were incubated overnight at 4°C. The cycle distribution was detected by the BD Accuri C6 Flow Cytometer. All cell cycle analysis experiments were performed at least 2 times.

3.4.5. *Immunohistochemistry*

For Ki-67 immunohistochemical analysis, tumours were removed, formalin-fixed and paraffin embedded. 4-μm tumour sections were deparaffinized in xylene, rehydrated through graded alcohols to water, and subjected to immunohistochemical analysis using the following antibody: anti-mouse monoclonal antibody Ki-67 (8D5#9449, Cell Signaling) at the dilution of 1:100. Nuclei were counterstained with hematoxylin.

For prtiostine staining, formalin-fixed, paraffin-embedded (FFPE) specimens from radical prostatectomies were obtained from the archive of the IRCCS Istituto Nazionale dei Tumori di Milano, following ethical approval procedures. Tissue sections of 4-μm were subjected to automated immunohistochemistry on Autostainer Link 48 instrument

(Agilent Technologies) using EnVisionFLEX+ Target Retrieval Solution, high pH (Dako, Agilent Technologies) detection system according to manufacturer's instructions. Briefly, tissue sections of 4-µm were deparaffinised in xylene and heat-induced epitope retrieval was performed in EnVisionFLEX+ Target Retrieval Solution, high pH (Dako, Agilent Technologies) for 30 minutes at 97°C. Periostin was identified using the anti-POSTN antibody (ab14041, Abcam) at the dilution of 1:1000. Adjacent sections were stained with hematoxylin and eosin for anatomical reference.

3.4.6. *Enzyme-linked immunosorbent assay*

Periostin, Sparc, Comp and Col10a plasma concentration was determined by solid phase sandwich enzyme-linked immunosorbent assays (ELISA), according to manufacturer's instructions. The following ELISA tests were used: Human Periostin ELISA kit (EHPOSTN; Invitrogen, Thermo Fisher Scientific), Human SPARC Quantikine ELISA (DSP00, R&D System), Human COMP Quantikine ELISA (DCMP0, R&D System), Human Collagen Alpha -1(X) Chain (COL10A1) ELISA kit (CSB-EL005715HU, Cusabio), Collagen Type XI Alpha 1 (COL11a1) ELISA kit (SEC157Hu, Cloud-Clone Corporation).

To obtain plasma sample, whole blood was collected in anticoagulant-tubs (BD Vacutainer™ Heparin Plasma Tubes,) and plasma was immediately separated by centrifugation at 2,200 g for 20 minutes by using a refrigerated centrifuge at 4°C. The supernatants obtained were further clarified for 10 minutes at 2,200 g, and stored at -80°C. Plasma samples were tested in duplicate, according to the manufacturer's instructions. The coloured product generated by the enzyme activity was detected by the plate-reader POLARstar optima (VWR International) at 450 nm.

3.5. *In vivo* experiments

Animal studies were performed in accordance with guidelines of animal care protocols approved by ethics committee for animal experimentation of IRCCS Istituto Nazionale dei Tumori of Milano. Male SCID mice were purchased from Charles River Laboratories and housed in specific pathogen-free conditions.

Prostate tumour xenografts were generated by subcutaneous injection of 1×10^7 DU145 cells in the right flank of SCID mice and when tumours reached ~100 mm^3 (Width2 x Length/2), mice were randomly assigned to control or treatment groups (n=6). Subsequently, mice were intratumourally treated (5 consecutive days for 2 weeks) with 250 µl of CM of WPMY-1, activated-WPMY-1 exposed or not to 1 µM amiodarone (Hikma Pharmaceuticals), 1 µM verapamil (Abbott Laboratories), 1 µM nifedipine (Meda AB) or 1 µM flecainide (Meda AB) and serum-free medium as control.

At two different time points (after 1 week and at the end of the treatments) subcutaneous tumours were harvested in order to investigate the impact on tumour plasticity by analysing the expression of specific epithelial-to-mesenchymal transition markers.

3.6. Bioinformatics analyses

For gene expression profiling, RNA samples were processed for microarray hybridation by Functional Genomics core facility at Fondazione IRCCS Istituto Nazionale dei Tumori, Milano Italy. RNA was reverse transcribed, labeled and amplified using the expression profiling tool human Clariom™ S Assay according to manufacturer's protocol. Raw data were normalized according to the RMA algorithm of the *oligo*

Bioconductor package. Probes not assigned to an official gene symbol were removed, while for probes mapping on the same gene symbol, the one with the highest variance value was selected. Besides, to reduce intervariability among samples, batch effects we adjusted with a linear model, using *ComBat* function of the *sva* package. Differential expression was estimated both in terms of fold change (FC) and *t*-value (paired t-test), using the *limma* Bioconductor package. Statistical significance was provided in terms of False Discovery Rate (FDR) taking into account the adjustment for multiple hypotheses testing, and considering a threshold of 0.05. All analyses were performed using the computing microenvironment R.

A single-sample GSEA (ssGSEA) was performed on normalized data, using Hallmark collection of MSigDB database [116]. This approach scores each individual sample against gene sets belonging to the collection. In this way, hierarchical clustering was represented in a heatmap, by plotting the normalized enrichment score (NES) and using Spearman correlation as a distance measure and average as a linkage method.

3.7. Statistical analyses

Data are presented as mean values ± standard deviation from at least three independent experiments. Two-tailed Students't test or chi-squared test were chosen as statistical analysis and performed by Prism GraphPad software. P-value <0.05 were considered statistically significant.

Results

4. RESULTS I: Drug repositioning approaches to counteract the activated phenotype of CAFs and affect CAF-PCa cell interplay

The first aim of the study is to evaluate the biological effects of cation channel inhibitors on CAF activated state. In the clinical routine, cation channels inhibitors, such as antiarrhythmics, are used to restore the normal rhythm and heart conduction in patients with cardiac arrhythmias [117]. Starting from our preliminary observation highlighting the up-modulation of ion channels in prostate CAFs compared to HPFs [89], we assumed to use antiarrhythmic drugs, in a drug-repositioning approach, to target the myocardiocyte-like phenotype of prostate CAFs, with the final aim of interrupting the crosstalk between CAFs and PCa (Figure 4.1).

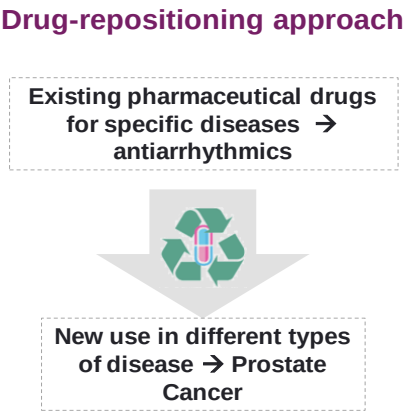

Figure 4.1. Schematic representation of drug-repositioning approach

Following this strategy, human primary fibroblasts were used to perform the experiments of the preclinical part of the project. Specifically, CAFs were isolated and established from tumoural areas of radical prostatectomy specimens and, for

comparison normal prostate fibroblasts (HPF) were obtained from non-tumoural stromal areas of the same clinical sample. In addition, for further biological functional validation, we used the prostate stromal cell line WPMY-1, purchased from ATCC.

Experimentally, we exposed activated fibroblasts to sub-toxic doses of antiarrhythmics and assessed the effect of the drugs on *i*) CAF activated state, and on *ii*) CAF-PCa cell interplay.

4.1. Evaluation of the relevance of ion channels on CAF activated state

4.1.1. *Validation of gene expression results*

Before investigating the effect of cation channel inhibitors on CAF activated state, the very first step of the study was the in silico and experimental validation of our gene expression data indicating up-regulation of cation channel genes in prostate CAFs.

Initially, we evaluated the expression levels of cation channels in publicly available gene expression datasets. In accordance with our observation, the analysis of GSE86260 dataset highlighted the significant enrichment of voltage-gated cation channel activity and voltage potassium activity gene sets (Figure 4.2) in genes up-modulated in prostate CAFs compared to normal fibroblasts, thus suggesting the involvement of cation channels in fibroblasts activation.

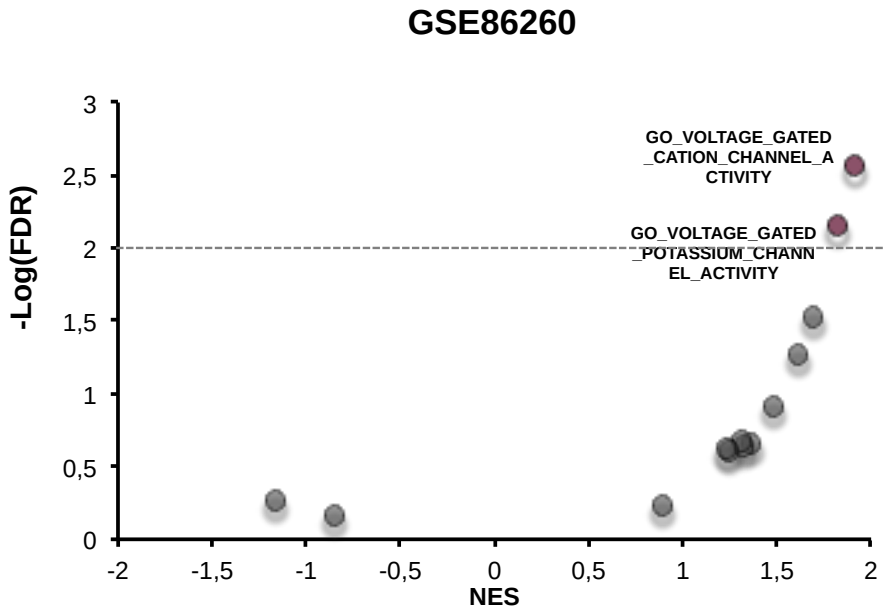

Figure 4.2. Evaluation of ion channel expression levels in GSE86260 database. Gens sets significantly up-modulated in seven CAFs samples isolated from radical prostatectomy with respect to normal fibroblast are highlighted in red (Log2 FDR ≥2), NES (normalised enrichment scores).

In a next step, we carried out a biological validation of our gene expression data. Specifically, the expression levels of selected ion channels belonging to the voltage-gated channel activity gene set (CACNA1H, CACNB1-3, SCN2A, SCAN1B, and KCNS3) were analysed by qRT-PCR and western blotting in an independent panel of paired CAFs and normal fibroblasts (HPFs) isolated from three patients who underwent radical prostatectomy at our Institute. Consistent with our preliminary observations, we confirmed that ion channels, especially sodium (SCN2A, SCN1B) and calcium channels (CACNAH1, CACNB1-3), were up-regulated both at the mRNA and protein level in the independent panel of CAFs, compared to paired HPFs (Figure 4.3). In contrast, despite KCNS3 mRNA was found to be down-modulate in our panel of CAFs compared to HPFs, however we confirmed its up-modulation at protein levels (Figure 4.3).

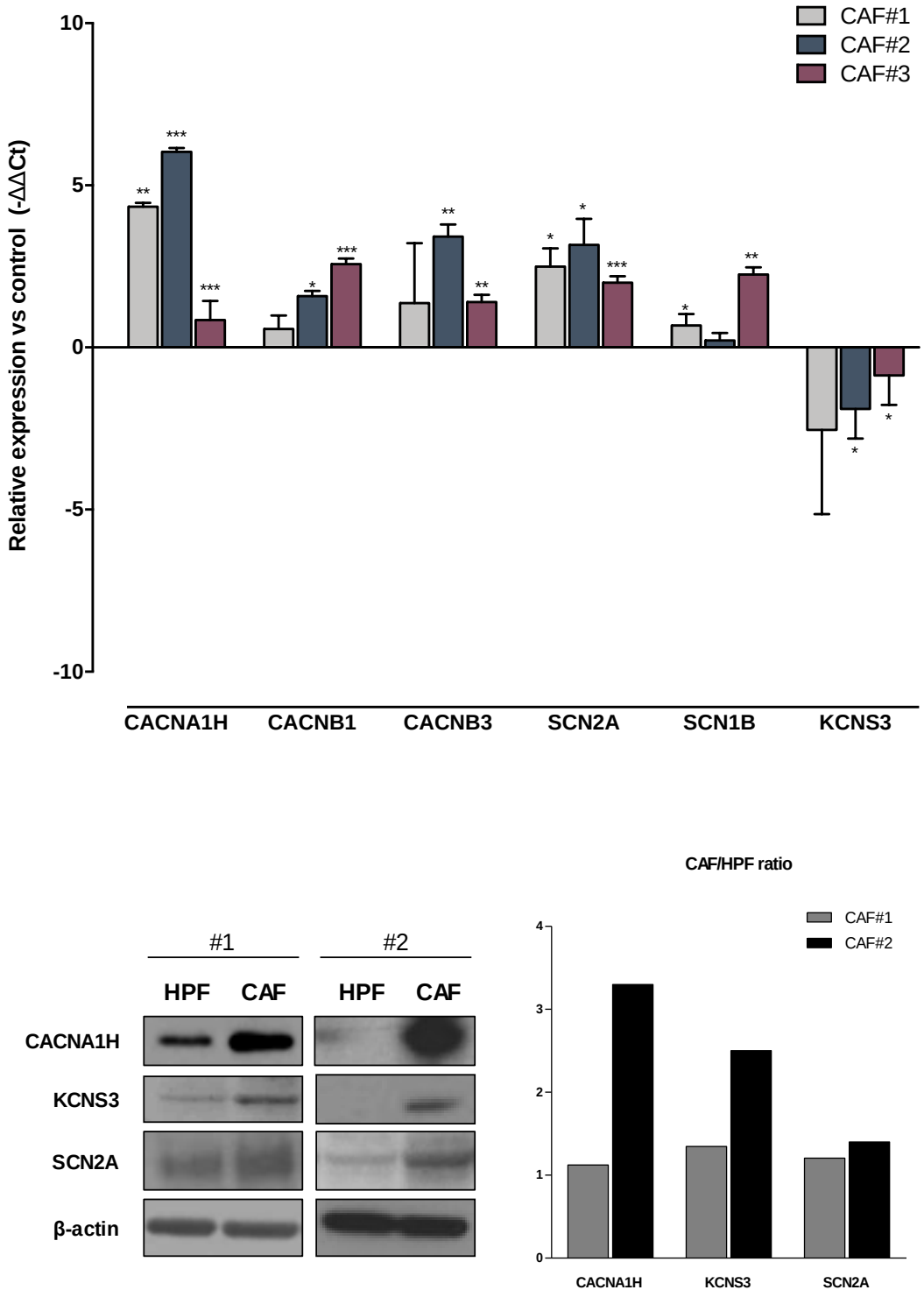

Figure 4.3. Validation of expression data obtained from GSEA analysis. (*Upper panel*) The expression levels of CACNA1H, CACNB1, CACNB3, SCN2A, SCN1B, and KCNS3 were evaluated in an independent setting of three paired CAFs and HPFs. Data are reported as relative expression compared to HPF. and are

representative of three independent experiments. (*Lower panel left*) Western blotting analysis showing selected ion channel protein levels in paired CAF#1/HPF#1 and CAF#2/HPF#2 samples. (*Lower panel right*) The bar plot reports quantification of western blot. Densitometry data are reported as raw normalized values (arbitrary units) towards the loading control (β-actin). The level of significance was represented as *p<0.05, **p<0.01, ***p<0.005, Student's t-test.

Overall, we confirmed our preliminary findings regarding the up-modulation of cation channels in prostate CAFs, by analysing public data and assessing the expression levels of cation channels in an independent panel of three CAF derived from radical prostatectomy samples collected in our Institute. Considering this preliminary observation, we were prompted to study the effects of ion channels inhibitions on CAF activated state.

4.1.2. *"In vitro" activation of fibroblasts confirms the up-modulation of ion channels*

In order to investigate the relevance of cation channels in fibroblasts activated phenotype, we performed an in vitro activation of fibroblasts by treating HPFs with conditioned medium (CM) of DU145 PCa cells with the aim to mimic the pathological environment, in which cancer cells condition the behaviour of normal stromal cells. Specifically, HPFs were exposed for 48 hours to CM of DU145 cells and the activated state was assessed by the evaluation of fibroblast activation markers. Additionally, to elucidate the involvement of ion channels in the shift from the inactivated to the activated phenotype, ion channels expression levels were investigated as well. qRT-PCR analysis showed that two sets of HPFs (HPF#1 and HPF#2) exposed to the CM of DU145 cells displayed an activated phenotype, as

indicated by increased α-SMA, FAP, COLLAGEN 1A1 and FSP mRNA levels (Figure 4.4).

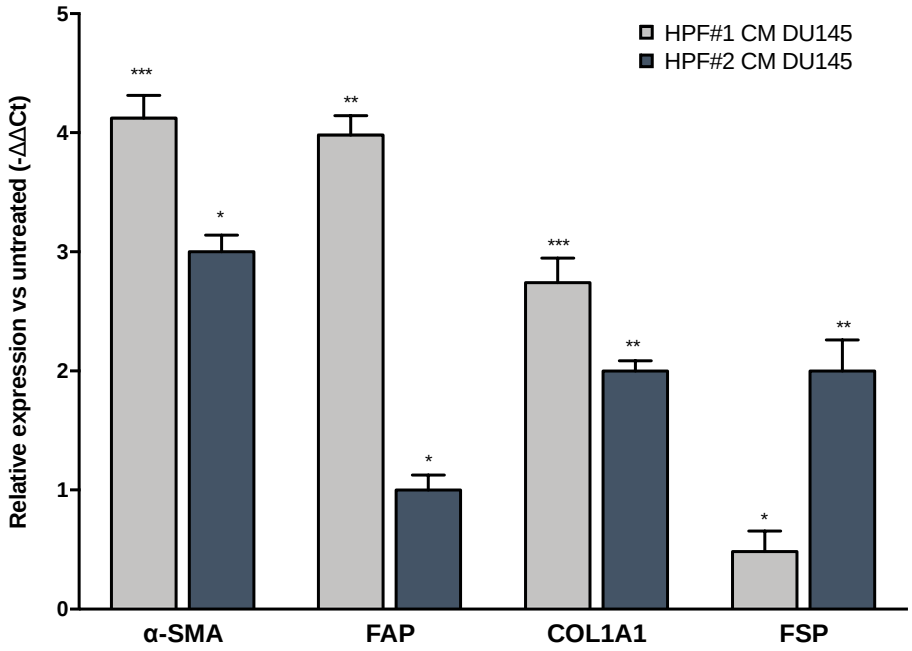

Figure 4.4. Increased activation marker expression levels in HPFs exposed to CM of DU145 cells. The expression levels of α-SMA, FAP, COL1A1 and FSP were evaluated in HPFs upon exposure to activation stimuli (Conditioned medium of DU145 cells). Data are reported as relative expression compared to untreated fibroblasts and are representative of three independent experiments The level of significance was represented as * $p<0.05$, ** $p<0.01$, *** $p<0.005$, Student's t-test.

Similarly, once assessed the activated state of treated HPFs, we investigated the expression levels of selected ion channels. Interestingly, qRT-PCR analysis revealed a marked up-regulation of CACNAH1, CACNB1, CACNB3, SCN2A, SCN2B and KCNS3 in HPFs upon exposure to CM of DU145 cells (Figure 4.5).

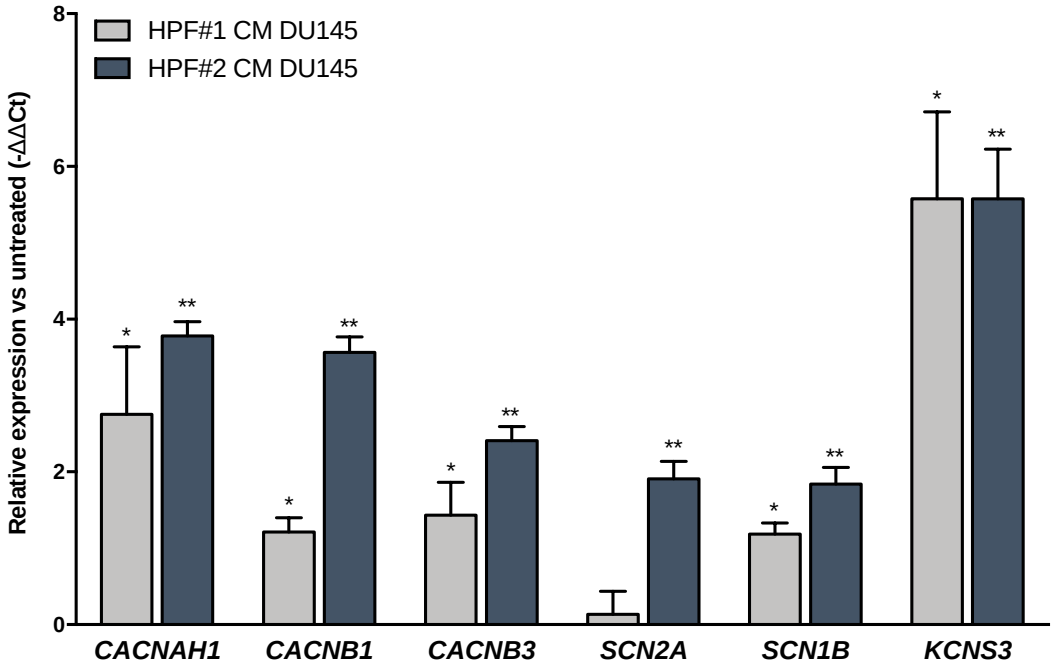

Figure 4.5. Evaluation of ion channel expression levels in in vitro activated HPFs. The expression levels of CACNAH1, CACNB1, CACNB3, SCN2A, SCN1B and KCNS3 were evaluated in HPFs upon exposure to activation stimuli (conditioned medium of DU145 cells). Data are reported as relative expression compared to untreated fibroblasts and are representative of three independent experiments. The level of significance was represented as * $p<0.05$, ** $p<0.01$, *** $p<0.005$, Student's t-test.

These results indicated that the activation state of fibroblasts, assessed by the up-modulation of specific fibroblasts activation markers, was associated with the concomitant up-modulation of cation channels. This evidence suggests that ion channels were actively involved in fibroblast activation and their up-modulation could represent a relevant step within the complex fibroblast activation process during tumourigenesis.

4.2. Evaluation of antiarrhythmic effects of CAF activated state

4.2.1. *Antiarrhythmic treatment of CAFs (experimental conditions)*

Once validated the up-regulation of cation channels in CAFs and their involvement in fibroblasts phenoconversion from an inactivated to an activated state, we sub-sequentially set up dose-response experiment in order to identify sub-toxic antiarrhythmic concentrations for treating CAFs. Following this strategy, we identified a panel of four antiarrhythmic drugs able to inhibit the activity of those cation channels that we found up-regulated in CAFs (Table 4.1).

UP-REGULATED GENE	CATION	ANTIARRHYTHMIC DRUG
CACNA1H CACNB1 CACNB2 CACNB3	Ca^{2+}	• Nifedipine • Verapamil
KCNS3 KCNH2 KCNQ2	K^{+}	• Amiodarone
SCN2A SCN1B	Na^{+}	•Flecainide

Table 4.2. List of ion channels up-modulated in CAFs and antiarrhythmic drugs able to inhibit the corresponding channel activity.

Specifically, we performed all the experiments by using the following antiarrhythmics: amiodarone, as a potassium channel inhibitor (against KCNS3,

KCNH2 and KCNQ2); verapamil and nifedipine to block calcium channels (CACNA1H and CACNB1-3); and flecainide to counteract the activity of sodium channels (SCN2A and SCN1B).

Initially, we tested different doses of each drug to identify the range of concentration appropriate to treat CAFs, without impact on cells viability. In details, we exposed CAFs to antiarrhythmics for 72 hours, with concentrations ranging from 0.1 µM to 5.0 µM. MTS assay results revealed that antiarrhythmics did not display major cytotoxic effects on a set of two different CAFs (CAF#1 and CAF#2) isolated from clinical samples (Figure 4.6). For this reason, we arbitrarily selected the sub-toxic concentration of 1 µM for each drug to perform all the experiments aimed at studying the effects of antiarrhythmics of CAFs activated state.

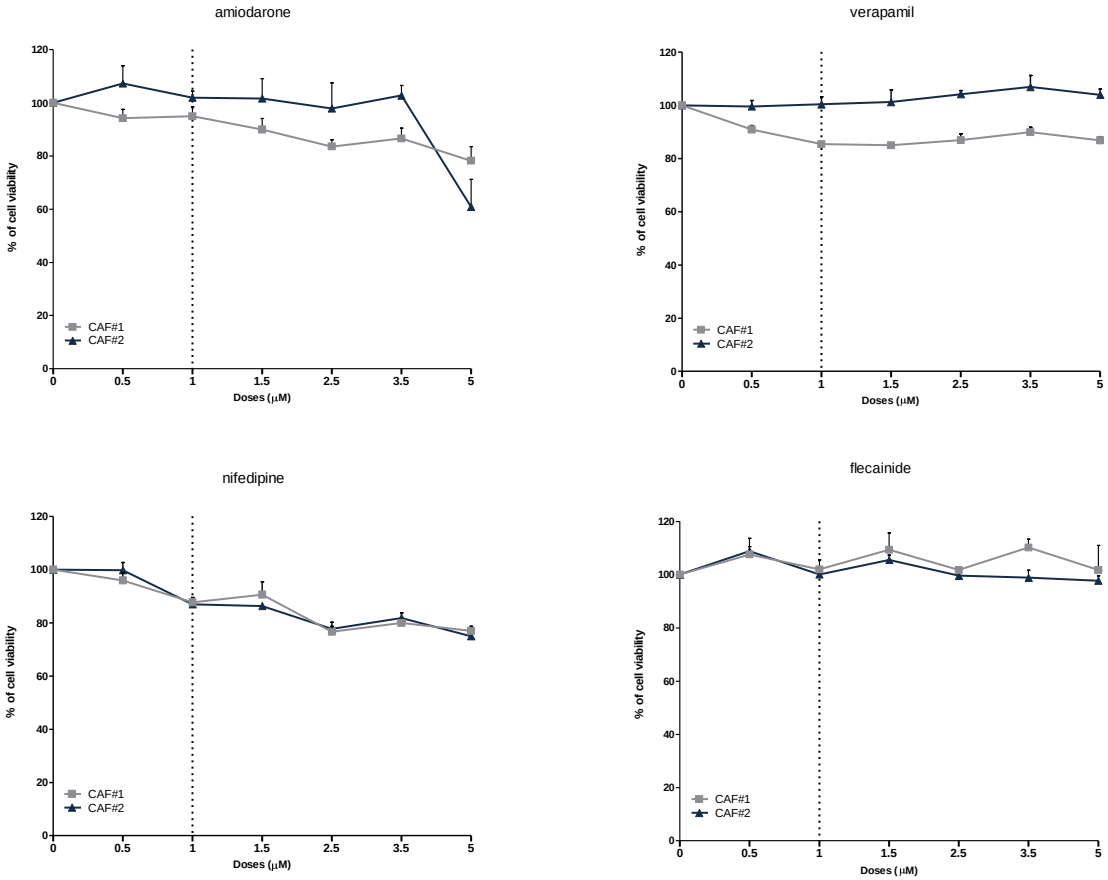

Figure 4.6. Antiarrhythmic drugs cytotoxic effects on CAFs. MTS assay of two panel of prostate CAFs derived from clinical samples (CAF#1 and CAF#2) exposed to amiodarone, verapamil nifedipine or flecainide for 72 hours. The cell viability following the indicated drug doses is reported as percentage of untreated cells. Data reported are representative of three independent experiments.

4.2.2. Antiarrhythmics treatment resulted in morphological changes and partial modulation of activation markers in CAFs.

Once identified the sub-toxic antiarrhythmic concentrations suitable for treating CAFs, we performed several experiments in order to assess whether antiarrhythmics were able to counteract the activated phenotype of CAFs. As first, we evaluated the effect of antiarrhythmics on CAF morphology and activation marker levels, which

reflect the activate state of CAFs. In details, the treatment of CAFs with sub-toxic doses (1 µM) of antiarrhythmics (amiodarone, verapamil, nifedipine or flecainide) for 48 hours resulted in marked morphological changes, which was particularly evident when CAFs where exposed to 1 µM of amiodarone. Morphologically speaking, as showed in the photomicrographs, amiodarone-treated CAFs exhibit a more elongated and thin shape, compared to control (Figure 4.7).

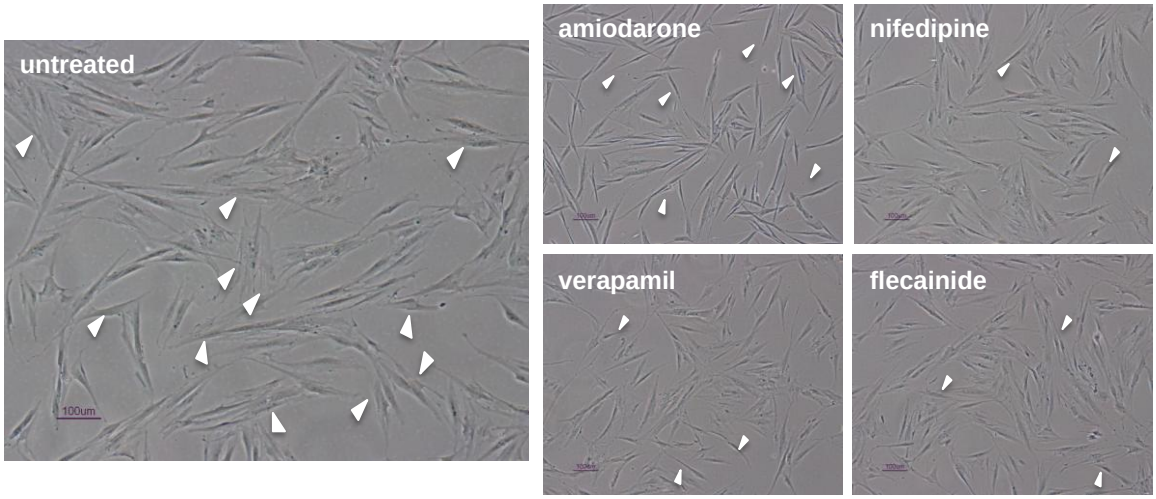

Figure 4.7. Antiarrhythmic drugs induced morphological changes in CAFs. Representative phase contrast microscopy images showing morphological changes in CAFs exposed to sub-toxic doses of antiarrhythmic drugs (scale 100 µm). White arrows highlighted flattened and enlarged cells, with visible stress fibres.

The effect of antiarrhythmic treatment of CAFs activate state was evaluated in terms of expression levels of specific activation markers. Specifically, upon the treatment of CAFs with three selected sub-toxic doses of antiarrhythmics (1 µM, 2.5 µM and 5 µM) for 48 hours, α-SMA and Col1a1 levels resulted partially decreased, which was particularly appreciable upon the treatment with amiodarone or verapamil, in a dose-dependent manner (Figure 4.8).

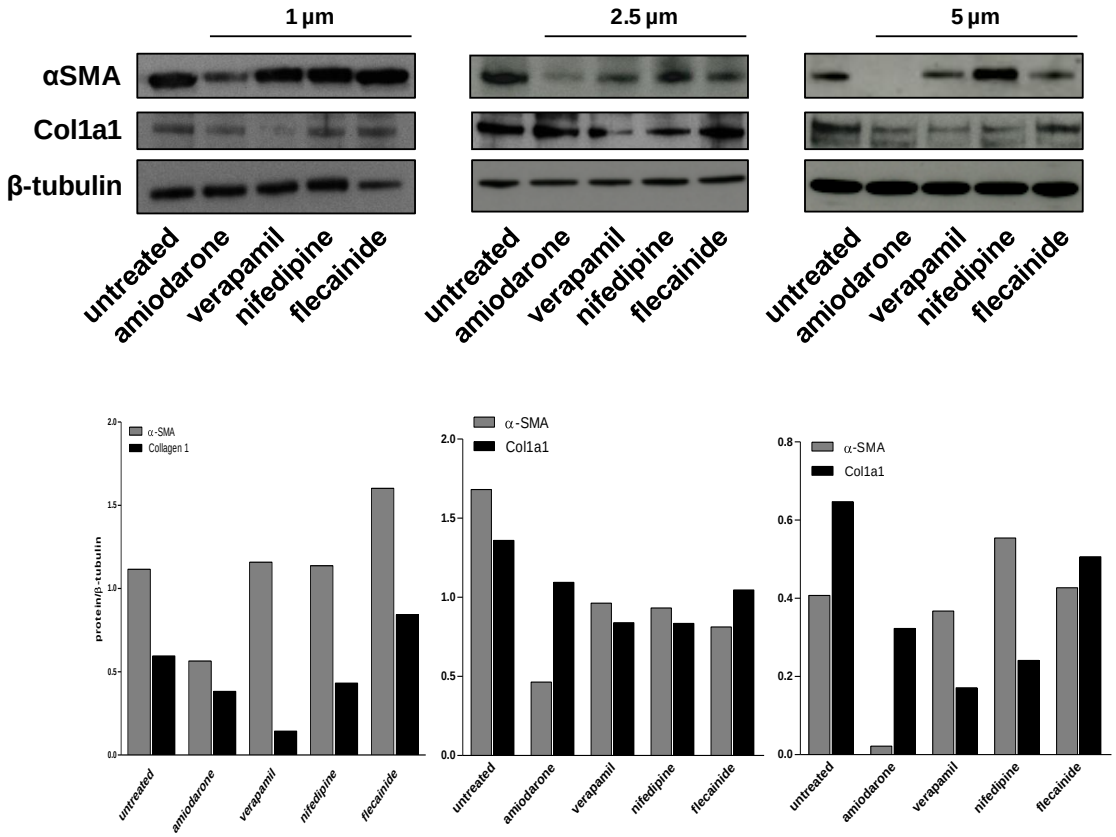

Figure 4.8. Antiarrhythmic drugs induced a partially down-modulation of specific fibroblast activation markers in a dose-dependent manner. Western blot analysis showing α-SMA and Col1a1 protein amount in CAFs treated for 48 hours with three sub-toxical doses of antiarrhythmics (1 µM, 2.5 µM and 5 µM), normalized to β-tubulin. The bar plot reports quantification of western blot. Densitometry data are reported as raw normalized values (arbitrary units) towards the loading control (β-tubulin).

Overall, the treatment of CAFs with sub-toxic doses of antiarrhythmic drugs was able to perturb fibroblasts morphology and partially reverts the activated state of CAFs, in a dose and drug-dependent manner, as indicated by the moderate down-modulation of fibroblasts activation markers, expecially upon the treatment with amiodarone or verapamil.

4.2.3. *Antiarrhythmic reduced CAF motility and FAK phosphorylation*

Considering the relevance of cell migration and extracellular matrix remodelling properties of activated fibroblasts, we evaluated the effect of antiarrhythmics on CAF migration potential by performing the traditional scratch assay. Specifically, CAFs were seeded and the monolayer of cells were wounded by manual scratching with a pipet tip, washed with PBS, photographed (0 h point) and media were replaced with serum-free-DMEM containing sub-toxic doses (1 µM) of amiodarone, verapamil, nifedipine or flecainide. Images of cell movement were captured at 24 hours. As indicated in the representative photomicrographs and in the bar plot, treated CAFs showed a significantly delayed closure of the wound than untreated cells, suggesting that antiarrhythmics decreased CAFs migration potential (Figure 4.9).

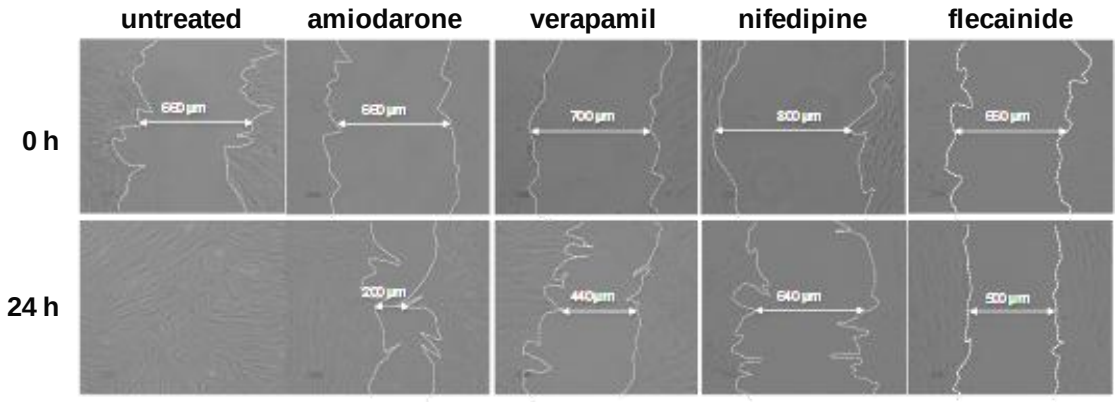

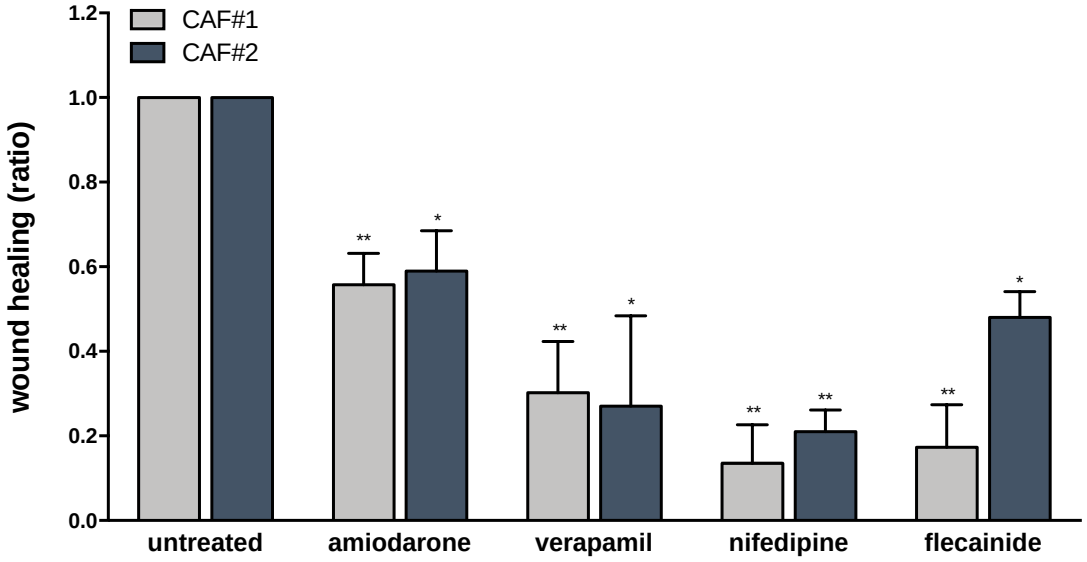

Figure 4.9. Antiarrhythmics impair CAF migratory capability. (*Upper panel*) Representative phase contrast microscopy images showing migration rate of CAFs exposed to sub-toxic doses of antiarrhythmic drugs (scale 100 µm). The dotted lines define the areas lacking cells. (*Lower panel*) Bar plots showing the wound-healing rate of CAFs assessed by scratch assay. Data are reported as wound healing ratio at 24 h compared to 0 h point and are representative of three independent experiments. The level of significance was represented as * $p<0.05$, ** $p<0.01$, Student's t-test.

Moreover, in accordance with the observed reduced migration rate, FAK signalling was found down-modulated in CAFs exposed to antiarrhythmic drugs. Immunofluorescence staining for p-FAK revealed less reactivity and a marked delocalization of the protein from the focal contacts, especially when CAFs were treated with verapamil (Figure 4.10). Similarly, as showed in the immunoblotting, the treatment with antiarrhythmics induced a marked reduction of p-FAK fraction protein levels (Figure 4.10). Overall, this experimental evidence further suggests that antiarrhythmic cation channel inhibition could effectively hinder CAF motility.

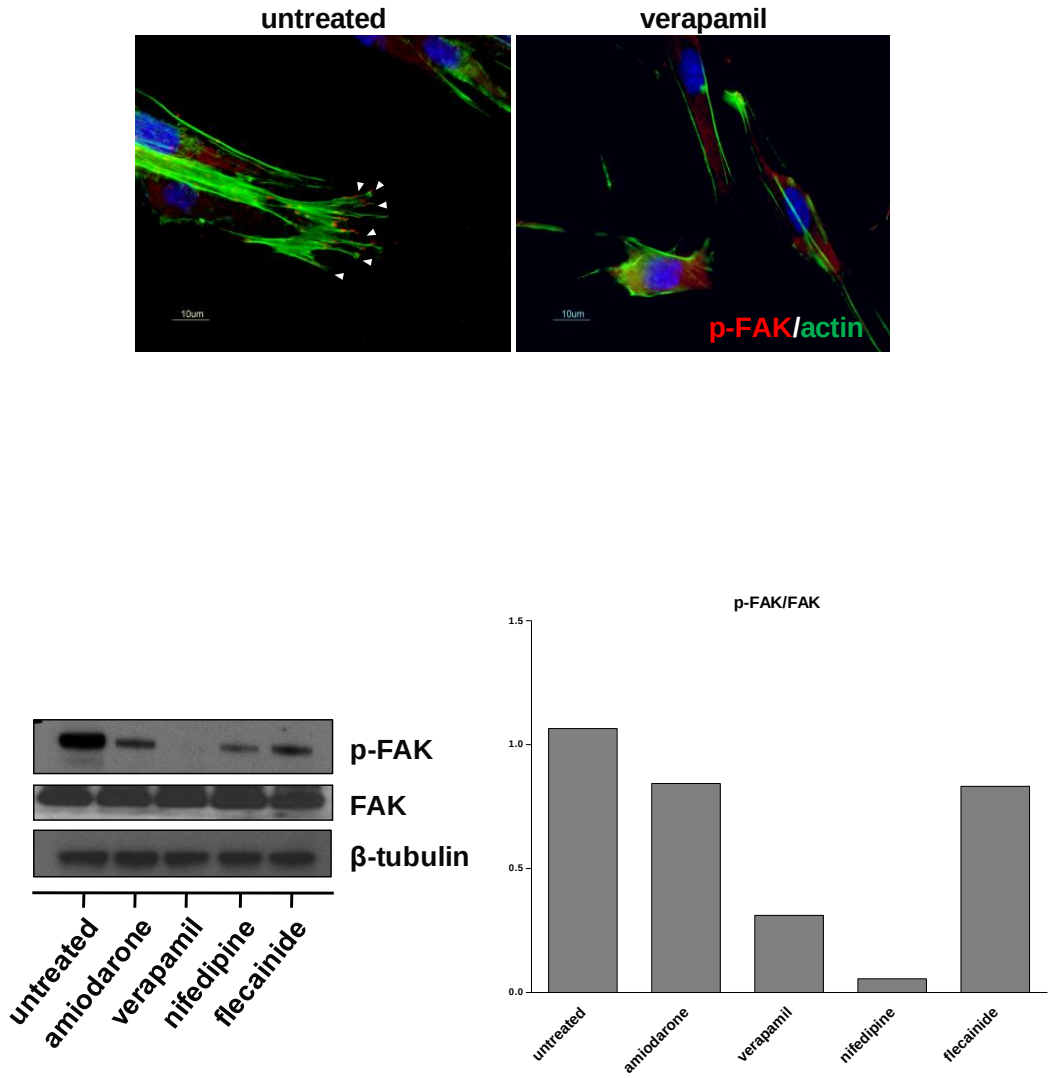

Figure 4.10. Antiarrhythmics hinder focal adhesion formation. (*Upper panel*) Representative immunofluorescence images showing reduction of p-FAK staining (red) and delocalization from cell membrane in verapamil-treated CAFs. Actin (green) was used to stain focal adhesion and DAPI (blue) to stain nuclei (scale bar 10 µm). (*Lower panel left*) Western blotting analysis showing p-FAK protein amount in antiarrhythmic treated CAFs. FAK and β-tubulin was used as loading control, respectively. (*Lower panel right*) The bar plot reports quantification of western blot. Densitometry data are reported as raw normalized values (arbitrary units) towards the loading control (β-tubulin).

4.2.4. Evaluation of CAFs capability to remodel the extracellular matrix

Consistent with their role in the tumour microenvironment, CAF pro-tumourigenic activity is also related to their capability to remodel the extracellular matrix (ECM) and create a desmoplastic environment, thus promoting tumour dissemination [118]. Considering this setting, we tested whether CAF ion channels inhibition, by using antiarrhythmics, would result in a reduction of ECM remodelling potential of CAFs. ECM remodelling ability could be recapitulated by cell capability to stress a 3D collagen gel, in which cells were seeded and then treated with antiarrhythmics. Cells that were characterised by a high remodelling capability display a greater gel contraction rate. Antiarrhythmic treatment of CAFs determined a significant reduction of their ability to cause 3D collagen gel stress compared to untreated CAFs, especially upon treatment with sub-toxic doses of verapamil, nifedipine or flecainide. Considering that this is a crucial feature of CAFs, this result suggests the involvement on ion channels in CAF ECM remodelling and indicated the possibility to revert such potential by using antiarrhythmics (Figure 4.11).

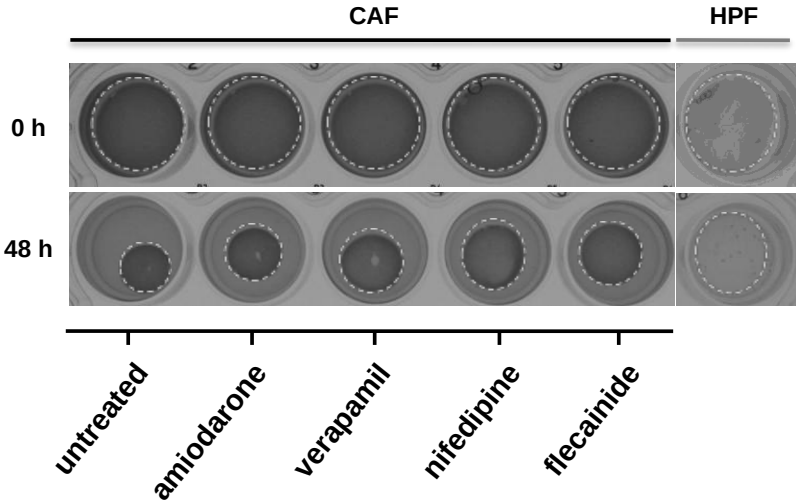

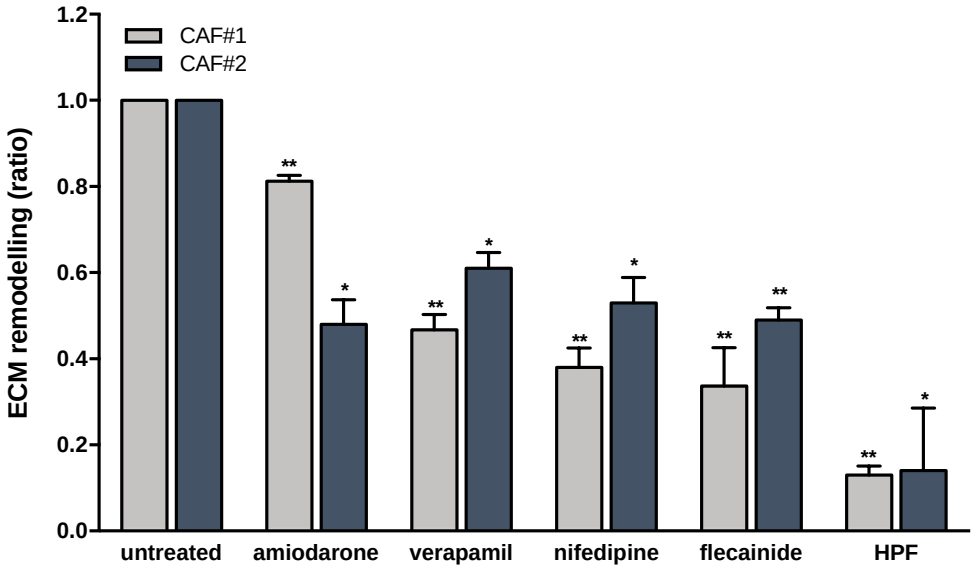

Figure 4. 11. Antiarrhythmics reduce CAF potential to remodel ECM. (*Upper panel*) Representative images showing 3D collagen gel rate remodelling of CAFs exposed to sub-toxic doses of antiarrhythmic drugs. (*Lower panel*) Bar plots showing the ECM remodelling ratio of treated CAFs assessed by 3D collagen gel assay. Data are reported as ECM remodelling ratio at 48 h compared to 0 h point and are representative of three independent experiments The level of significance was represented as * $p<0.05$, ** $p<0.01$, Student's t-test.

4.2.5. Antiarrhythmic effect on CAF gene expression profile.

With the aim of studying the effects of antiarrhythmics on CAF transcriptome, gene expression profiling was conducted. For this experiment, we sought to focus on those antiarrhythmics that showed, in our hands, a grater capability to impact on ECM remodelling process mediated by CAFs (Figure 4.11), and a prominent reduction of CAF migration potential (Figure 4.9). Specifically, a panel of three different CAFs were exposed to nifedipine and flecainide for 48 hours. Upon the treatment, the total RNA was isolated and analysed using Clariom S array. For comparative purposes, we included matched HPFs isolated from the same patients.

As shown in figure 4.12, the principal component analysis (PCA) identified three different clusters of samples, separated along the first principal component (PC1). Specifically, we observed a cluster composed of CAFs and a completely distinct cluster characterized by HPFs. More interestingly, although close to the CAF cluster, a third group represented by CAFs treated with antiarrhythmics were identified. In addition, the different shaping schemes applied to the samples highlighted that the cluster separation was not associated with the patient. These findings further suggest that antiarrhythmics were able to perturb CAFs activated phenotype by inducing gene expression changes that make them resemble to HPFs.

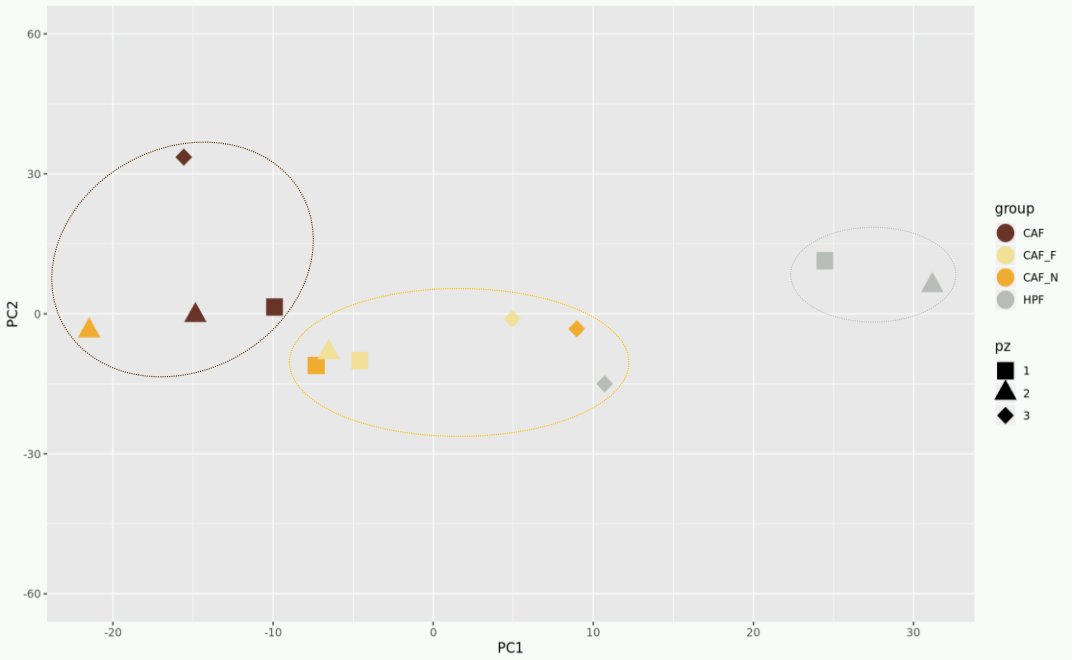

Figure 4. 12. PCA plot of gene expression data from antiarrhythmics-treated CAFs. PCA was performed on gene expression data from a panel of three CAF primary cultures treated or not with nifedipine or flecainide and matched HPFs (colour code: HPFs grey, CAFs brown, CAFs treated with nifedipine-yellow-CAF_N, CAFs treated with flecainide orange-CAF_F). Batch effects were removed by applying combat algorithm. Samples were plotted along the first two principal components (PCs). Different colouring schemes revealed that clustering was associated with different activated fibroblast state.

In addition, in order to compare gene expression changes induced by antiarrhythmics and highlight commonalities and differences among fibroblast profiles, we performed a single sample gene set enriched analysis (ssGSEA) by using Hallmark collection from The Molecular Signatures Database (MSigDB) (https://www.gsea-msigdb.org/gsea/msigdb/collections.jsp). The Hallmark collection summarizes and represents specific well-defined and relevant biological states or processes, and the major molecular mechanisms of cells. These gene sets were generated by a computational strategy, based on the identification of genes shared by other collections but that show a coherent behaviour (116). In line with this evidence, we selected Hallmarks since they reduce noise and redundancy, providing a more refined and concise inputs of the molecular mechanisms implicated in fibroblasts activation profile.

As shown in figure 4.13, the unsupervised clustering grouped 2 major categories defined as “normal-like” and “tumour-like” groups. Specifically, the “normal-like” cluster is mainly represented by HPFs and the “tumour-like” is composed of CAF samples. Surprisingly, the antiarrhythmic treated-CAF samples are spread across the 2 groups, independently from the patient origin and treatment, thus indicating that the treatments are able to perturb CAFs expression profile and in part resembling of HPFs (Figure 4.13).

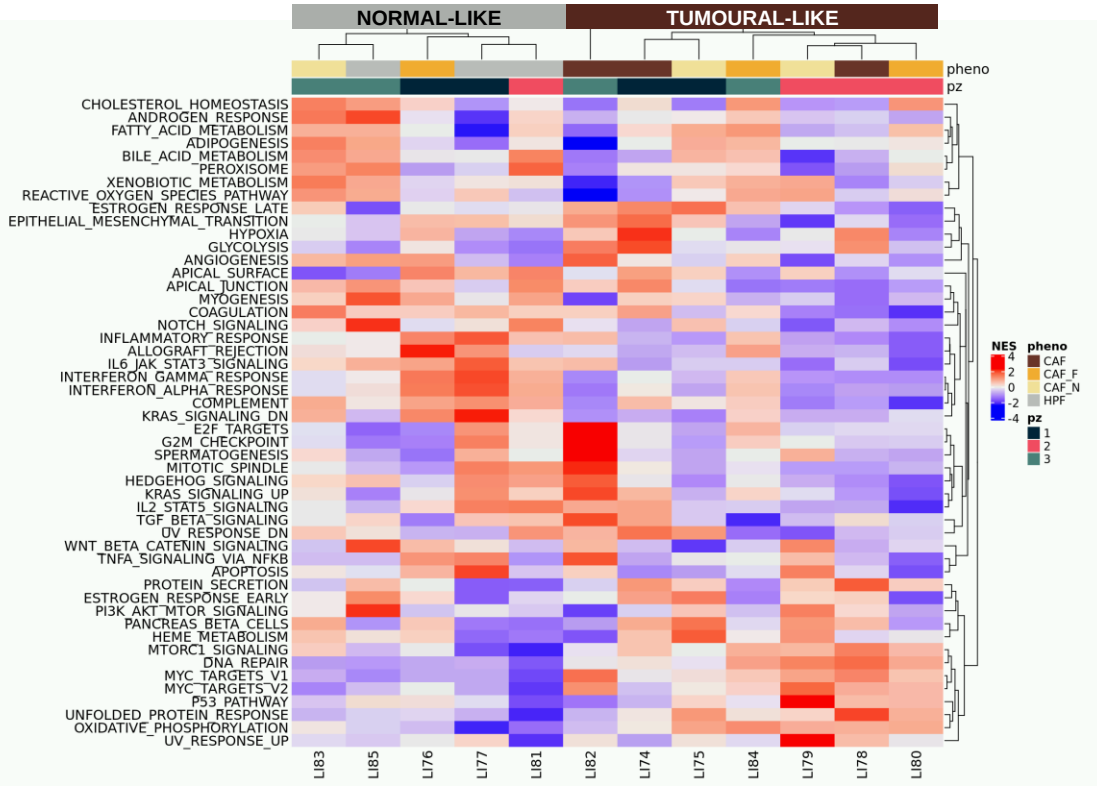

Figure 4.13. Heatmap of ssGSEA on hallmark canonical gene sets. The unsupervised hierarchical clustering of columns grouped HPFs, antiarrhythmic-treated CAFs, and CAFs in 2 major categories based on their differential expression levels of genes belonged to hallmark collection. Each row represents a gene set, while each column represents a different biological sample. The first line annotation indicates fibroblasts phenotype (colour code: HPFs grey, CAFs brown, CAFs treated with nifedipine-yellow-CAF_N, CAFs treated with flecainide orange-CAF_F). The second line depicts patient origin (colour code: patient 1 black, patient 2 red, patient 3 green). Red-white-blue colormap is used to visualize the magnitude of the normalized enrichment score (NES) value of the specific signature in the specific sample, where red is up-regulation and blue is down-regulation.

Moreover, a classical GSEA approach was performed on the same collection. Only significant (FDR threshold < 0.05) comparisons with the same magnitude among all the three contrasts were considered. To share light on the genes involved in the signatures of interest, the intersection of the leading edges of each single contrast was considered, retaining only the common genes.

The GSEA revealed interesting commonalities between HPFs and treated CAFs compared to CAFs that belong to the normal-like cluster. Especially regarding the down-modulation of genes implicated in epithelial to mesenchymal transition, glycolysis, hypoxia, and protein secretion pathways (Figure 4.14). Contrarily, CAFs showed an induction of the abovementioned gene sets, which completely reflect their role in the tumour microenvironment. Overall, the expression landscape of treated CAFs indicated the shift of specific pathways, suggesting that nifedipine and flecainide were able to affect CAFs phenotype by inducing the modulation of crucial pathways involved in their activation.

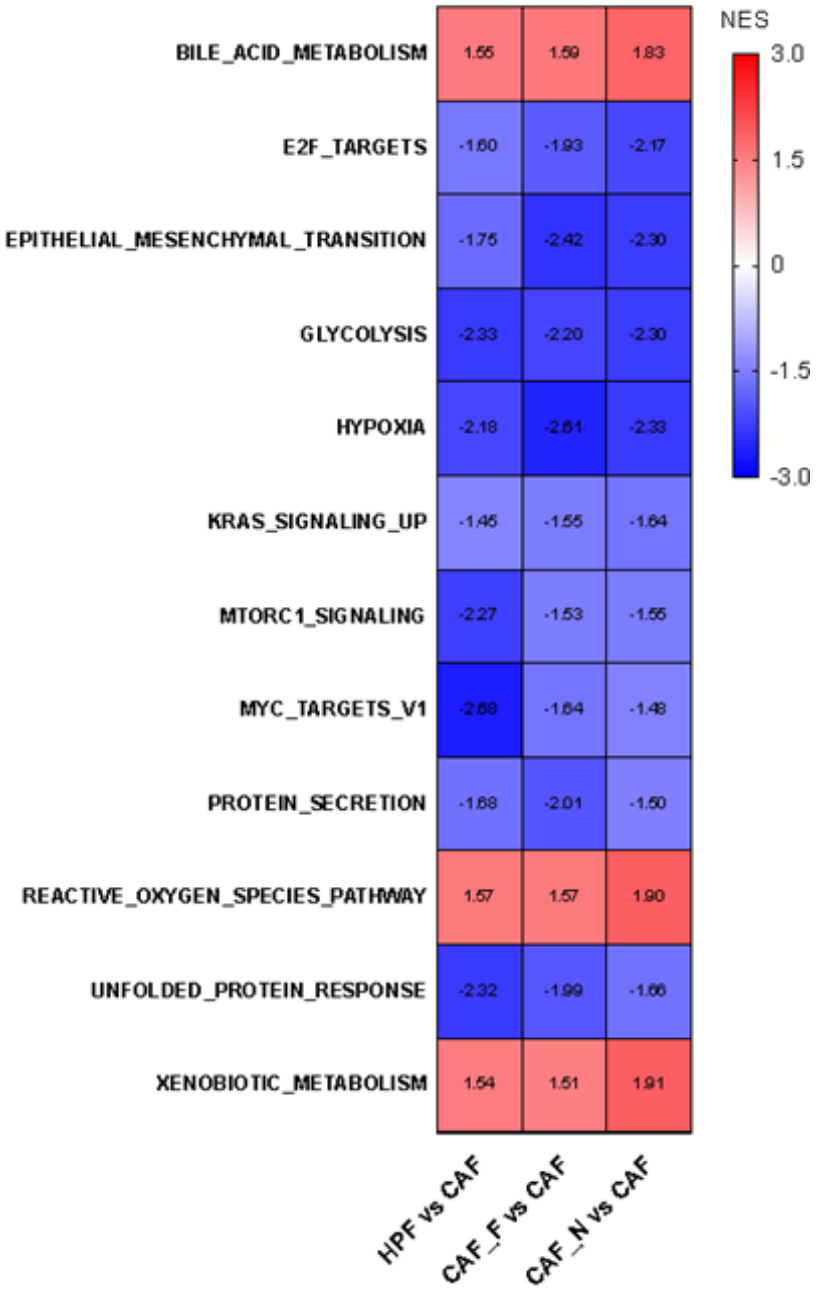

Figure 4.14. GSEA highlighted crucial communities between antiarrhythmic-treated CAFs and HPFs. Heatmap representing gene sets from hallmark collection with significant modulation. The normalized enrichment score (NES) was used.

4.3. Evaluation of antiarrhythmic drug effect on CAF-PCa cell interplay

In order to investigate whether the inhibition of CAF cation channel activity could affect CAF pro-tumoural boost, co-culture approaches for studying the *in vitro* interaction between CAFs and PCa cells were carried out. In this regard, indirect co-culture experiments, which represent the relevant *in vitro* techniques to study paracrine interactions, were set up to test the effects of antiarrhythmics treatment on CAF-PCa cell interplay. Specifically, conditioned media (CM) of antiarrhythmics-treated CAFs were used to culture PCa cells, and the effects on PCa cells were evaluated. CAFs were initially treated with sub-toxic doses of antiarrhythmics (amiodarone, verapamil, nifedipine or flecainide) for 48 hours, then culture media were switched to fresh serum-free medium and treated CAFs were incubated for additional 24 hours. Then CM were harvested, clarified by centrifugation, and used freshly to culture PCa cell lines (DU145 or PC-3). CAF-CM effects were evaluated in terms of cell growth and prostate cancer cell plasticity (Figure 4.15).

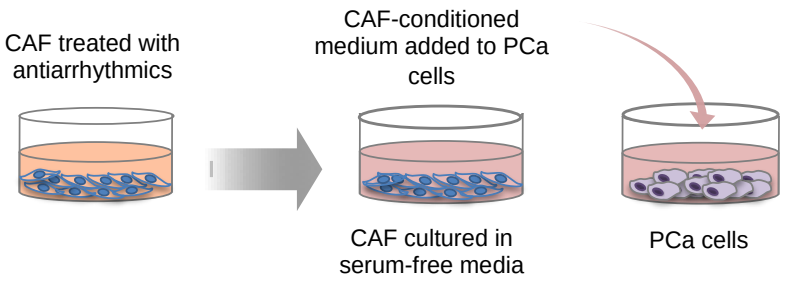

Figure 4.15. Schematic representation of CAF-PCa indirect co-culture system based on the use of conditioned medium.

4.3.1. *CM from CAFs treated with antiarrhythmics affect PCa cell growth and cell cycle distribution*

By using a indirect co-culture approach, PCa cells (DU145 and PC-3) were exposed to CM of CAFs pre-treated or not with sub-toxic doses of antiarrhythmics and cultured until 72 hours. The number of cells was evaluated by cell counting. As showed in figure 4.16, the CM of CAFs displayed a slightly promoting effect on PCa cell growth compared to control, which was more appreciable in DU145 than PC-3 cells. In contrast, CM from HPFs induced a marked inhibition of PCa cell growth in both cell lines. Surprisingly, the treatment of CAFs with antiarrhythmics reduced their capability to sustain PCa proliferation and let them acquire a more growth-inhibitory phenotype, thus recapitulating the trend observed with CM of HPFs.

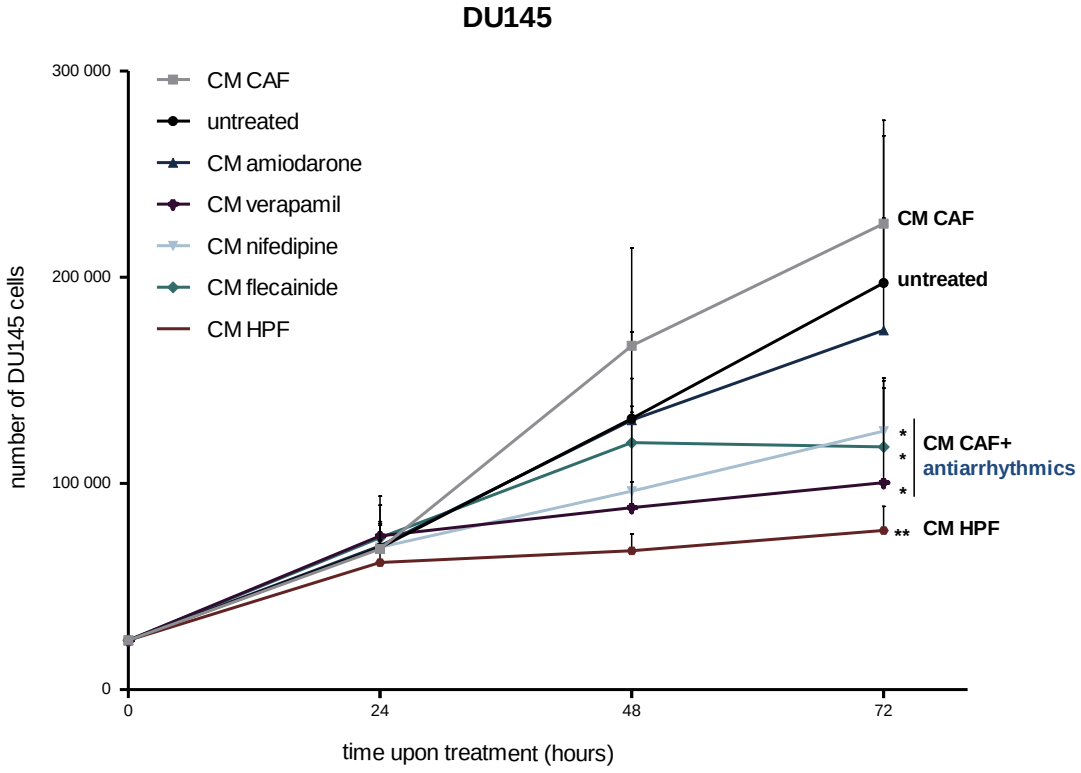

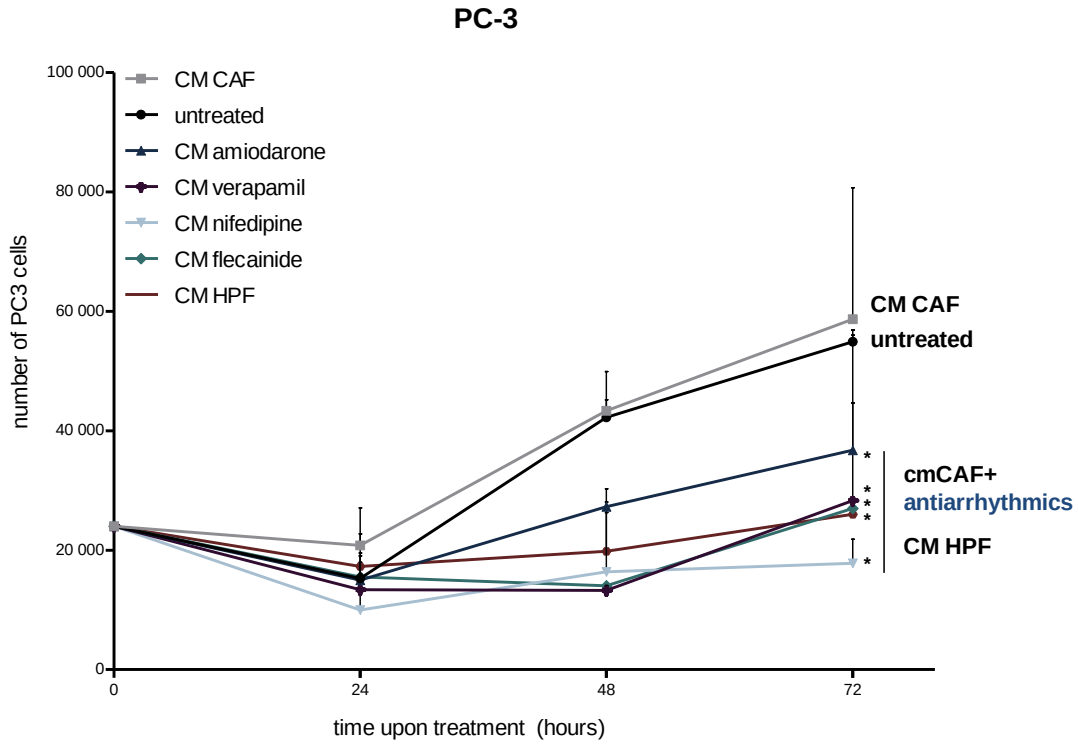

Figure 4.16. Antiarrhythmics-treated CAFs recapitulate HPFs capability to suppress PCa cell growth. Cell growth evaluation of DU145 (*upper panel*) and PC-3 (*lower panel*) cells cultured with CM of CAFs treated or not with antiarrhythmics, or CM of HPF at different time points (24, 48, 72 hours). Data are representative of three independent experiments. The level of significance was represented as * $p<0.05$, ** $p<0.01$, Student's t test.

In addition, a cell cycle analysis has been performed in order to assess whether CM of treated CAFs could affect PCa cell cycle phase distribution. Specifically, DU145 cells were exposed to CM of CAFs pre-treated or not with sub-toxic doses of antiarrhythmics and cultured until 72 hours. As shown in figure 4.17, DU145 cells exposed to CM of antiarrhythmic treated-CAFs or CM of HPFs displayed a significantly higher percentage of cells in the subG1/G1 phase compared to untreated cells, with a corresponding reduction

in the percentage of cells in S phase. In contrast, the treatment with CM of CAFs resulted increase the percentage of cells in S phase.

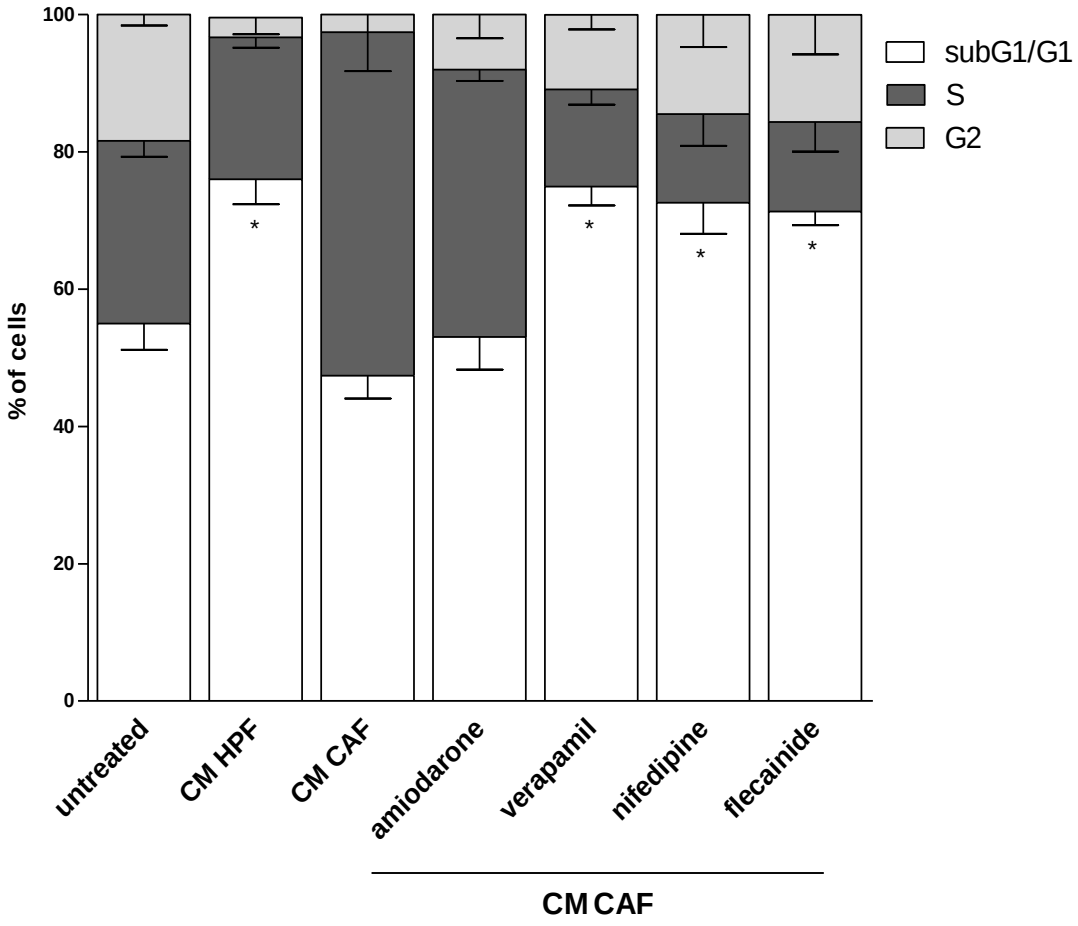

Figure 4. 17. Antiarrhythmics-treated CAFs recapitulate HPFs capability to perturb DU145 cell cycle phase distribution. Cell cycle phase distribution of DU145 cells cultured with CM of CAFs treated or not with antiarrhythmics, or CM of HPF at 72 hours until treatment. Data are representative of two independent experiments. The level of significance was represented as * $p<0.05$, Student's t test with respect to untreated cells.

4.3.2. *DU145 cells exposed to CM of antiarrhythmics-treated CAFs displayed a more epithelial-like phenotype*

To further investigate the effect of antiarrhythmics on CAF-PCa cell interplay, we evaluated CAF ability to remodel DU145 cell plasticity. Specifically, upon exposure to CM of CAFs treated or not with antiarrhythmics, the number of DU145 cells displaying a polygonal shape and cluster organization or a elongated morphology/spindle-like shape was assessed. Morphologically speaking, photomicrographs and bar plot quantification showed an increase of individual spreading/elongated cells upon exposure of DU145 cells to CM of CAFs, suggesting the acquisition of a more mesenchymal-like phenotype. In contrast, the number of spreading DU145 cells was significantly reduced upon culturing with antiarrhythmics-treated CAF CM, indicating that antiarrhythmics were able to reduce CAF-induced DU145 cell plasticity boost. These preliminary observations suggest that antiarrhythmic treatment could affect the ability of CAFs to promote the epithelial to mesenchymal shift of PCa cells (Figure 4.18).

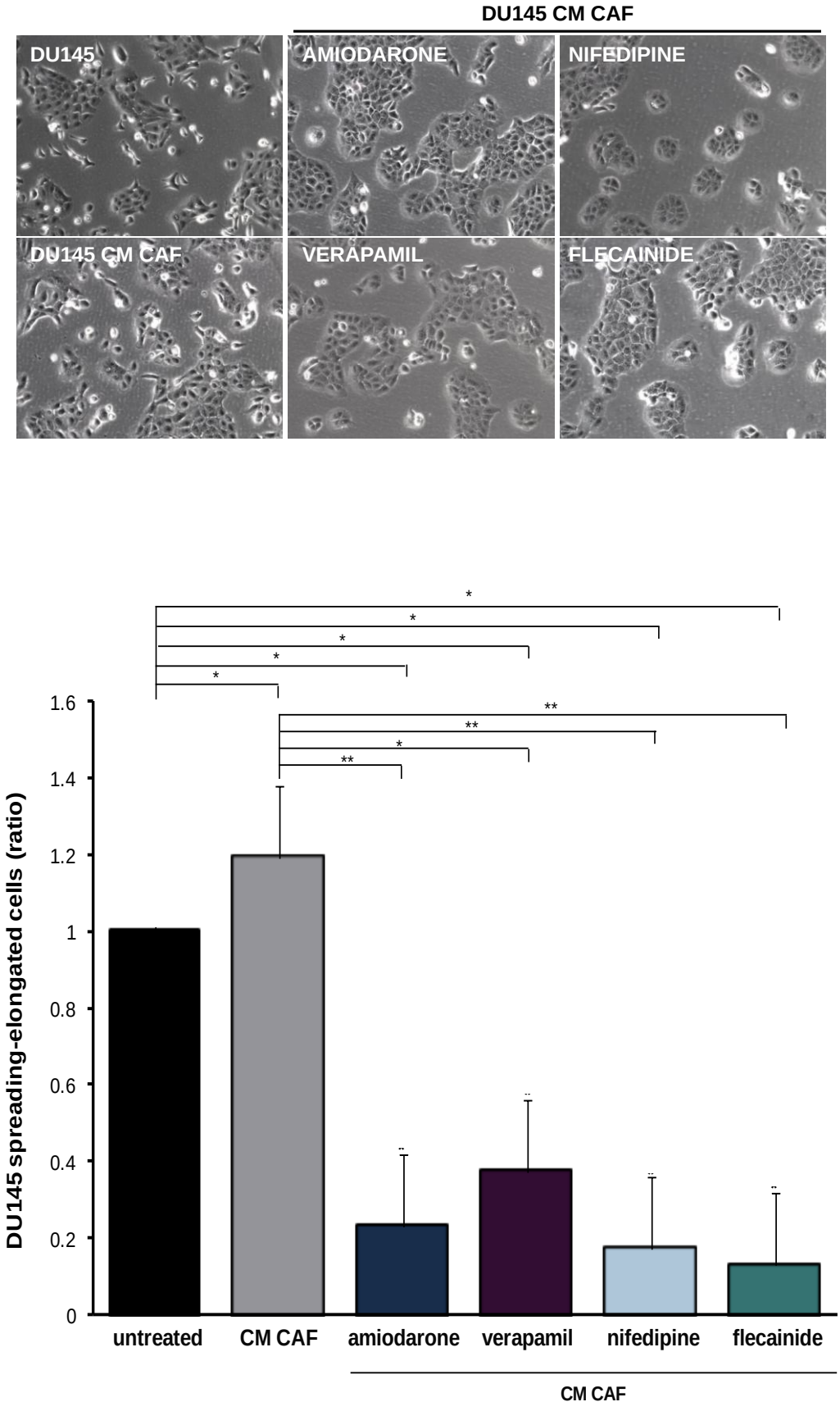

Figure 4. 18. Antiarrhythmics reduce CAF capability to induce plasticity in DU145 cells. (*Upper panel*) Representative phase contrast microscopy

images showing morphological changes of DU145 cells cultured with CM CAFs treated or not with antiarrhythmics (scale bar 100 μm). (*Lower panel*) Bar plot indicating the number of DU145 cells with a spreading-elongated cell morphology obtained by counting five fields for each experimental condition and compared to untreated. Data are representative of three independent experiments. The level of significance was represented as * $p<0.05$, Student's t-test.

4.3.3. *Antiarrhythmics reduce CAF-induced EMT in PCa cells*

It has been largely reported that CAFs are able to enhance malignancy features of PCa cells, promoting the switch from an epithelial-like phenotype to a more mesenchymal one [119]. In order to verify whether antiarrhythmics treatment of CAFs was able to revert such pro-tumoural effects, we performed qRT-PCR evaluation of different EMT-related markers, such as *CHD1* (E-cadherin), *CTNNB1* (β-catenin), *VIMENTIN* and *SNAI1* (Snail) in DU145 and PC3 cells cultured with CM of CAFs (CM-CAF), CM of CAFs treated with antiarrhythmics (CM antiarrhythmic-CAF) or CM of HPFs (CM-HPFs). Accordingly, we observed that CM-CAF was able to down-modulate the epithelial markers *CDH1 and CTNNB1* in PCa cells, inducing a more mesenchymal phenotype as assessed by the up-modulation of *VIMENTIN* and *SNAI1*. The treatment of CAFs with antiarrhythmics partially reverted such EMT-promoting effect on PCa cells. Specifically, qRT-PCR analysis showed that the CM from antiarrhythmic-CAFs was less able to down-modulate *CDH1* in DU145 and PC-3 cells, and in some cases it even increased it, partially recapitulating the effect observed with the CM-HPFs, which is recognised has tumour-suppressive features [120]. More interestingly, western blot analysis on DU145 cells confirmed the down-modulation of E-cadherin (CDH1) and β-catenin (CTNNB1), and up-modulation

Vimentin and Snail (SNAIL1) upon exposure to the different aforementioned stimuli (Figure 4.19),. These results suggest that CM from antiarrhythmic-treated CAFs on DU145 and PC-3 cells could impact on cell plasticity, by modulating EMT.

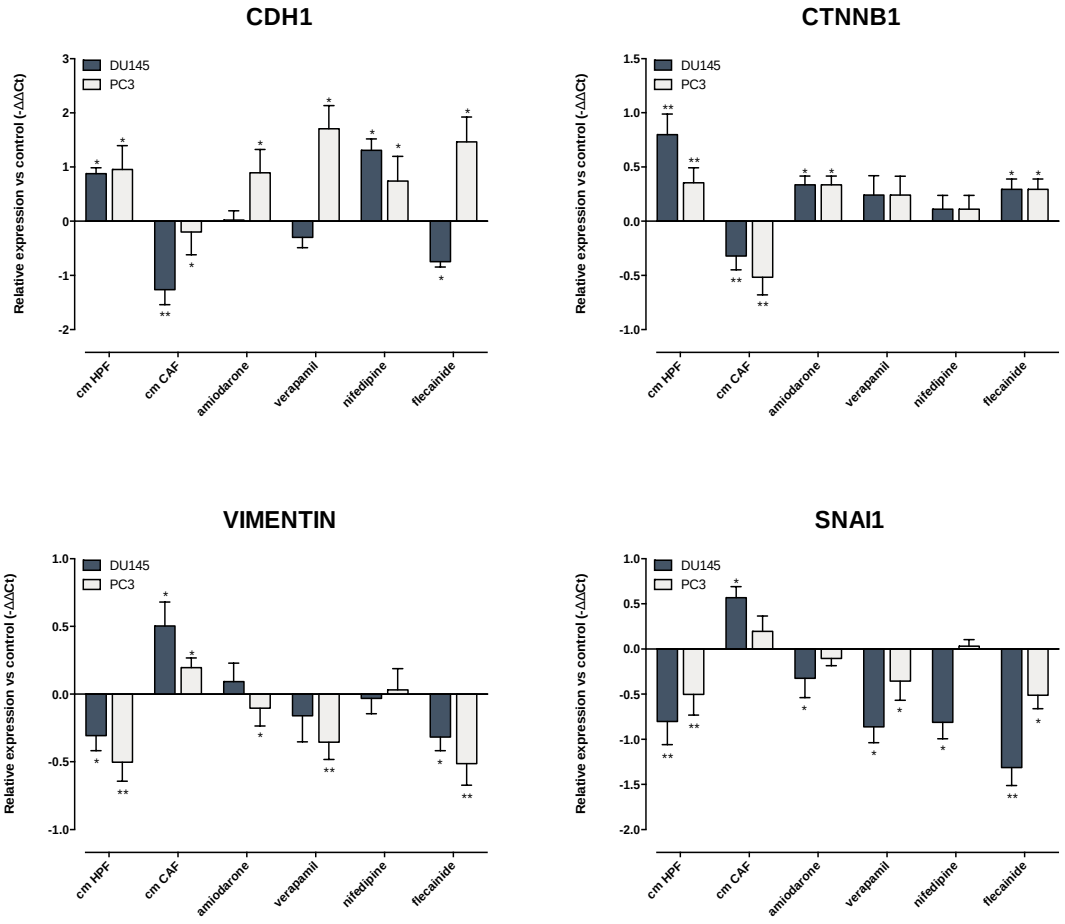

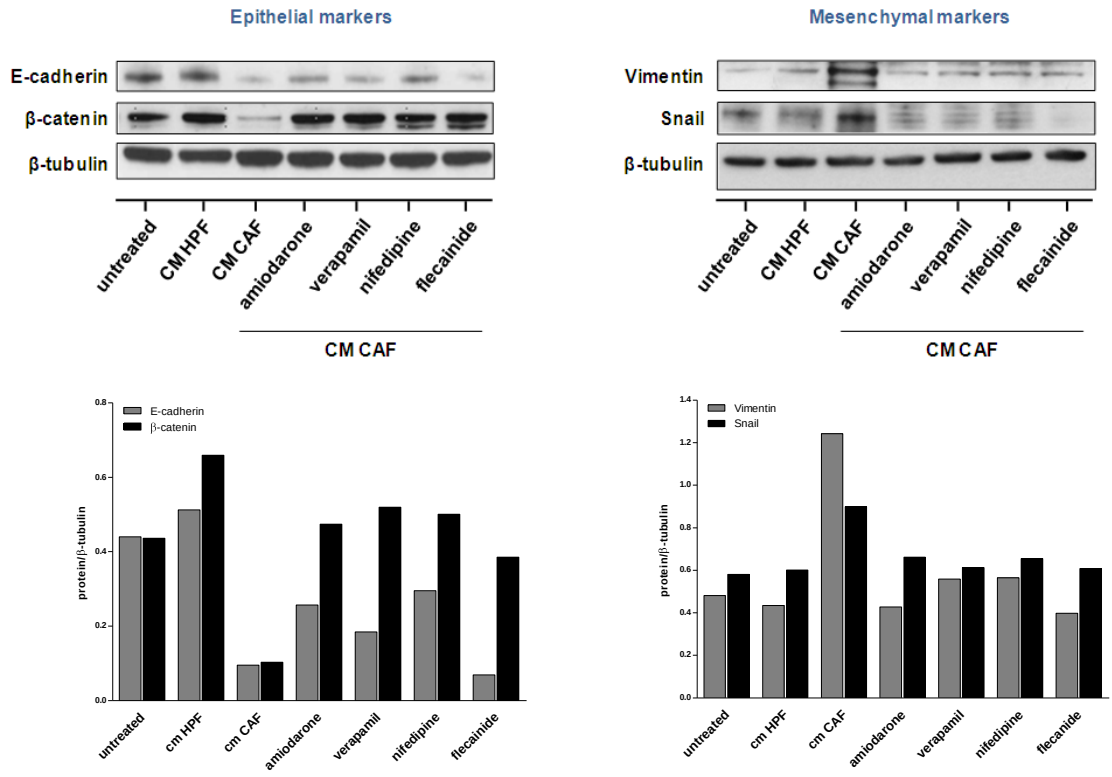

Figure 4. 19. Antiarrhythmics impair CAF-mediated EMT in PCa cells. (*Upper panel*) Expression levels of the epithelial markers (*CDH1 and CTNNB1), and mesenchymal markers (VIMENTIN and SNAI)* assessed by qRT-PCR in DU145 and PC-3 cells exposed to CM of HPF or CM of CAF exposed on not to antiarrhythmics. Data are reported as relative expression with respect to untreated cells and are representative of three independent experiments . (*Middle panel*) Western blotting analysis showing E-cadherin, β-catenin, Vimentin and Snail protein amount in DU145 cells exposed to CM of HPF or CM of CAF exposed on not to antiarrhythmics, normalized to β-tubulin. (*Lower panel*) The bar plot reports quantification of western blots. Densitometry data are reported as raw normalized values (arbitrary units) towards the loading control (β-tubulin). The level of significance was represented as *p<0.05, **p<0.01, Student's test.

4.3.4. *Antiarrhythmics affect CAF pro-migratory boost on DU145 cells*

Considering the relevance of migratory capability in the dissemination process, and knowing that such relevant pro-metastatic feature is strongly induced by CAFs in the

PCa context [120], we evaluated whether antiarrhythmics treatment could revert CAF-promoted migratory boost on DU145 cells. For this sub-set of experiments, we sought to focus on those antiarrhythmics that showed, in our hands, a greater capability to impact on ECM remodelling process mediated by CAFs (Figure 4.11), and a prominent reduction of PCa cell growth and EMT modulation in CM co-culture experiments (Figure 4.16 and 4.19). For this purpose, the capability of DU14 to migrate and recover a wound were tested using a common scratch assay. Specifically, DU145 cells were seeded, and the monolayer of cells were wounded by manual scratching with a pipet tip, washed with PBS, photographed (0 h point) and media were replaced with CM of HPFs or CM of CAFs treated or not with nifedipine or flecainide. Images of cell movement were captured at 24 hours. As indicated in the representative photomicrographs and bar graph, DU145 cells exposed to CM of CAFs displayed a high capacity to close the wound. Conversely, the CM of antiarrhythmic treated CAFs significantly reduced DU145 cell effectiveness to close the wound, showing a wound-healing ratio that partially recapitulated CM of HPFs effect, which is known to acts as a tumour suppressor. These findings suggest that nifedipine and flecainide decreased CAF mediated pro-migratory boost on DU145 cells, thus confirming the repressor effects on CAF protumoural spur (Figure 4.20).

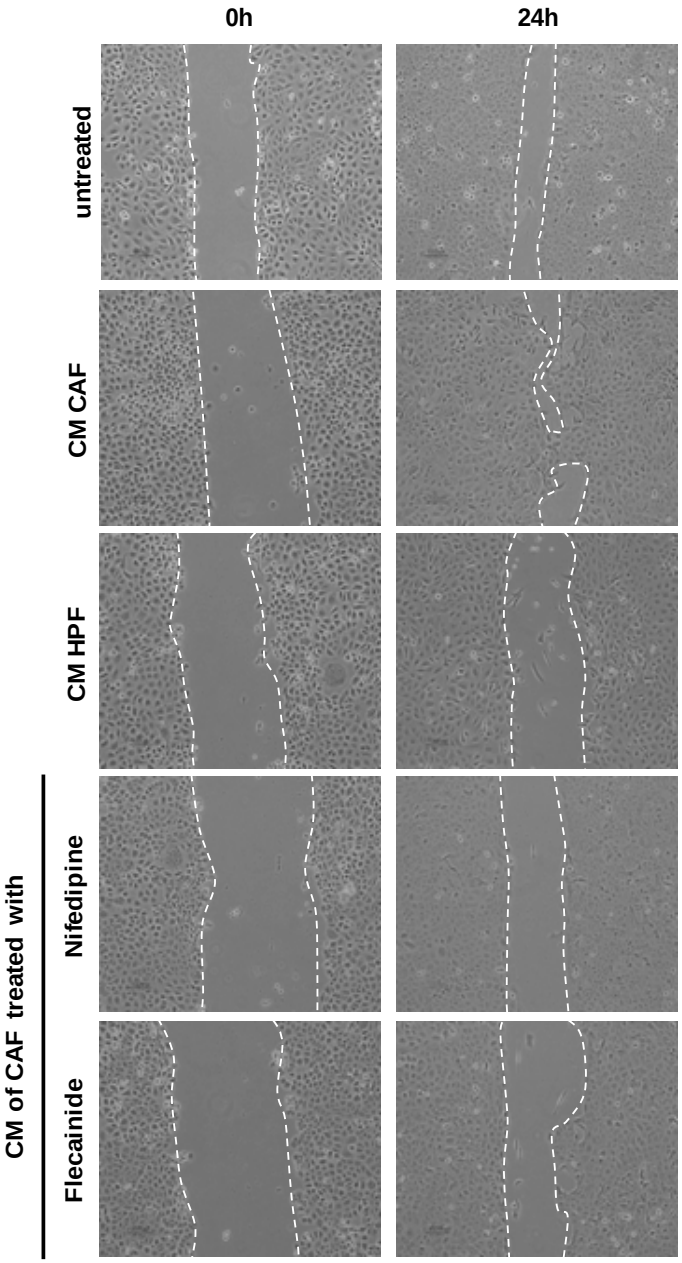
0h
24h
untreated
CM CAF
CM HPF
CM of CAF treated with
Nifedipine
Flecainide

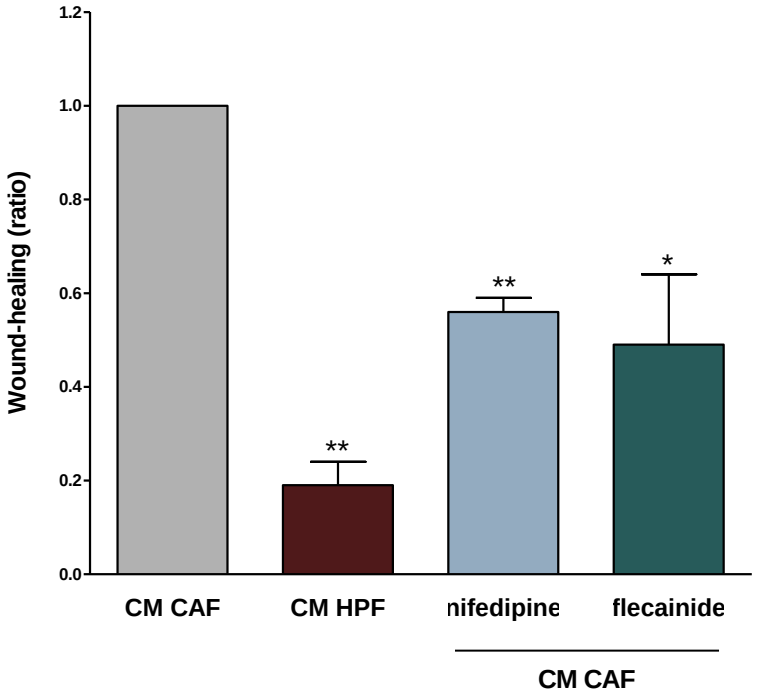

Figure 4. 20. CM of antiarrhythmics-treated CAFs impairs DU145 cell migratory capability. (*Upper panel*) Representative phase contrast microscopy images showing migration rate of DU145 cells exposed to CM of HPF, or CM of CAFs treated or not with nifedipine or flecainide (scale 100 µm). The dotted lines define the areas lacking cells. (*Lower panel*) Bar plots showing the wound-healing rate of DU145 cells upon the indicated treatments, as from scratch assay. Data are reported as wound healing ratio at 24 h compared to 0 h and are representative of three independent experiments. The level of significance was represented as * $p<0.05$, ** $p<0.01$, Student's t-test.

4.3.5. *Antiarrhythmics reduced MMP secretion by CAFs*

Considering our data showing that upon antiarrhythmic treatment CAFs lose their migratory and ECM remodelling capability and display a reduced pro-tumoural potential, we attempted to investigate soluble factors involved in these aspects. Since MMP up-regulation is well established to be associated with an increase in cell motility and extracellular matrix remodelling in PCa setting [121], we assessed MMP

expression levels in CAFs exposed to antiarrhythmics, and HPFs as comparison. Specifically, we sought to focus on MMP-2, which is reported to be largely released by CAFs and also associated with the presence of bone metastasis in PCa patients. Western blotting analysis confirmed that CAFs were able to release high levels of MMP-2 in the CM. Controversially, CAFs treated with nifedipine or flecainide, showed a substantial reduction of MMP-2 production, both for the pro-MMP2 and the relative activated form, thus recapitulating HPF status. Surprisingly, as shown in figure 4.19, the amount of MMP-2 was not decreased in cell lysate with respect to the corresponding CM sample, suggesting that antiarrhythmics could specifically affect MMP-2 release in the CM. (Figure 4.21).

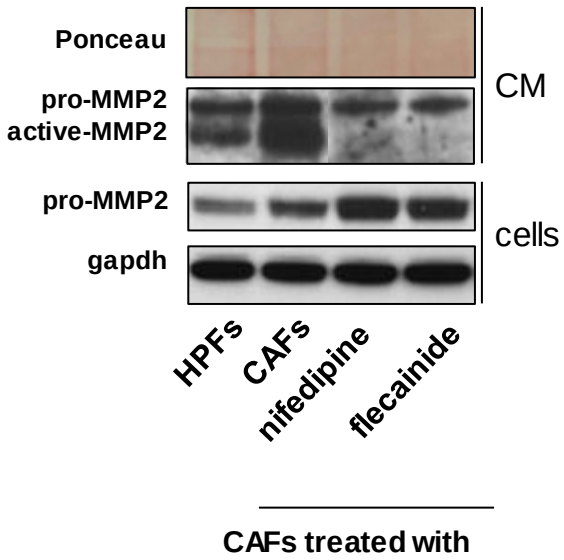

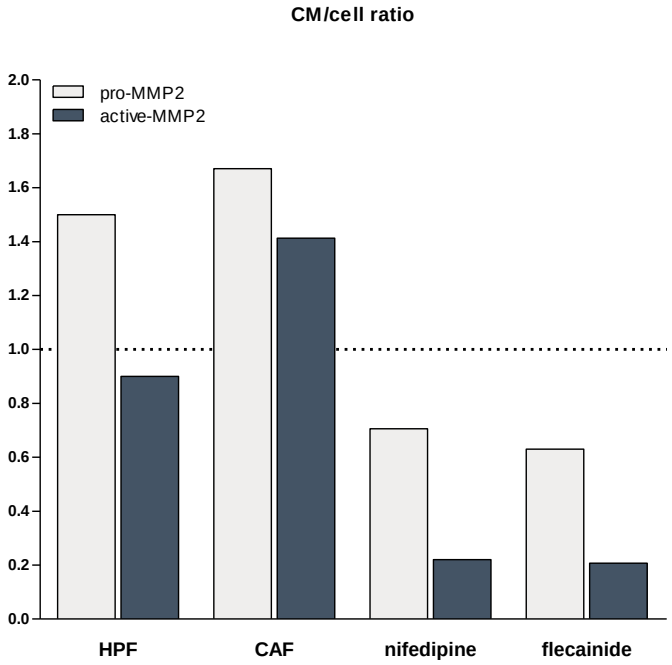

Figure 4. 21. Antiarrhythmics reduced MMP-2 release in the CM. (*Upper panel*) Western blotting analysis showing pro-MMP-2 and active-MMP-2 protein levels in CM and cell lysate of CAFs treated or not with nifedipine or flecainide, and HPFs. (*Low panel*) Quantification of MMP-2 western blotting analysis showing the CM/cells ratio.

4.3.6. *Antiarrhythmic-treated CAFs impaired tumour growth of PC* xenografts

To further confirm the obtained results showing that antiarrhythmics treatment can modulate CAF activated phenotype and reduce their pro-tumoural boosts, we tested the antiarrhythmic-mediated effects on CAF-PCa interplay by performing in vivo experiments.

First of all, we investigated the possibility of performing in vivo experiments by on the immortalized stromal cell line WPMY-1, which would be more easy to expand in culture as compared to the primary fibroblasts used in the previous part of the

project. Following this strategy, WPMY-1 cells were exposed to CM of DU145 cells, in order to induce their activation in vitro, then we tested the activated state through the evaluation of specific fibroblast activation markers and cation channel expression levels. As shown in figure 4.22, WPMY-1 cells exposed to CM of DU145 cells displayed an activated phenotype indicated by the up-modulation of α-SMA, COL1A1 and FAP, and the concomitant up-modulation of ion channel CACNA1H, CACNB1, SCN2A and SCN1B, as assessed by qRT-PCR and western blotting analysis.

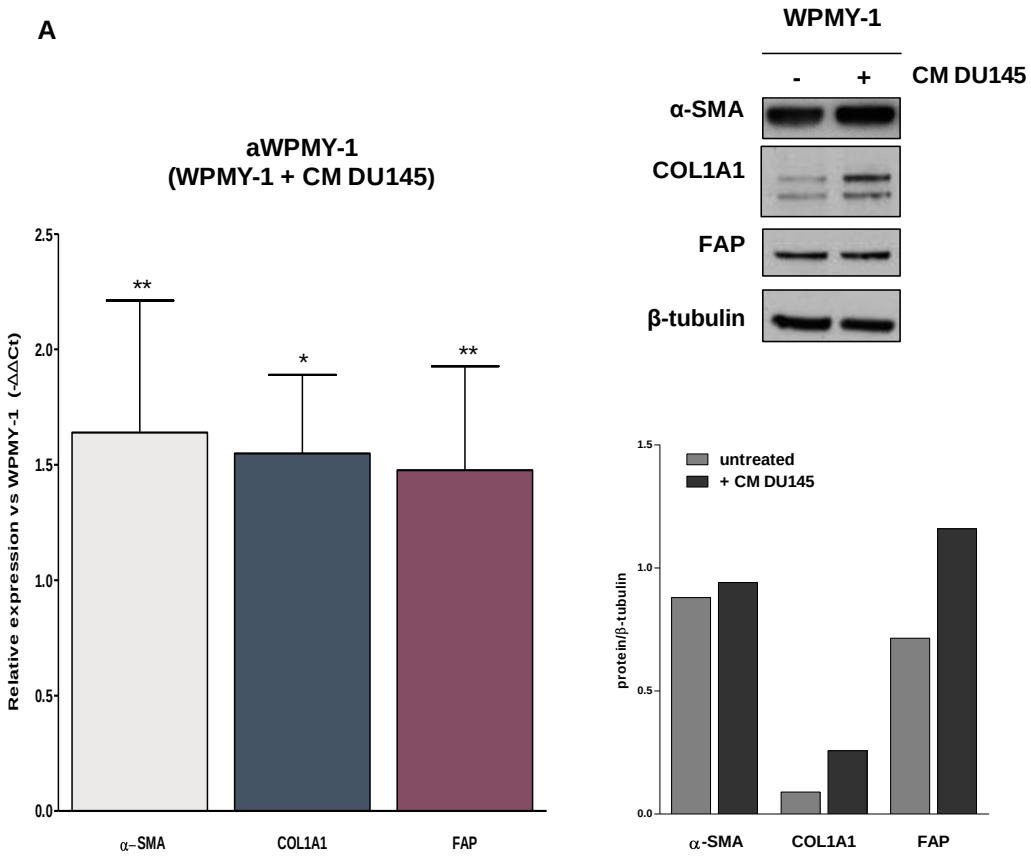

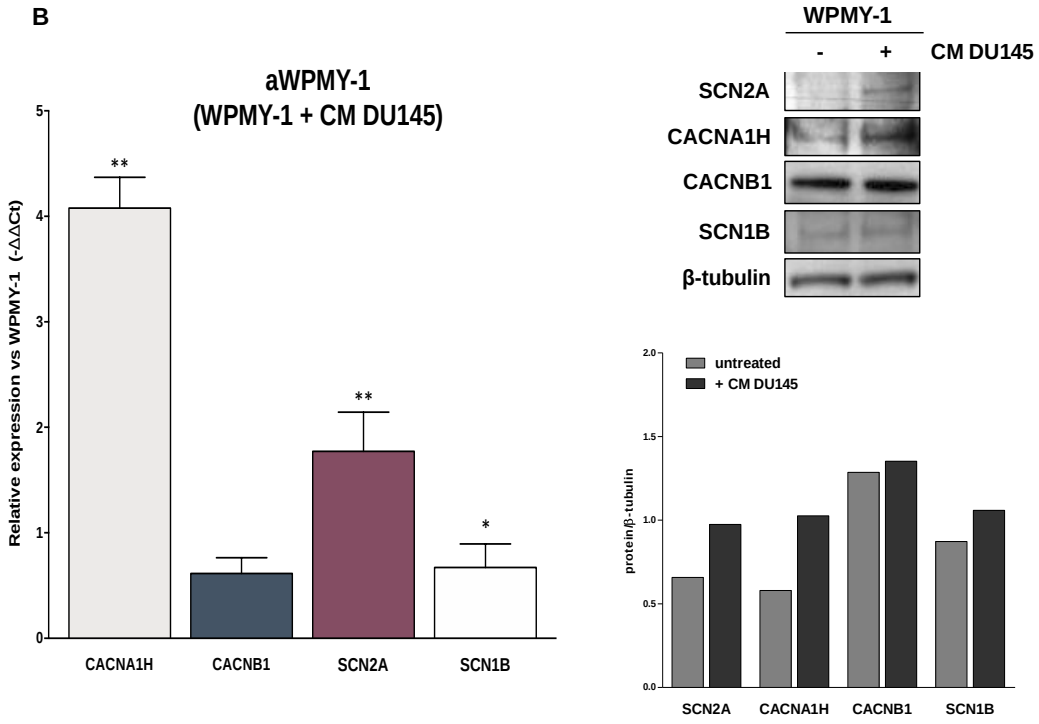

Figure 4. 22. Evaluation of WPMY-1 activated state. (*Panel A - left and upper right*) qRT-PCR and western blotting analysis showing fibroblast activation marker expression levels (α-SMA, COL1A1 and FAP) in WPMY-1 cells exposed to CM of DU145 cells. (*Panel B-left and upper right*) qRT-PCR and western blotting analysis showing the expression of ion channels CACNA1H, CACNB1, SCN2A and SCN1B in WPMY-1 cells exposed to CM of DU145 cells. (*Lower panel right A and B*) Western blots quantifications are reported as bar blots and densitometry data as raw normalized values (arbitrary units) towards the loading control (β-tubulin). qRT-PCR data are reported as relative expression with respect to untreated WPMY-1 cells and are representative of three independent experiments. The level of significance was represented as * $p<0.05$, ** $p<0.01$, Student's t-test.

To assess whether antiarrhythmic treatment was able impair to WPMY-1 activated state and reduce their tumoural promoting effects, as observed in fibroblast primary cultures, we exposed activated-WPMY-1 cells (aWPMY-1) to nifedipine and flecainide. As shown in figure 4.23, antiarrhythmics treatment was able to partially reduce WPMY-1 activation, as indicated by the reduction of α-SMA, COL1A1 and FAP mRNA levels and partially modulate COL1A1 and FAP protein levels.

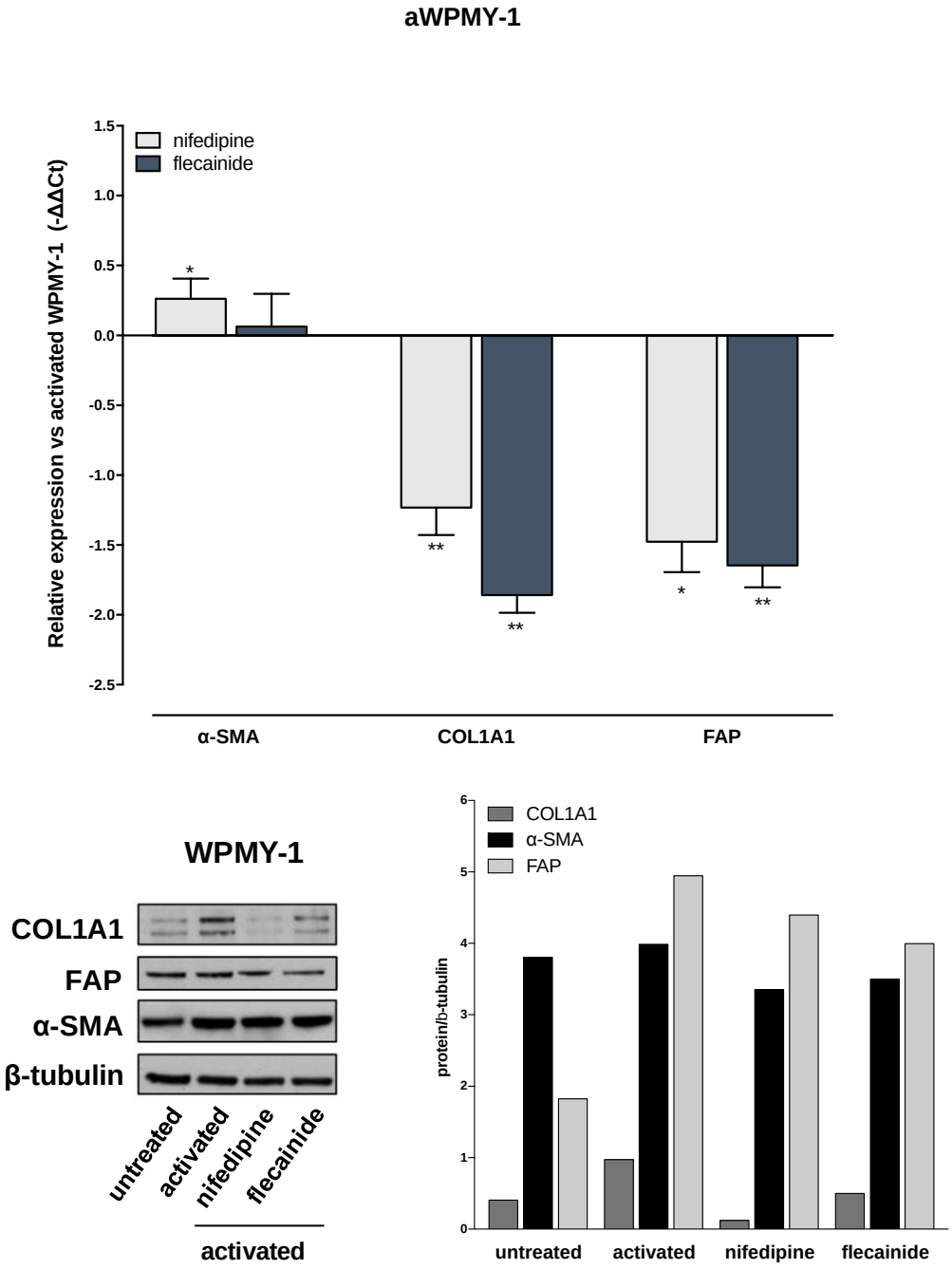

Figure 4. 23. Antiarrhythmics effects on WPMY-1 activated state. (*Upper and lower left panels*) qRT-PCR and western blotting analysis showing fibroblast activation marker expression levels (α-SMA, COL1A1 and FAP) in aWPMY-1 cells exposed to nifedipine or flecainide, compared to WPMY-1 cells. (*Lower right panel)* Western blots quantifications are reported as bar blots and densitometry data as raw normalized values (arbitrary units) towards the loading control (β-tubulin). qRT-PCR data are reported as relative expression

with respect to aWPMY-1 cells and are representative of three independent experiments. The level of significance was represented as * $p<0.05$, ** $p<0.01$, Student's t-test.

Finally, we evaluated antiarrhythmics impact on aWPMY-1 and PCa interplay. In this regard, as performed above for fibroblast primary cultures, we performed an indirect co-culture experiment. Specifically, DU145 cells were exposed to CM of parental WPMY-1 or aWPMY-1 cells treated or not with nifedipine or flecainide and cultured until 72 hours. The treatment of aWPMY-1 cells with antiarrhythmics reduced their capability to sustain DU145 cells proliferation, as indicated by the significant reduction of cell growth rate as compared to that of cells stimulated with CM from untreated aWPMY-1, recapitulating the trend observed when PCa cells were exposed to CM of parental WPMY-1 cells (Figure 4.24).

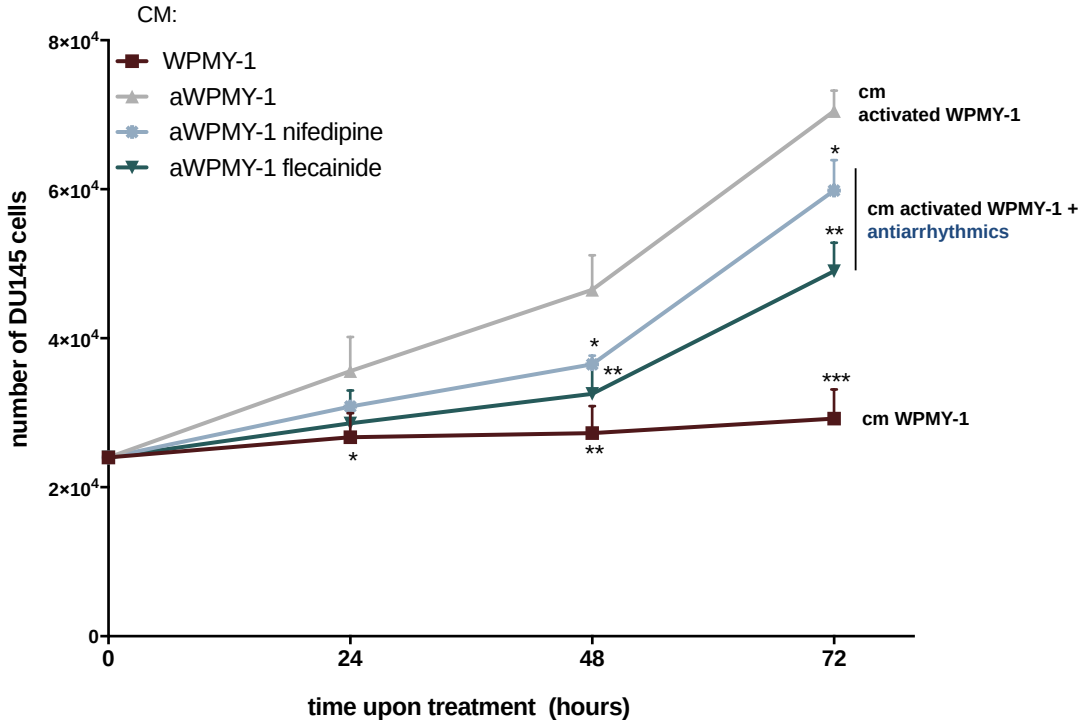

Figure 4. 24. Antiarrhythmics impair CAF capability to promote DU145 cell growth. DU145 cell growth evaluation cultured with CM of parental WPMY-1 or aWPMY-1 cells treated or not with nifedipine or flecainide at different time points (24, 48, 72 hours). Data reported are representative of three independent experiments. The level of significance was represented as * $p<0.05$, ** $p<0.01$, *** $p<0.001$ Student's t test.

Once verified the suitability of the fibroblast cell model for in vivo experiments, DU145 cells were injected in to the right flanks of SCID mice, and let to grow thus leading to the onset of subcutaneous PCa tumours. When the tumours reached a volume ≈ 150 mm^3, CM of parental WPMY-1 or of aWPMY-1 cells exposed or not to nifedipine or flecainide was intratumourally injected into PCa xenografts for 5 consecutive days for a total of 2 weeks. Tumour volumes were determined every 4 days with a Vernier caliper. In consonance with what observed before, the tumours exposed to CM of aWPMY-1 cells treated with antiarrhythmics displayed a significant tumour growth delay, resembling the trend observed for tumours treated

with CM of parental WPMY-1 cells, which is recognized as tumour suppressive stimulus (Figure 4.25).

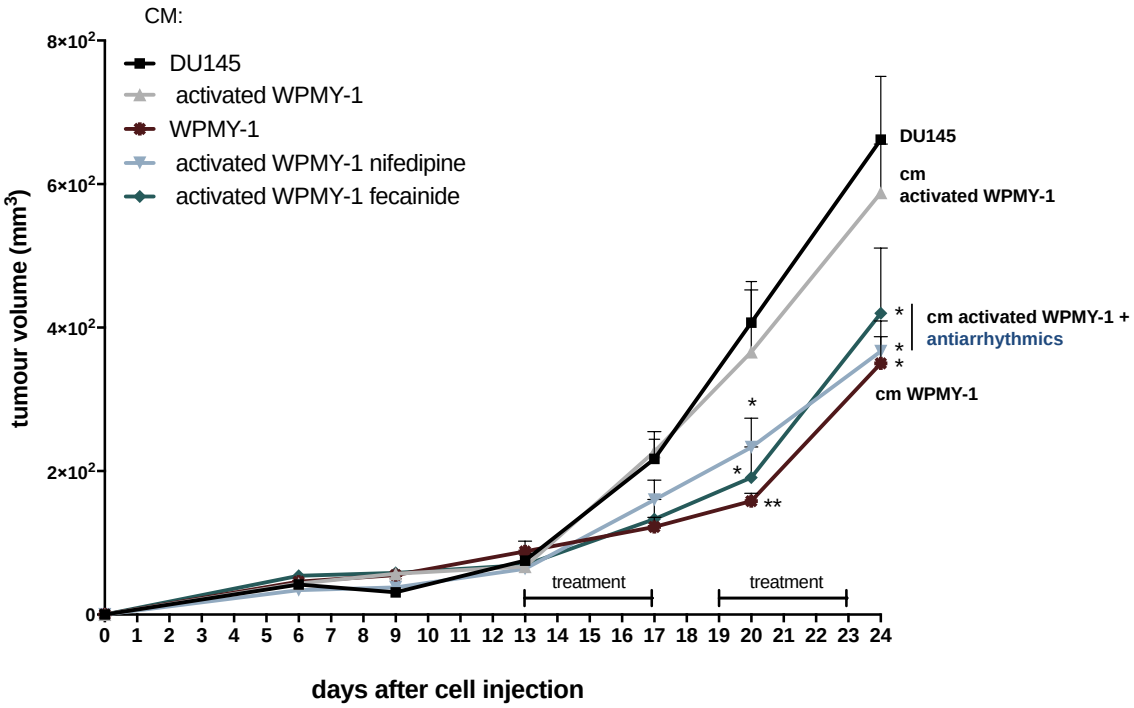

Figure 4.25. Antiarrhythmics significantly impair the capability of activated fibroblasts to sustain tumour growth in vivo. DU145 cells were subcutaneously injected into the right flanks of SCID mice. When tumours reached the volume of 150 mm^3, mice were randomly separated in five groups (six mice/group) and were intratumourally treated 5 days for 2 weeks with CM of parental WPMY-1 or of aWPMY-1 cells treated or not with nifedipine or flecainide. The level of significance was represented as * $p<0.05$, ** $p<0.01$, *** $p<0.001$ Student's t test with respect to DU145.

In addition, in order to investigate the impact on tumour growth upon intratumourally treatment with CM of aWPMY-1 exposed or not to antiarrhythmics, immunohistochemical analysis of Ki-67 in tumour xenograft tissues has been performed. Results indicated a significant decrease of Ki-67 rate in the groups intatumourally treated with CM of aWPMY-1 exposed to

nifedipine (6.0% ± 1.1%) or flecainide (7.2% ± 2.0%) compared to untreated group (21.3% ± 4.2%), resembling the trend observed for tumours treated with CM of parental WPMY-1 cells (6.3 ± 1.4%). No significant differences were identified between untreated and CM aWPMY-1 groups (19.9% ± 2.9%).

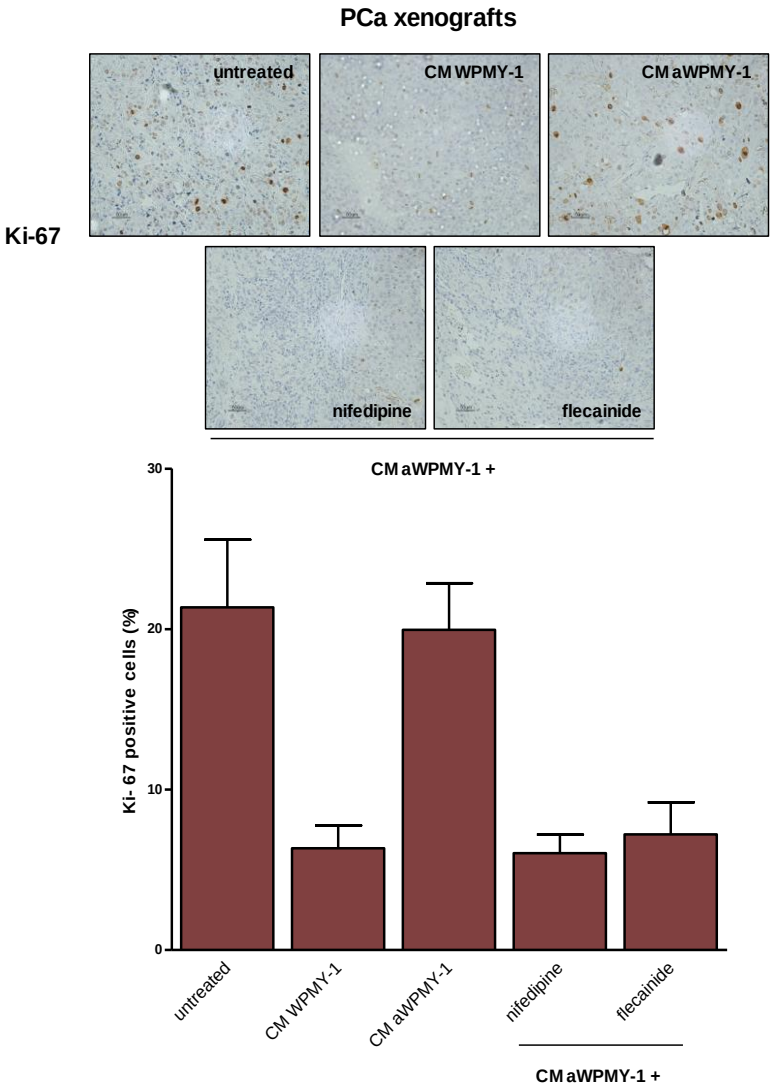

Figure 4.26. Proliferation rate in PCa xenografts. (*Upper panel*) Representative images of KI-67 immunohistochemical staining (stained in brown) in PCa xenografts intratumouraly treated with CM of parental WPMY-1, aWPMY-1 exposed or not to nifedipine of flecainide. (*Lower panel*) Percentage of Ki-67 positive cells evaluated by counting 8 different fields for

each samples. The level of significance are represented as * $p<0.05$, Student's t test with respect to untreated group.

Moreover, western blotting and qRT-PCR analysis revealed that intratumoural administration of CM of aWPMY-1 cells exposed to antiarrhythmics was able to affect PCa xenograft plasticity, as indicated by E-cadherin up-modulation. As shown in figure 4.27, E-cadherin levels were slightly decreased in xenografts treated with CM of aWPMY-1 cells. In contrast, CM of aWPMY-1 cells exposed to nifedipine or flecainide was no longer able to decrease E-cadherin, rather it increased its levels, similarly to what observed in xenografts treated with CM from parental WPMY-1 cells.

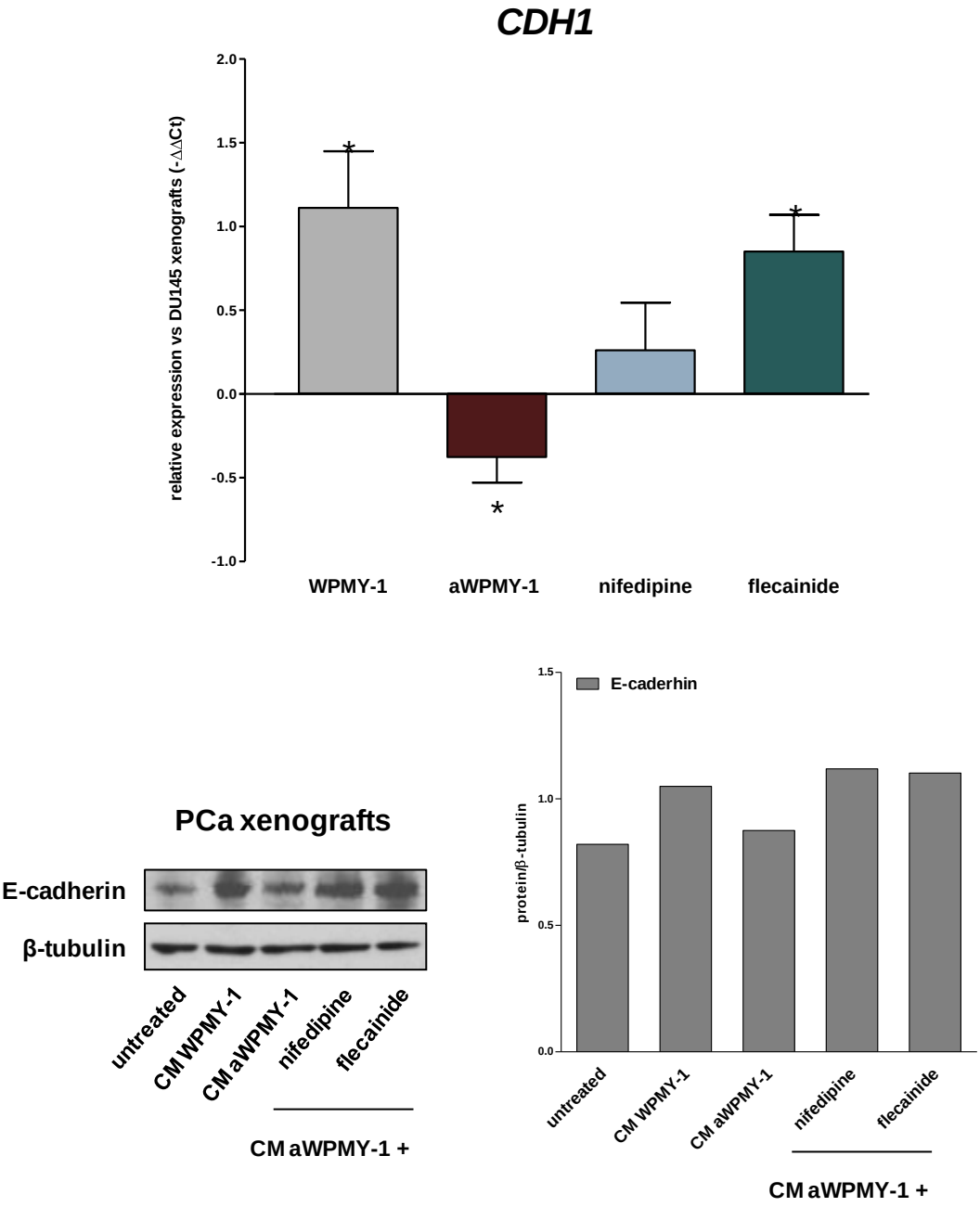

Figure 4.27. Antiarrhythmics revert CAF-mediated EMT in PCa xenografts. (*Upper panel*) Expression levels of the epithelial marker *CDH1* assessed by qRT-PCR in PCa tumours treated with CM of parental WPMY-1 or of aWPMY-1 cells exposed or not to nifedipine or flecainide. Data are reported as relative expression with respect to untreated tumours. (*Lower panel left*) western blotting analysis showing E-cadherin protein amount in PCa tumours treated with CM of parental WPMY-1 or of aWPMY-1 cells exposed on not to nifedipine or flecainide, normalized to β-tubulin. (*Lower panel right*) Western blots quantifications are reported as bar blots and densitometry data as raw normalized values

(arbitrary units) towards the loading control (β-tubulin). The level of significance was represented as *p<0.05, **p<0.01, Student's test.

5. RESULTS II. Identification of potential stromal biomarkers for risk assessment in Active Surveillance patients

In PCa setting, active surveillance (AS) has evolved as an alternative to radical treatment for patients with very low risk, potentially indolent tumours. AS patients are strictly monitored and curative treatments are avoided or deferred until evidence of more aggressive PCa [122]. Eligible AS patients have clinical stage T1/T2 PCa, PSA levels in the blood ≤10 ng/ml, PSA density <0.2 ng/ml per millilitre, one or two positive biopsy cores, and Gleason pattern score (GPS) ≤ 6.

Patients enrolled in AS are monitored by measuring PSA levels every 3–6 months, and follow-up biopsies are scheduled after 1, 4, and 7 years of AS inclusion [122]. Despite this stringent protocol, the aforementioned selection criteria are suboptimal and about 1/4 of patients discontinue AS because of PCa reclassification/progression, mainly for up-grading (change from GPS ≤ 6 to GPS > 6), or for the detection of more than two positive cores at the time of the first repeated biopsy [123]. This frame highlights the urgent need of novel biomarkers for an unequivocal classification of indolent disease, thus allowing the early identification of occult high-risk PCa tumours during biopsy procedures. In this regard, the PCa stroma, characterized by an increased desmoplastic and inflammatory environment, could potentially improve AS patients' classification.

Considering our recently observation on the crucial role of reactive stroma in PCa setting [89], we hypothesized that the existence of peculiar reactive stroma in GPS=6 core biopsies (or even in negative biopsies) could be indicative of an adjacent undetected high-grade PCa tumour, and therefore potentially reduce disease misclassification during needle biopsy procedures. In addition, the choice of

investigating the potential of stromal biomarkers for high-grade PCa detection was supported by literature evidence reporting that the percentage of myofibroblasts is increased in the stroma of poorly differentiated GPS > 6 compared to GPS ≤ 6 tumours [70]. Moreover, the expression of α-SMA stromal marker in radical prostatectomy specimens has been reported to correlate with PCa grade [74]. Considering this premise, the aim of this translational part of the project is to define the potential of selected stromal genes found to be consistently up-regulated PCa activated stroma as novel stromal tissue and/or circulating biomarkers for risk assessment in AS patients.

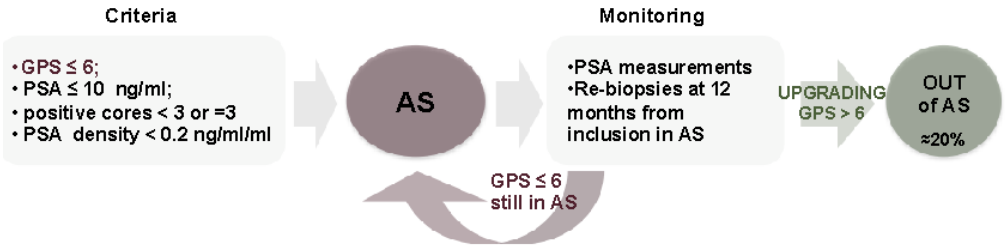

Figure 5. 1. Schematic representation of AS protocol, selection criteria and monitoring.

5.1. Identification of potential stromal biomarkers in PCa sample.

Despite intensive efforts in the characterization of tumour-stroma interplay have led to the identification of factors that contribute to sustain this crosstalk, further attempts are required to understand the crucial molecular pathways that govern tumour stroma activation. In this regard, defining a stromal gene signature relevant for cancer progression could be a successful strategy to identify novel prognostic biomarkers for PCa. Recently, we have performed a gene expression profiling analysis comparing prostate CAFs and normal fibroblasts stimulated with IL-6 or TGF-β, to examine the molecular signatures involved in fibroblast activation. This analysis highlighted that PCa reactive stroma was influenced by IL-6 and TGF-β signalling, even if with different extent and most likely with different roles [89]. Specifically, GSEA highlighted that genes related to ECM modulators were positively enriched in CAFs, IL-6- or TGF-β-activated fibroblasts.

Whit the aim of identifying gene functionally involved in fibroblast activation and potentially suitable as stromal biomarkers for AS patients, we selected a set of genes related to reactive stroma and up-modulated in CAFs or HPFs activated in vitro with IL-6 or TFG-β. Combining these criteria, we identified POSTN, COL10A1, COL11A1, SPARC and COMP, genes related to extracellular matrix remodelling and tumourigenesis process [124], as significantly up-modulated in at least one of our activated fibroblast sets (Figure 5.2). Among these genes, we focused on POSTN. As shown in figure 5.2, POSTN was found to be significantly up-modulated in all activated fibroblasts (CAFs, normal fibroblasts activated in vitro with IL-6 and TGF-β) with respect to HPFs. POSTN gene codes for the protein periostin, which is a secreted structural protein involved in cell proliferation, migration and EMT processes [125].

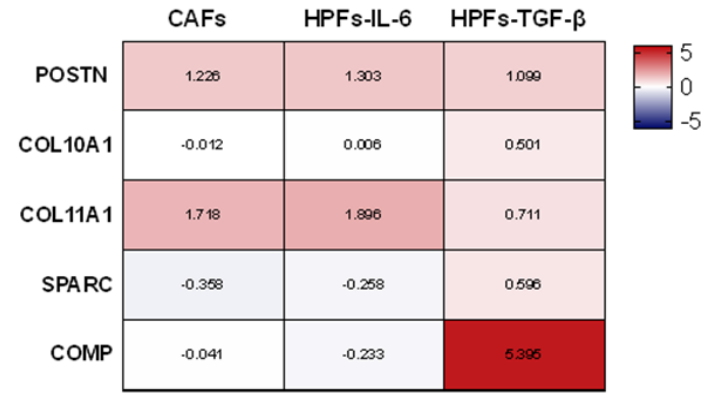

	CAFs		HPFs-IL6		HPFs-TGF-β	
	logFC	p-value	logFC	p-value	logFC	p-value
POSTN	1.226143	0.00763	1.303061	0.00126	1.194951	0.0002
COL10A1	-0.01245	0.91915	0.06279	0.66751	0.500536	0.08124
COL11A1	1.718046	0.07488	1.896297	0.04705	0.710533	0.01056
SPARC	-0.35811	0.23563	-0.25752	0.478502	0.595899	0.00128
COMP	-0.04116	0.94404	-0.23303	0.72200	5.39523	3.69E-06

Figure 5. 2. Stromal related genes showing differential expression in activated fibroblasts compared to HPFs. List of extracellular matrix related genes found to be associated with fibroblast activation phenotype in CAFs and HPFs activated in vitro with IL-6 or TGF-β, compared to HPFs.

5.1.1. *POSTN expression in PCa setting*

The reason why we selected POSTN (i.e. periostin) is that this gene was found to be up-regulated in prostate CAFs and HPFs activated in vitro with IL-6 and TFG- β and that, moreover POSTN expression was found to be associated with is tumourigenesis processes [125]. These findings indicate that POTSN could be a valid candidate biomarker for improve AS patient selection. In support to this, high expression levels of POSTN mRNA were found to significantly correlate with a higher probability to experience biochemical recurrence (BCR), which is the rise of PSA blood levels upon radical

treatment (e.g. radical prostatectomy or radiotherapy), in ≈ 100 clinical PCa samples (Taylor dataset GSE21032) [126] (Figure 5.3).

	BCR			
	HR	CI. low	CI. up	p-value
POSTN	2.613288	1.515	4.506	0.0005

Figure 5. 3. POSTN mRNA expression correlates with BCR in clinical PCa samples from Taylor data set. Hazard Ratio (HR) indicating a significant association of POSTN mRNA expression in ≈ 100 clinical PCa samples with BCR.

Moreover, to both check the suitability and the reliability of our hypothesis, we validated our gene expression results in an independent panel of three CAFs isolated from tumoural areas of PCa specimens with respect to the HPFs. qRT-PCR analysis showed a considerable up-modulation of POSTN mRNA in the independent panel of CAFs, thus confirming our preliminary observation (Figure 5.4).

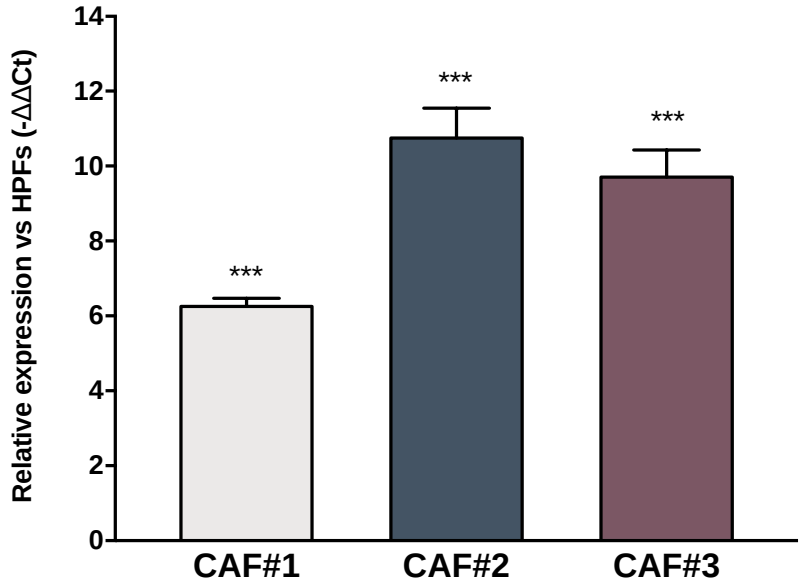

Figure 5. 4. POSTN is overexpressed in CAFs. Expression levels of POSTN assessed by qRT-PCR in three different CAFs isolated from tumoural area of radical prostatectomy samples. Data are reported as relative expression with respect to matched-HPFs. The level of significance was represented as p*<0.00, Student's t-test.

5.1.2. *Evaluation of periostin (POSTN) protein expression in radical prostatectomy samples*

Our initial hypothesis was to test the presence of a specific reactive stromal signature in GPS=6 core biopsies (or even in negative biopsies) collected at the time of PCa diagnosis, and correlates such unique feature with disease reclassification during AS monitoring. Unfortunately, the use of diagnostic core biopsies raises several issues related to the very small sample size (technical issue) and the actual possibility to completely deplete such small samples (legal issue) during investigation analyses. In this scenario, we sought to take advantage from a large series of Formalin Fixed and Parafin Embedded (FFPE) radical prostatectomies collected in our institute, and use

this valuable cohort i) to set up the appropriate conditions to detect periostin (e.g. POSTN) protein expression in the stroma infiltrating tumour foci, by using immunohistochemistry (IHC) techniques, and ii) to preliminary assess the clinical relevance of periostin expression, in terms of association with clinico pathological features and patient outcome. The case series consisting of FFPE tissue sections from 116 PCa patients subjected to radical prostatectomy with a minimum follow-up of 5 years, including 31 patients that experienced biochemical failure and 85 that had no evidence of recurrence. To simulate the AS setting, specimens characterized by GS ≤ 6 cancers were included. At first, the samples were evaluated by an expert uro-pathologist to identify proper areas to be macro-dissected for IHC. Under close supervision of the uro-pathologist, we analysed IHC periostin staining to provide a semi quantitative score to be used to assess correlation between protein expression in the stroma and clinico pathological characteristics of the tumour and/or patient outcome. We designed a semi quantitative score, by setting up an arbitrary scale ranging from 0 to 3, where 0 represents no periostin stromal staining and 4 the highest stromal staining observed in the tissue sections. Once defined the score, sections with stromal tumoural score from 0 to 1 were classified as “low”, and sections with score of 2 or 3 were classified as “high”. As shown in figure 5.5, we found that periostin (in red) is manly expressed in the stroma area (labelled with S) surrounding tumoural foci (labelled with T). Moreover, results from 116 FFPE prostatectomy samples showed a significant correlation between stromal periostin score and tumour grade. Specifically, we observed that higher expression of periostin was found in the stroma of GS > 6 tumours. In fact, the 81% of the tumours classified as GS > 6 displayed a high periostin score, and only 19% were classified as low periostin score. Conversely, low score was assigned to the 87% of GS ≤ 6 tumours and high score to 13% (Figure 5.5).

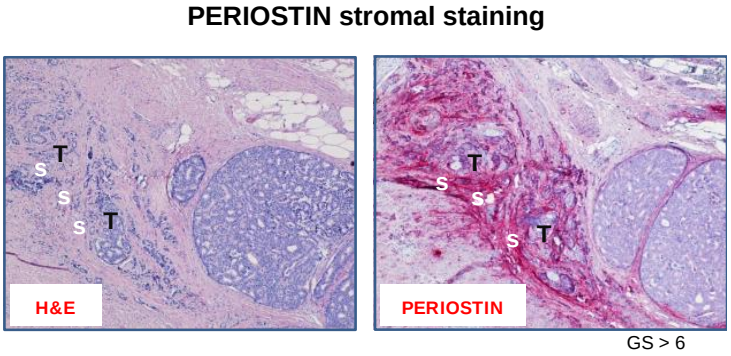

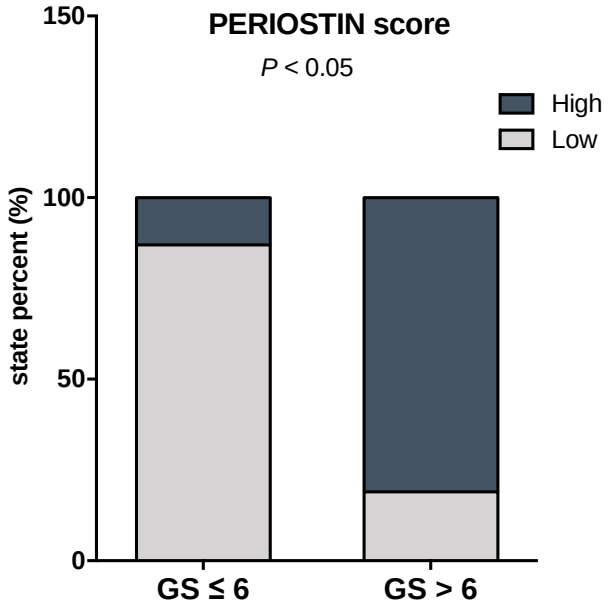

		PERIOSTIN stromal score	
	Total n	**Low** n (%)	**High** n (%)
GPS ≤ 6	38	33 (87%)	5 (13%)
GPS > 6	78	15 (19%)	63 (81%)

Figure 5.5. Periostin stromal staining correlates with tumour grade in PCa specimens. (*Upper panel*) Representative image of a FFPE section of high grade PCa stained for H&E and periostin protein (red), showing an intense staining in the stroma (S) surrounding tumour foci (T). (*Low panels*) Bar plot and table comparing periostin stromal score (high or low) and GPS in the PCa cohort. The level of significance was represented in accord to chi-squared test.

Moreover, we highlighted an interesting correlation between periostin score and a specific subgroup of GS 7 tumours. Tumour GS is defined by adding the two most common Gleason patterns observed in PCa specimens. The GS 7 tumours are mainly composed of the patterns 3 and 4 (3+4 or 4+3). Patients with GS 7 demonstrate a wide range in clinical outcomes, suggesting the urgent need of novel outcome predictors in this setting. Recently, uro-pathologist observed that a subgroup of patients characterised by cribriform morphology tumour growth in pattern 4 displayed a poor prognosis, indicating that this specific histological pattern requires an unequivocal annotation and identification during diagnosis due to the relevant impact on patient's outcome [127] .

In this regard, we observed a significant association of periostin score and the presence of cribriform morphology in pattern 4 tumours of our cohort of 74 FFPE prostatectomy samples displaying GS 7. As shown in figure 5.6, we found that 100% of tumours with cribriform morphology in the pattern 4 displayed a high periostin score. Conversely, despite the high periostin score was anyway found to be relevant for GS 7 tumours, the 76% of the tumours characterised by non-cribriform morphology was classified as high score and the 14% as low. These pieces of evidence suggest a possible correlation between a peculiar reactive PCa stroma and cribriform tumour growth.

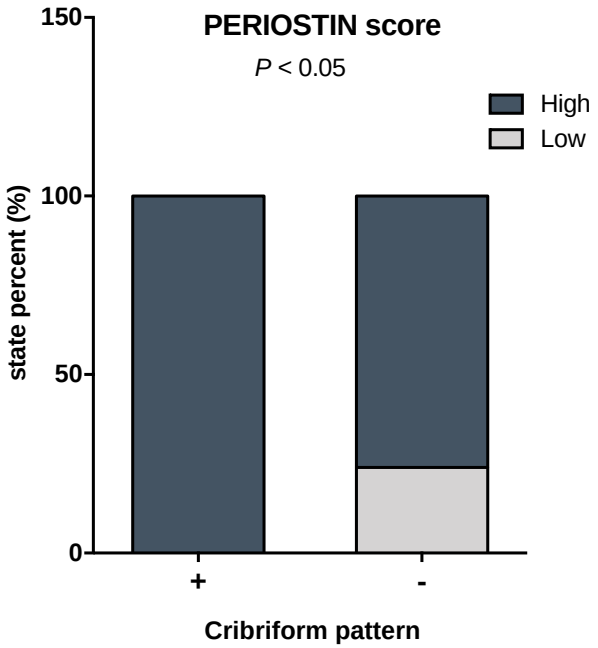

Cribriform pattern	Total n	PERIOSTIN stromal score	
		Low n (%)	High n (%)
+	16	0 (0%)	16 (100%)
-	58	14 (24%)	44 (76%)

Figure 5.6. Periostin score correlates with cribriform growth in the sub-group of GS 7 tumours. Bar plot and table comparing periostin stromal score (high or low) and cribriform pattern in a sub-group of 74 GS 7 tumours. The level of significance was represented in accord to chi-squared test.

5.1.3. *Evaluation of periostin as a potential prognostic tissue biomarker for risk assessment in PCa setting*

Once assessed the correlation between stromal periostin staining and tumour grade in the cohort of prostatectomy specimens, we investigated the prognostic value of periostin score. In PCa, the crucial event that is indicative of a possible failure of curative therapies (e.g. prostatectomy or radiotherapy) is disease relapse in the form of

biochemical recurrence (BCR) that is rising of PSA levels in the blood after radical treatments. In order to investigate the prognostic potential of periostin, we initially performed a univariate analysis considering several clinico-pathological characteristics, including: surgical margin, extraprostatic extension (EPE), seminal vesicle invasion, perineural invasion, GS and periostin score. As shown in figure 5.7, the univariate analysis indicated that periostin score (HR=6.98; IC 95%: 2.11, 22.95), surgical margin (HR=3.83; IC 95%: 1.77, 8.29), EPE (HR=3.83; IC 95%: 1.77, 8.29), seminal vesicle invasion (HR=3.57;IC 95%: 1.51, 8.47), perineural invasion (HR=2.25; IC 95%: 1.01, 5.02) and GS (HR=2.62; IC 95%: 1.00, 6.86) were all related to BCR, with periostin score having the highest HR. Moreover, 7-year BCR probability stratified for periostin score indicated that high periostin score displayed a moderate capability to predict biochemical failure event in PCa patients.

Variable	HR	95%CI	
Surgical margin			
> 1 vs 0	3.83	1.77	8.29
Periostin score			
high vs low	6.96	2.11	22.95
EPE			
yes vs no	3.38	1.54	7.39
Seminal vesicle invasion			
1 vs 0	3.57	1.51	8.47
Perineural invasion			
yes vs no	2.25	1.01	5.02
GS			
> 6 vs 6	2.62	1.00	6.86

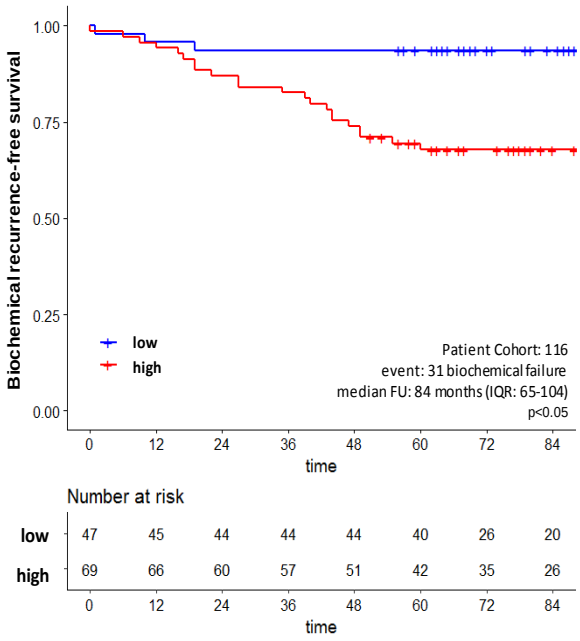

Figure 5. 7. Univariate Cox model and Kaplan-Meier analysis of biochemical-relapse free survival in PCa patients according to periostin score. (*Left panel*) Table reports Hazard Ratio (HR) value obtained considering several clinico-pathological variables (surgical margin, EPE extraprostatic extension, seminal vescicle invasion, GS= Gleason score) and

periostin staining. (*Right panel*) Periostin stromal score with respect to biochemical recurrence (BCR) free survival in 116 PCa patients.

5.2. Identification of potential stromal circulating biomarkers in PCa sample

Considering the abovementioned critical aspects related to the assessment of stromal biomarkers in core biopsies obtained from AS patients, we sought to investigate their prognostic potential as circulating biomarkers. Our findings indicating a positive correlation between periostin score and aggressive disease (GS > 6) (Figure 5.5) and a moderate association of periostin score with disease outcome (Figure 5.7) prompted us to investigate the potential of periostin as a circulating biomarker for disease reclassification in AS patients. With the same aim, we decided to extend our explorative evaluation adding a panel of four ECM proteins that we previously described as up-modulated in CAFs or normal fibroblasts activated in vitro with IL-6 or TGF-β, compared to normal fibroblasts (Figure 5.1): col11a1, col10a1, sparc and comp.

5.2.1. *Evaluation of ECM signature in CM of CAFs and PCa plasma patients*

With the aim of investigating the potential value of stromal circulating biomarkers, we initially performed an explorative evaluation of ECM protein amounts in the CM of patient-derived CAFs and HPFs, in order to assess the reliability of our hypothesis. Western blotting analysis indicated that periostin, col11a, col10a, sparc and comp were detectable in the CM of fibroblasts and, in agreement with gene expression data, their expression levels were found to be increased in CM of CAFs with respect to HPFs (Figure 5.8).

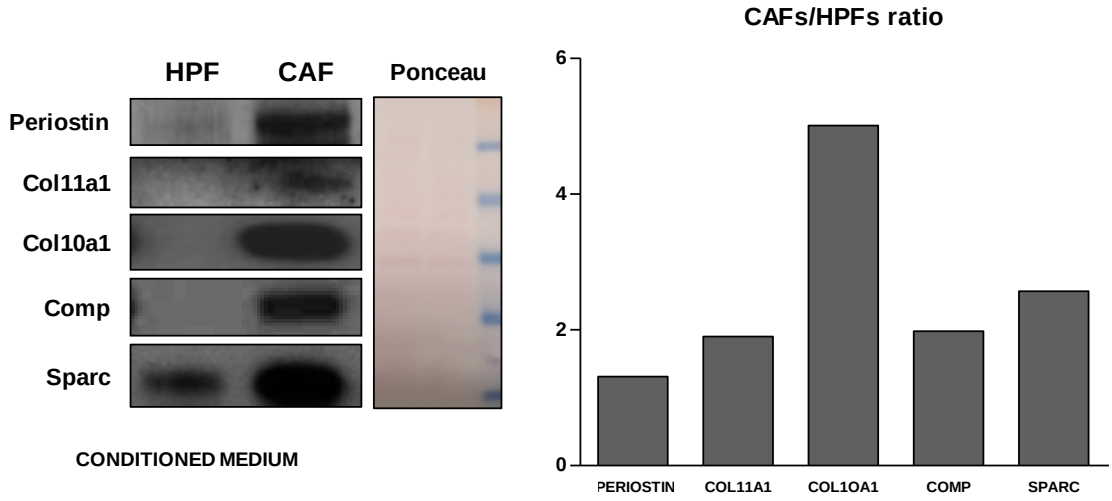

Figure 5.8. ECM proteins were increased in CM of CAFs. Western blotting showing reactive ECM-related protein amount (periostin, col11a, col10a, comp and sparc) in CM from CAFs with respect to that from HPFs. The bar plot reports quantification of western blot. Densitometry data are reported as raw normalized values (arbitrary units).

Moreover, we assessed the expression levels of our ECM signature in plasma samples collected at inclusion in AS (baseline) of two patients who dropped out of AS protocol due to disease reclassification (upgrading), two patients who remained in AS for more than 5 years (indolent), and for comparison we analysed the levels of ECM proteins in the plasma obtained at diagnosis (baseline) of two patients with a clinically significant disease subjected to radical treatment. A shown in figure 5.9, we found a high amount of perostin, col10a1, comp and sparc in the plasma of patients with clinically relevant tumours and moderated levels in that of AS patients belonging to the upgrading group. Conversely, the indolent group showed lower levels of ECM proteins, especially for periostin.

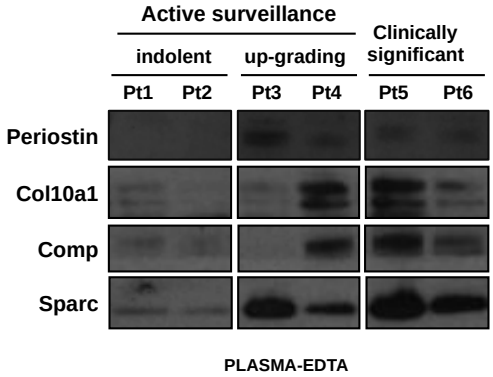

Figure 5.9. ECM proteins were increased in baseline plasma samples of upgrading AS patients and clinically significant PCa patients. Western blotting showing periostin, col10a, comp and sparc amounts in plasma samples obtained at the diagnosis in indolent or upgrading AS patients and patients with clinically significant disease.

5.2.2. *Evaluation of ECM protein levels in plasma sample from AS patients*

In order to identify circulating biomarkers able to discriminate between PCa patients with indolent tumour, truly eligible for AS, and patients who discontinued AS due to upgrading at the fist re-biopsy, we tested the potential of our ECM signature on plasma samples collected at the inclusion in AS protocols. At first, in order assess the reliability of our stating point, we evaluated periostin, col11a1, col10a1, sparc and comp baseline plasma levels in an explorative cohort of 40 AS patients, including 20 patients who discontinued AS due to upgrading at the fist re-biopsy (1 year) and 20 patients still in AS for at least 5 years. ELISA-based assessment analysis indicted that only sparc displayed a moderate differential expression between the two groups of upgrading (UP) and indolent (IND) patients (Figure 5.10).

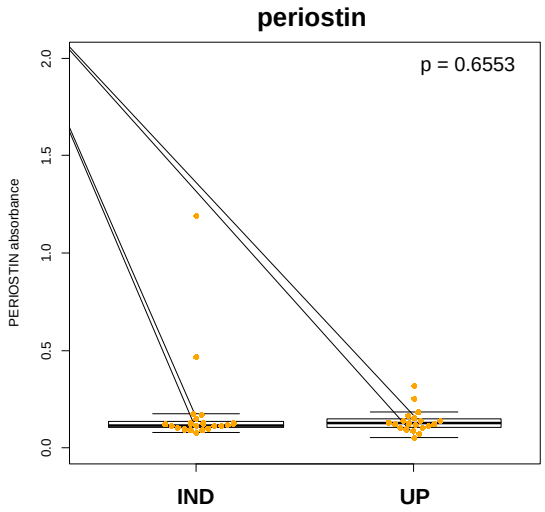
periostin
p = 0.6553
PERIOSTIN absorbance
0.0
0.5
1.0
1.5
2.0
IND
UP

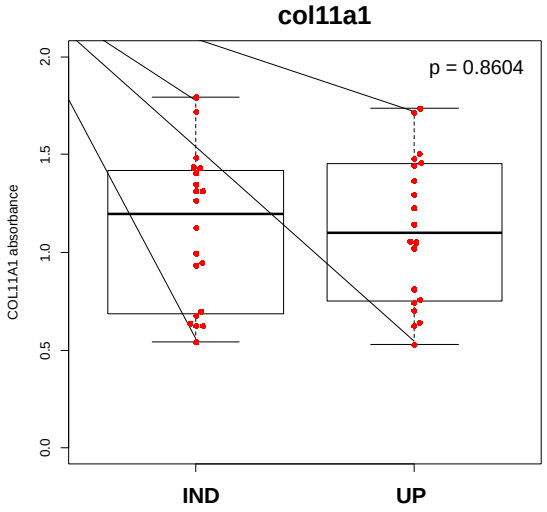
col11a1
p = 0.8604
COL11A1 absorbance
0.0
0.5
1.0
1.5
2.0
IND
UP

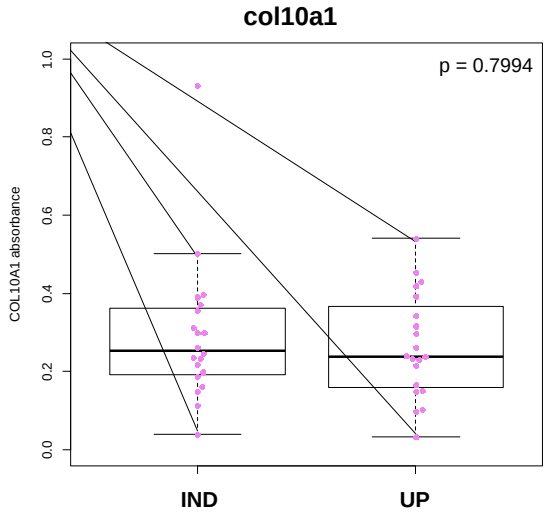
col10a1
p = 0.7994
COL10A1 absorbance
0.0
0.2
0.4
0.6
0.8
1.0
IND
UP

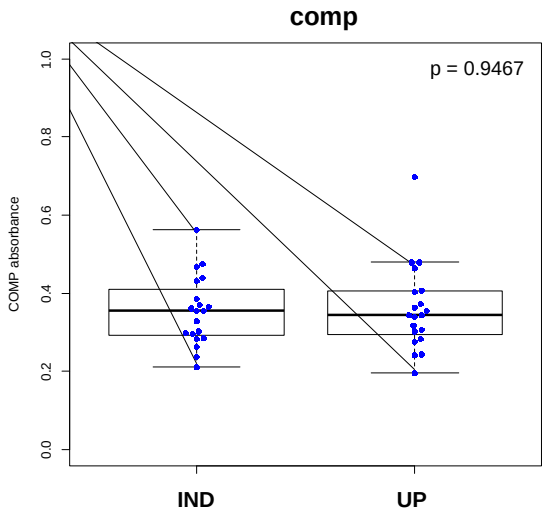
comp
p = 0.9467
COMP absorbance
0.0
0.2
0.4
0.6
0.8
1.0
IND
UP

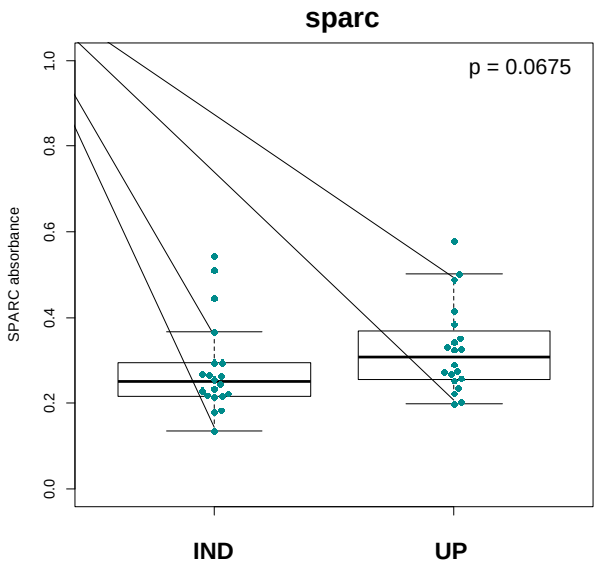

Figure 5. 10. ECM signature plasma levels in an explorative cohort of AS patients. Quantification of periostin, coll11a1, coll10a1, comp and sparc plasma levels using ELISA assay in 40 AS patients, of which 20 from the indolent (IND) and 20 from the upgrading (UP) group. Data are reported as absorbance (optical density). Wilcoxon test was performed and $p<0.05$ was considered significant.

5.2.3. *Evaluation of a logistic model for AS risk assessment based on circulating periostin and sparc*

Considering our findings that indicated a moderate association of sparc with disease reclassification, and with the aim of improving the relevance of our circulating signature, we sought to define a prognostic model combining sparc and periostin predictive values. At first, logistic models were developed by considering circulating sparc levels as a continuous or as a categorical variable (index score). The logistic model with sparc modulated as a continuous variable revealed to have an area under the curve ROC (AUC) of 0.695 (AUC: 0.695; IC 95% 0.52-0.850), indicating that the

levels of circulating sparc had a moderate capability to discriminate between the indolent and upgrading AS patients (Figure 5.12, left panel). More interestingly, when sparc was combined with periostin, we observed an increase of the AUC value from 0.695 to 0.725 (AUC: 0.725; 0.555, 0.867), suggesting that the combination slightly improved the moderate predictive power of the model (Figure 5.11, right panel). As shown in table 5.13 (low panel), sparc also showed moderate association with the probability of upgrading occurrence (Odds Ratio (OR) 4.14; IC 95%: 1.04;-16.51). When combined with periostin, the model displayed a higher probability to predict upgrading in AS patients (OR 4.89; IC 95%: 1.14-20.96).

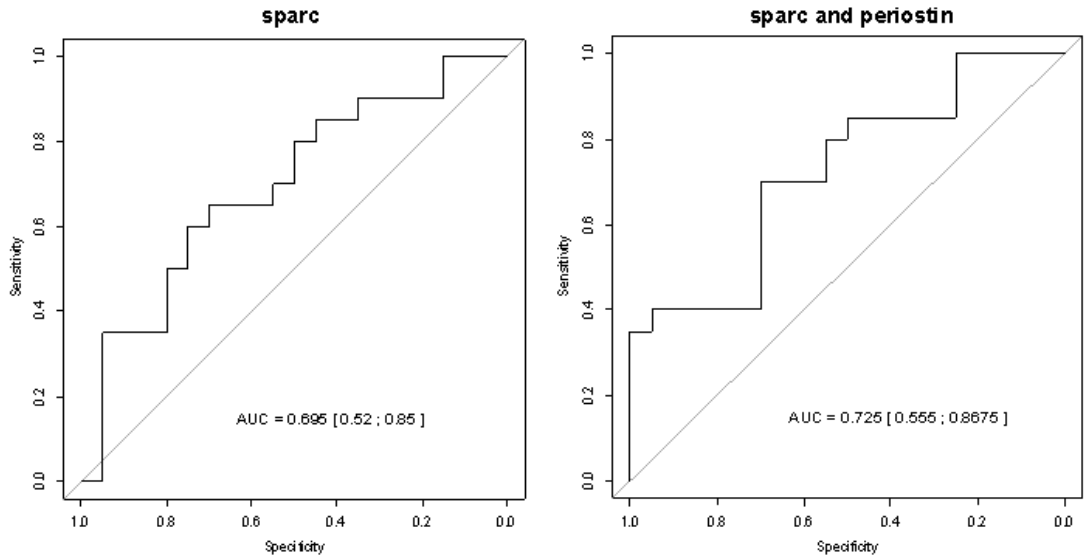

LOGISTIC MODELS WITH CONTINUOUS VARIABLE

	OR [CI]	p	C
Model 1			
SPARC	4.14 [1.04; 16.51]	0.103	0.696
Model 2			
SPARC	4.89 [1.14; 20.96]	0.07	0.722
PERIOSTIN	1.38 [0.58; 3.26]	0.362	

Figure 5. 11. Receiver Operating Characteristics (ROC) curves and Odds Ratio (OR) value for potential predictors in AS patients. (*Upper panel*) Areas under the ROC curves (AUC) and relative 95% confidence interval measurement of sparc or of saprc/periostin combination. The area AUC represents the accuracy of the individual and combined potential biomarkers for distinguishing upgrading patients in AS protocols. (*Lower panel*) OR values were defined by using of sparc (model 1) or sparc and periostin circulating levels (model 2) as continuous variable to estimate the risk to experience upgrading event during AS. Abbreviations: AUC= Area Under the ROC Curve, OR = Odds Ratio, CI = 95% Confidence Interval, p= p-value, C = Harrell's C discrimination index.

To further investigate the potential of sparc and periostin as predictors of upgrading event in AS patients, we developed a logistic model based on index score. Specifically, the index was defined by combining arbitrary scores assigned to specific sparc and periostin quantification levels. Following this strategy, we confirmed that high

expression levels of sparc was per se indicative of an increased probability of experiencing upgrading (OR 4.33 IC95%: 1.15-16.32; C 0.675) and that, by adding periostin to the model, such probability was improved (OR 4.33; IC95%: 1.15-16.32; C 0.702). Overall, these findings indicated that both logistic models were improved by the addition of periostin.

LOGISTIC MODELS WITH INDEX SCORE

	OR [CI]	p	C
SPARC	4.33 [1.15; 16,32]	0.030	0.675
SPARC and PERIOSTIN	20.54 [1.59; 265.02]	0.021	0.702

Figure 5. 12. . Logistic model with index score for risk assessment in AS patients. OR values were defined by combining sparc and periostin circulating levels as categorical variables to estimate the risk to experience upgrading event during AS. Abbreviations: AUC= Area Under the ROC Curve, OR = Odds Ratio, CI = 95% Confidence Interval, p= p-value, C = Harrell's C discrimination index.

5.2.4. *Evaluation of periostin and sparc as potential predictors in an extended cohort of AS patients*

To further support these results, we investigated the ability of circulating sparc and periostin to predict upgrading in an extended cohort of AS patients, including plasma samples collected at inclusion in AS protocol form a total of 60 patients, of whom 20 discontinued AS due to upgrading at the re-biopsy, and 40 still in AS for at least 5 years. As described for the explorative experiments, we assessed circulating sparc and

periostin protein levels in baseline plasma samples by using ELISA assays. In agreement with what we observed in our explorative experiments, the results derived from the combination of the two series (explorative and extended cohort) consisting of 100 patients (40 up-grading and 60 indolent) highlighted that the ability of sparc to discriminate between the two groups of patients was better than that of periostin, although the data did not reach statistical significance (Figure 5.13).

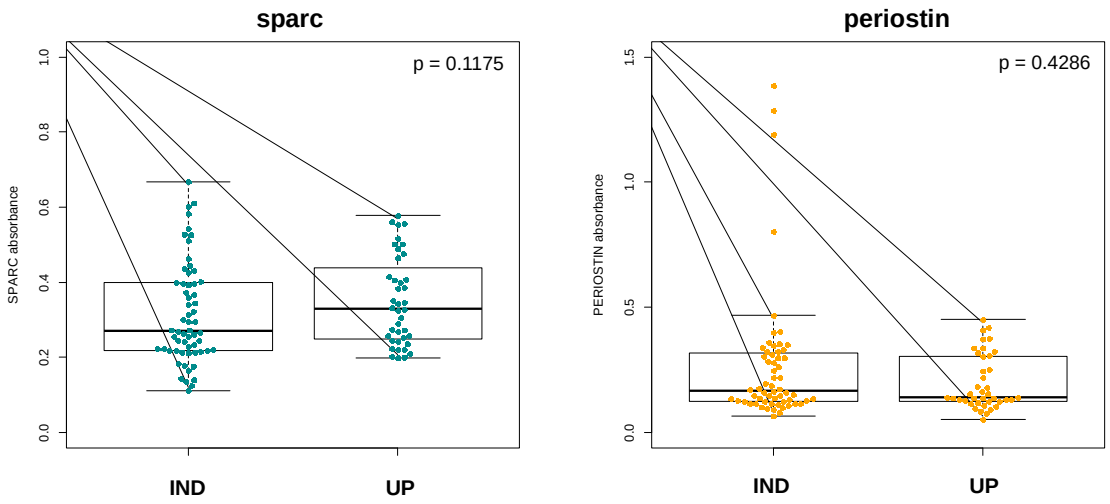

Figure 5. 13. Sparc and periostin plasma levels evaluated in a cohort of 100 AS patients. Quantification of sparc and periostin plasma levels using ELISA assays in 100 AS patients, 60 from the upgrading group (UP) and 40 from the indolent group (IND). Data are reported as absorbance (optical density). Wilcoxon test was performed and $p<0.05$ was considered significant.

In contrast to our previous observation, the logistic models obtained by modulating sparc as a continuous variable indicated that the AUC of sparc reached a value of about 0.598 (figure 5.14, left panel), lower than our previous model (figure 5.12). Unfortunately, our results indicated that when periostin was added to the logistic model, the risk predictive value of two candidate biomarkers was not sufficient to

discriminate between patients really suitable for undergoing an AS protocol and patients who experience upgrading event at the first re-biopsy (AUC: 0.616; IC 95% 0.505-0.726) (Figure 5.14).

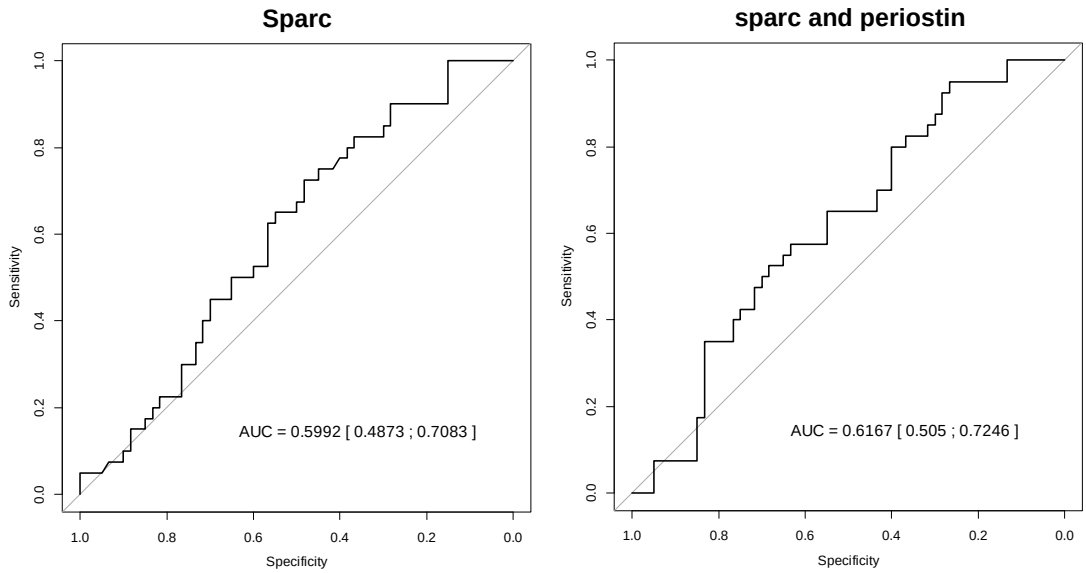

LOGISTIC MODELS WITH CONTINUOUS VARIABLE

	OR [CI]	p	C
Model 1			
SPARC	2.41 [1.04; 5.58]	0.115	0.598
Model 2			
PERIOSTIN	0.78 [0.36; 1.71]	0.417	0.564
Model 3			
SPARC	1.60 [0.88; 2.92]	0.124	0.617
PERIOSTIN	0.65 [0.37; 1.14]	0.134	

Figure 5. 14. Receiver Operating Characteristics (ROC) curves and Odds Ratio (OR) value for potential predictors in AS patients. (*Upper panel*) AUC and relative 95% confidence interval value of sparc and sparc combined with periostin. The area AUC represents the accuracy of the individual and combined potential biomarkers for distinguishing upgrading patients in AS protocols. (*Lower panel*) OR values were assessed by using of sparc or sparc and periostin circulating levels as continuous variable to estimate upgrading event during AS. Abbreviations: AUC= Area Under the ROC Curve, OR = Odds Ratio, CI = 95% Confidence Interval, p= p-value,C = Harrell's C discrimination index.

5.2.5. *Circulating periostin levels are elevated in patients with clinically significant PCa*

Considering the limitations of studying novel prognostic biomarkers in AS cohorts, which include patients characterised by low-grade tumoural foci (GS ≤ 6) and low tumoural burden (n<2 of positive cores biopsy at the diagnosis), we sought to assess the prognostic potential of circulating periostin in patients with clinically relevant organ-confined PCa, who are subjected to radical therapies. In this setting, we assessed exclusively the plasma levels of periostin due to our findings highlighting the correlation between periostin score and PCa tumour grade. Specifically, we evaluated periostin levels in the plasma collected at the diagnosis (baseline) from 21 patients with GS >6 PCa tumours treated with radical radiotherapy, by using ELISA assays. Interestingly, in this cohort of PCa patients, we found significantly enhanced circulating periostin levels with respect to AS patients. This piece of evidence further confirmed our previous observations, suggesting that elevated periostin plasma levels could reflect the presence of high-grade PCa foci (Figure 5.15).

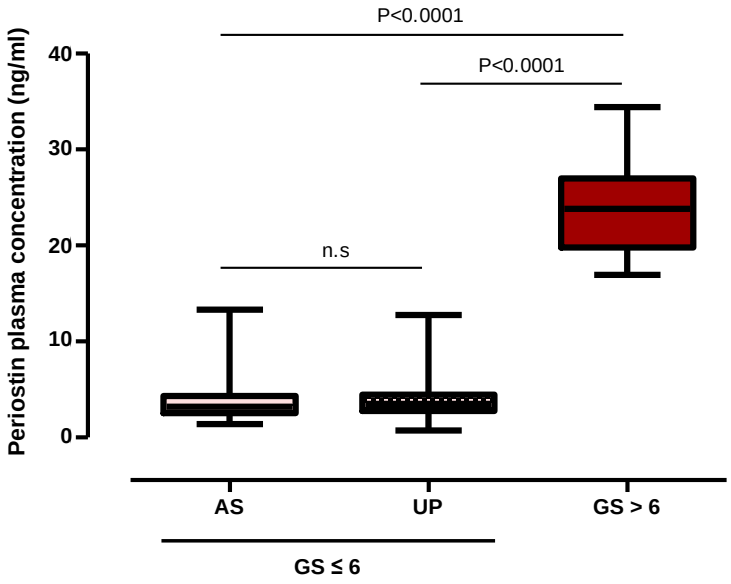

Figure 5. 15. Periostin plasma levels evaluated in PCa patients. Quantification of periostin plasma levels using ELISA assays in 100 AS patients (60 upgrading group (UP), 40 indolent group (IND)) and 21 clinically relevant PCa patients (GS>6). Data are reported as plasma concentration (ng/ml). The level of significance was reported as p-value according to Students' test. Abbreviation: n.s= not significant.

Discussion

6. DISCUSSION

6.1. Drug repositioning approaches to counteract the activated phenotype of CAFs

Tumours display a complex and heterogeneous microenvironment consisting of stromal cells, structural components, and immune infiltrating cells [128]. In the last decade, several studies highlighted the important role of tumour microenvironment in promoting cancer progression and dissemination [129]. Among the cellular populations within the tumour microenvironment, fibroblasts are the most represented cells of the reactive stroma. In normal tissues, fibroblasts are quiescent and play suppressive functions, covering the regulation and the repression of abnormal epithelial cell growth [130]. However, in the tumour microenvironment cancer-associated fibroblasts (CAFs) become activated, thus changing their cell functions and structure. CAF functions range from promoting tumour cell proliferation, migration and invasion, to modulating tumour immunosuppressive environment and pro-inflammatory factors secretion [131]. In PCa, it has been reported that the reactive stroma fosters tumour progression and affects response to therapies. However, the mechanisms that underlie such processes are not clear and further investigations are needed [81132]. In this regard, defining relevant reactive stromal gene signatures for PCa progression could help understand tumour-stroma crosstalk and promote the development of novel therapeutic strategies aimed at targeting the stroma rather than tumour cells.

For this reason, we have recently performed a gene expression profiling analysis comparing CAFs isolated from radical prostatectomy specimens and normal fibroblasts

stimulated with interleukin-6 (IL-6) or transforming growth factor-β (TGF-β), in order to define the molecular signatures involved in fibroblast activation [89]. Results from this study showed that prostate-derived CAF transcriptome strictly resembles that of normal fibroblasts stimulated in vitro with IL-6, showing for the first time that IL-6 is able *per se* to induce most of the transcriptional changes characteristic of patient-derived CAFs. Interestingly, gene sets related to glycolysis/gluconeogenesis and muscle contraction, including the so-called "cardiomyopathy" gene set and "voltage-gated cation channel activity", were found positively enriched in all types of activated fibroblast profiled, suggesting a crucial role for such pathways in stromal phenoconversion [89]. Hence, an intriguing scenario emerged concerning a possible similarity between prostate CAFs and myocardiocytes.

Based on these findings, we were encouraged to pursue the identification of stromal gene signature functionally involved in fibroblast activation, in order to investigate therapeutic approaches aimed at targeting CAFs in the PCa microenvironment. Among the genes that we found differently expressed and up-modulated in CAFs, we focused on "voltage-gated channel activity" gene set, which includes genes coding for cation channel proteins involved into the regulation of cation flux across cell membranes [89].

Currently, scanty information is available on cation channels' role in prostate CAFs. In this regard, Vancauwenberghe and collaborators reported that stromal TRPA1-calcium channel was able to reduce resveratrol-induced apoptosis in PCa cells [133]. However, the role of cation channels has been widely studied in physiological and pathological processes, including carcinogenesis. Noteworthy, Prevarskaya and colleagues categorised the carcinogenesis process as a special type of "channelopathy", due to the tight association that has been observed between cation channel dysfunctions and

cancer hallmarks, including aberrant cellular proliferation and differentiation, uncontrolled apoptosis, and increased cellular motility [134].

Encouraged by the relevance of cation channel involvement in physiological processes and in multiple carcinogenesis steps, which are clearly influenced by reactive stroma, we investigated the role of cation channels in the tumour-stroma crosstalk.

Starting from this, the most up-modulated voltage-gated channel genes in CAFs, namely CACNA1H, CACNB1, CACNB3, SCN2A, SCN1B and KCNS3, were selected and their role in fibroblast activation was evaluated. Initially, we validated our gene expression data by assessing the expression levels of the following cation channels CACNA1H, CACNB1-3, SCN2A, SCAN1B, and KCNS3 in an independent panel of three paired CAFs and HPFs isolated from clinical samples collected at our Institute. Such cation channels were confirmed to be significantly up modulated in CAFs compared to HPFs, at both the mRNA and protein levels (Figure 4.3). Moreover, in agreement with our starting point, observations derived from the analysis of a public data set, which includes several paired prostate CAFs and HPFs (Figure 4.2), confirmed that the “voltage-gated cation channel activity” gene set was enriched in genes up-regulated in CAFs.

Once validated our gene expression results, we experimentally confirmed the involvement of cation channels in fibroblast activation, by performing an in vitro activation of fibroblasts, in which HPFs were exposed to conditioned medium (CM) of DU145 cells. As a result, HPFs exposed to PCa stimuli were characterised by a simultaneous up-modulation of fibroblast activation markers and cation channels, thus suggesting the involvement of ion channels in fibroblast activation process (Figure 4.4 and 4.5).

These observations provided the first functional evidence of a possible role of cation channels in prostate CAF activated phenotype, and prompted us to investigate drug-based strategies aimed at counteracting CAF activated phenotype by targeting cation channels.

Once the involvement of cation channels in fibroblasts activation was confirmed, the potential of specific drugs able to block the activity of the channels that we found up-regulated was assessed in order to potentially revert CAF activated phenotype. By following a drug-repositioning approach, we selected amiodarone, verapamil, nifedipine and flecainide, which are common antiarrhythmic drugs used in the clinical practice to control and regulate the cardiac rhythm [117]. Specifically, we packed-out amiodarone, a class II agent able to inhibit potassium (e.g. KCNS3) as well as calcium and sodium channels [135], verapamil and nifedipine, class IV agents able to counteract the activity of calcium channels (e.g. CACNA1H, CACNB1-3) [136], and flecainide, a class Ic drug active against sodium channels (e.g. SCN2A, SCAN1B) [137].

Several studies defined CAFs as a heterogeneous cell population, characterised by the expression of various mesenchymal proteins. However, none of the CAF markers described so far is peculiar for this cell type [138]. According to the variety of factors associated with CAF activated phenotype, we found that α-SMA and collagen1a1, which are the most widespread fibroblast activation markers, were slightly reduced in CAFs upon antiarrhythmics treatment, even if with different extent depending on the drug and the doses (Figure 4.8).

In order to create a permissive environment for cancer cells, CAFs are characterised by an enhanced cell motility and an increased extracellular matrix (ECM) production and remodelling activities [118]. Therefore, the impact of antiarrhythmics on CAF migratory

potential and ECM remodelling effectiveness were assessed. Interestingly, antiarrhythmics were able to reduce CAF motility (Figure 4.9) by impairing focal adhesion formation during CAF migration process, as assessed by a decreased FAK phosphorylation expression (Figure 4.10). Moreover, ECM remodelling capability of CAFs was affected upon the treatment (Figure 4.11), suggesting that antiarrhythmics could reduce CAF-induced desmoplastic reaction and potentially affect metastatic processes. Altogether, these changes indicated that antiarrhythmics were able to induce in CAFs a phenoconversation from an activated phenotype, characterised by the up-modulation of fibroblast activation markers, migration and ECM remodelling potential, to a more quiescent state that resembled that of HPFs.

Despite the elevated inter-individual heterogeneity that characterises CAF phenotype, the similarities between HPFs and antiarrhythmic treated-CAFs were further confirmed by gene expression profiling analysis. According to PCA analysis, antiarrhythmic treated-CAF profiles were found spatially aligned in-between HPF and CAF profiles, which instead were clearly sorted (Figure 4.12). Moreover, interesting communalities between HPFs and antiarrhythmic-treated CAFs were clarified by GSEA. Notably, , EMT-related gens, glycolysis, hypoxia, protein secretion pathways and TGF- β signalling were found to be simultaneously down-modulated in antiarrhythmic-treated CAFs and HPFs compared to CAFs (Figure 4.13 and 4.14). In contrast, the up-modulation of those gene sets was found in CAFs (Figure 4.13 and 4.14). These findings are in line with the role of TGF-β signalling in PCa tumour microenvironment. As well established, TGF-β signalling activation in prostate fibroblasts is associated with a tumour-promoting phenotype, which relies on the secretion of tumourigenic factors, such as CXCL-12 [139]. In addition, CAFs in PCa tumour microenvironment are subjected to a metabolic reprogramming to provide crucial metabolites for cancer cell

growth. Specifically, cancer cells are able to induce the shift of CAFs from an oxidative phosphorylation metabolism to aerobic glycolysis, through TGF-β signalling activation [68,69,140]. Interestingly, in our antiarrhythmic-treated CAFs setting, the simultaneous down-modulation of TGF-β signalling, glycolysis, hypoxia and protein secretion pathways was indicative of a possible role of antiarrhythmics as suppressors of the metabolic boost provided by CAFs to PCa cells.

Overall, these findings highlighted that antiarrhythmics are able to substantially shift CAF-activated phenotype into HPFs, mainly by inhibiting CAF motility and ECM remodelling capability and also suppressing CAF-metabolic reprogramming induced by PCa cells.

It is well known that the progression of cancer cells into a fully malignant tumoural mass is actually supported by tumour-stroma interactions [141]. In PCa, as well for many types of tumours, it has been reported that CAFs are engaged in cancer progression, mainly by inducing the EMT shift and metastatic dissemination, and as well by establishing a mutual metabolic reprogram of cancer cells [83,120]. On this basis, we investigated the biological effects of antiarrhythmics on CAF-PCa cell interplay, by performing CM-based indirect co-culture. Considering the relevance of CAF-promoting effects on cancer cell growth, the impact of antiarrhythmics on CAF-mediated PCa cell proliferation was evaluated. Interestingly, CM of CAFs treated with antiarrhythmics was able to significantly reduce PCa cell growth, partially recapitulating tumour suppressive effects mediated by CM of HPFs on PCa cells (Figure 4.16). In addition, the reduction of PCa cell proliferation induced by CM of CAFs exposed to antiarrhythmics was associated mainly with the induction of subG1/G1 arrest (Figure 4.17). However, a substantial improvement of PCa cell

proliferation by CAFs was not observed in our experimental setting. In this regard, controversial information has been reported regarding the ability of CAFs to promote cell growth of PCa cell lines. In fact, metastatic-PCa cell lines were shown to be less sensitive to the CAF-induced proliferative spur than non-metastatic cell lines [79]. Regarding EMT modulation, the role of CAFs in promoting EMT in tumour cells has been instead established in many cancers, as well in the PCa setting [120]. Consistent with this role, a shift from a epithelial-like to a mesenchymal-like phenotype was observed in DU145 cells exposed to CM from CAFs (Figure 4.18). Surprisingly, a significant improvement of cell organised in clusters was found in DU145 cells cultured with CM of antiarrhythmic-treated CAFs, as well with CM-HPFs (Figure 4.18). These changes were consistent with the increased amount of E-cadherin and β-catenin found in DU145 cells cultured with CM of antiarrhythmic-treated CAFs or of HPFs. In contrast, decreased levels of E-cadherin and β-catenin, with concomitant up-modulation of vimentin and snail were detected in DU145 cells exposed to CM from untreated CAFs (Figure 4.17). Altogether, these findings indicate that antiarrhythmics are able not only to abrogate CAF-induced EMT in DU145 cells but also to revert the mesenchymal phenotype, as observed with HPFs. Given the relevance of migration processes in cancer dissemination, we also found that antiarrhythmics were able to influence CAF-mediated PCa cell migration. Specifically, CM of CAFs treated with nifedipiine and flecainide – two of our most promising drugs – was able to significantly reduce DU145 cell migratory potential (Figure 4.20). Furthermore, since MMPs are essential for cell migration and invasion, we investigated whether antiarrhythmics were able to counteract their expression/secretion by CAFs (120) . Interestingly, the levels of MMP-2 were found to be reduced in the CM of CAFs treated with nifedipine or flecainide (Figure 4.21). In line with our observation, Giannoni and collaborators indicated that

MMP-2 was produced and released in the interstitial tissues by prostate CAFs, thus promoting a marked remodelling of the stroma, and fostering PCa invasion and dissemination [121]. Overall, these findings indicated that antiarrhythmics were able to act on CAF-PCa interaction, mainly by reverting the CAF-induced EMT and potentially by impairing PCa cell invasion

On this promising basis, we were strongly encouraged to pursue the investigation of antiarrhythmics effect in the in vivo setting. Consistent with the in vitro observations, intratumoural injection of CM of CAFs treated with antiarrhythmics was able to significantly delay tumour growth (Figure 4.25 and Figure 4.26) and reduce E-cadherin expression of PCa xenografts (Figure 4.27).

Overall, this study provided evidence that antiarrhythmics could act as promising inhibitors of CAF-PCa interplay in vitro and in vivo. Actually, CAF-mediated tumour promoting effects, especially with respect to the ECM remodelling capability and CAF-induction of EMT in PCa cells, were substantially affected by antiarrhythmics treatment. in addition considering the impact of the tumour microenvironment in shaping PCa cell metabolism and *vice versa*, antiarrhythmic promising suppressive potential of CAF metabolic pathways could be further invistigated in order to abrogate the reciprocal metabolic interaction between PCa cells and reactive stroma. Our findings may open new innovative opportunities for the translation of drugs already used in the cardiovascular field, specifically those targeting voltage gated cation channels, into novel anticancer regimens, aimed at interrupting the tumour-supportive spur provided by reactive stroma.

6.2. Identification of potential stromal biomarkers for risk assessment in AS patients

AS is a conservative management approach aimed to prevent overtreatment in PCa patients with very low-risk and clinically insignificant disease, characterised by a limited metastatic potential [142]. During AS the signs of the disease are monitored every 3 months, trough PSA level evaluation and digital rectal examination, and a prostate core biopsy is scheduled every 12-24 months [122]. However, the criteria for the correct identification of AS candidates are actually suboptimal and approximately 25% of the patients enrolled discontinue the protocol due to disease reclassification, mainly for the detection of GS>3+3 tumour cores at the first re-biopsy [143]. In this regard, together with the commitment to avoid low-risk PCa overtreatment, the main purpose of a successful AS protocol is the early and correct discrimination between truly clinically insignificant PCa patients and carriers of occult high-risk cancer, in order to guide patients toward the most appropriate treatment [144]. This frame highlights the immediate need of novel selection criteria for AS patients, which may reduce misclassifications. To address these limits, we hypothesized that the presence of a reactive stroma could be relevant for the early detection of significant PCa foci. This hypothesis was sustained by the emerging evidence highlighting the role of tumour microenvironment in PCa carcinogenesis. In this regard, it has been largely reported that stromal changes occur as an early phenomenon in PCa and correlate with the aggressiveness of the disease. For instance, the number of CAFs present in the reactive stroma was increased in higher-grade disease, with respect to prostatic intraepithelial neoplasia (PIN) or low-grade PCa [70]. Specifically, Ayala and collaborators showed that the reactive stroma volume correlates with biochemical recurrence in PCa patients, highlighting that patients with abundant reactive stroma displayed a reduced disease free-survival [74]. Moreover,

extracellular matrix (ECM) proteins, including collagen, fibronectin and tenascin, were found up-modulated in the PCa reactive stroma. Among these proteins, the authors identified desmin and α-SMA as reactive stroma hallmarks associated with recurrence in PCa patients [74]. In addition, Mo and colleagues characterised a stroma-derived metastatic signature able to discriminate between metastatic and non-metastatic PCa PDX models [145], further confirming that the stromal component could be actually considered as an important source of information useful to predict patient outcome.

In this frame, our idea was to define a peculiar reactive stroma signature associated with high-grade PCa foci, in order to improve AS selection criteria and potentially predict patient outcome. As anticipated, we performed a gene expression profiling of prostate derived-CAFs and normal fibroblasts (HPFs) activated in vitro with IL-6 and TGF-β. In this setting, we analysed and selected those genes that we found to be significally up-modulated in at least one of our set of activated fibroblasts. This criterion of selection is based on the assumption that CAFs and "in vitro activated fibroblasts" reasonably up-modulate genes actively involved in the formation of a reactive stroma [89].

Accordingly, considering the relevance of ECM deregulation in reactive stroma, we found a panel of five ECM proteins up-modulated in our set of activated fibroblasts (Figure 5.2). Specifically, we identified postn, col11a1, col10a1, sparc and comp, which encode for ECM proteins found to be associated with reactive stroma in several tumours [146]. Initially, we focused on POSTN, which is the most up-modulated ECM gene in CAFs and in vitro activated fibroblasts (Figure 5.2). POSTN gene encodes for periostin, a glycoprotein protein involved in the ECM deposition that has been reported to be associated with development and progression of several tumours, including PCa

[147148149]. In 2018, Cattrini and collaborators established the relevance of periostin in PCa stroma. In this study, they showed the association of periostin expression levels and patient outcome [150]. Consistent with the emerging role of periostin in the PCa tumour we observed that high expression levels of periostin mRNA were significantly correlated with a higher probability to experience biochemical recurrence (BCR), which is the rise of PSA blood levels upon radical treatment (e.g radical prostatectomy or radiotherapy), in PCa samples from public database (Figure 5.3).

These observations prompted us to investigate the potential of periostin as a risk-assessment biomarker in AS setting. Specifically, our hypothesis was to correlate stromal periostin expression levels with the presence of undetected high-grade PCa foci, in order to reduce the disease misclassification during PCa diagnosis. Consistent with literature data, results derived from our explorative cohort of 116 prostatectomy samples, collected in our institute, indicated that periostin expression was significantly increased in the tumoural stroma component surrounding Gleason score (GS) > 7 PCa foci, with respect to GS ≤ 6 (Figure 5.5). More interestingly, high periostin expression levels were found significantly associated with a specific subgroup of GS 7 tumours (Figure 5.6). The GS 7 tumours are mainly classified by the detection of the Gleason patterns 3 and 4 (3+4 or 4+3) within the tumour foci. Patients with GS 7 tumours were characterised by a wide spectrum of clinical outcomes, ranging from a more favourable outcome to the worst one [151]. This scenario highlighted the urgent needed of novel outcome predictors for these intermediate PCa tumours. Recently, has been shown that a subgroup of GS 7 tumours are characterised by cribriform growth in the Gleason pattern 4. Unfortunately, these patients display a worse prognosis with respect to GS 7 tumours without cribriform morphology. This finding suggests that cribriform morphology requires an unequivocal annotation and identification during diagnosis due

to the relevant impact on patient outcome of this subgroup of tumours [127]. The significant association of periostin staining and cribriform morphology in pattern 4 (Figure 5.5) further supports our idea that the presence of a peculiar reactive stroma could be relevant for the early identification of specific subset of aggressive PCa foci. Finally, given the ability of a reactive stroma to support cancer progression, the prognostic relevance of periosin staining was evaluated. Despite the expectations, the univariate models indicated that periostin displayed a moderate capability to predict biochemical failure in our cohort (Figure 5.7).

As mentioned above, our initial hypothesis was to detect the presence of specific reactive stroma in core biopsies obtained at the diagnosis of AS patients in order to identify the presence of a suspicion aggressive disease and avoid the inclusion in AS apparently indolent PCa patients. Unfortunately, several technical issues and legal aspects, related to the concrete possibility of destroy these precious samples prompted us to investigate alternate strategies for achieving our aim.

Given the well-documented possibility to detect circulating tumour cells (CTCs) and as well tumour-derived molecules, including mRNAs and exosomes, in the blood of cancer patients, we sought to test the relevance of our ECM signature as circulating biomarker for AS patients risk assessment [152]. Currently, no considerable evidence has been collected regarding the potential of stromal circulating signatures in the PCa context. However, our hypothesis was supported by the evidence that tumour-derived molecules, as well CTCs, were found in the blood of PCa patients and their levels correlate with disease classification and patient outcome. Specifically, it has been showed that CTCs obtained from PCa patients harbour peculiar alterations such as TMPRSS2-ERG fusions, PTEN deletions and AR copy number changes, typically associated with PCa [153]. Moreover, Wang and colleagues found that an increased

number of CTCs correlates with poor overall survival in castration-resistant PCa patients [154]. Concerning the potential of miRNAs as novel PCa biomarkers, altered miRNA expression profiles were found in tumoural tissues, as well as in serum and plasma of PCa patients compared to normal tissues and healthy donors [155]. Specifically, a panel of 15 miRNAs (miRNA-16, miRNA-31, miRNA-125b, miRNA-145, miRNA-149, miRNA-181b, miRNA-184, miRNA-205, miRNA-221, miRNA-222, miRNA-96, miRNA-182, miRNA-182*, miRNA-183, miRNA-375) displayed a considerable capability to discriminate normal prostate from PCa tissue with accuracy up to 84% [156]. Moreover, Mitchell and colleagues reported that serum levels of miRNA-141 were able to distinguish PCa patients from healthy donors [157]. Due to their obvious potential and stability in the biologic fluids, miRNAs have emerged as promising diagnostic and prognostic biomarkers able to define tumour staging and treatment responses in PCa patients [158]. Finally, in the last decade, exosomes have emerged as novel circulating disease biomarkers in PCa setting. Interestingly, tumour derived-exosomes could carry specific miRNAs and proteins associate with the tumour. In this regard, an increased amount of prostate-derived vesicles was found to be associated with aggressive disease in PCa patients [158]. In addition, miRNA-profiling analysis of serum-derived exosomes revealed an association of miR-141 and miR-375 with metastatic PCa [159,160] Moreover, higher levels of Survivin were found in plasma-derived exosomes isolated form PCa patients compared to donors, suggesting that tumour-derived molecules, including proteins, could be uses as circulating biomarkers for early detection of PCa [161].

Notably, the cells of origin of such circulating molecules, which reflect the tumour stage and patient outcome, are unknown and it cannot be excluded that circulating molecules could be released in the biologic fluid by reactive stroma surrounding the cancer cells rather than by tumour cells.

In this study, we assessed plasma levels of periostin, col11a1, col10a, comp and sparc in order to correlate their expression with AS patients' outcome. The feasibility of our hypothesis was initially supported by the evidence that periostin, col11a1, coll10a1, sparc and comp were found extensively released in the CM of CAFs (Figure 5.8) and in the plasma of PCa patents (Figure 5.9), especially in those who harbour clinically significant disease.

On this basis, we evaluated the plasma levels of periostin, coll11a1, col101, comp and sparc in an explorative cohort of AS patients by using ELISA assay. No significant difference was found between plasma levels of ECM proteins at the baseline in upgrading vs indolent patients (Figure 5.10). Interestingly, only sparc displayed a limited capability to discriminate upgrading patients from indolent ones (Figure 5.10). However, the combination of sparc and periostin in logistic models revealed a moderate potential of our candidates to predict upgrading event at the baseline (Figure 5.11 and 5.12). Unfortunately, this moderate predictive potential obtained by combining sparc and priostin was not confirmed in an additional cohort of AS patients (Figure 5.13 and 5.14).

Overall, considering the several limitations concerning the study of this peculiar subgroup of PCa patients, our preliminary findings could provide the basis for develop novel strategies for the investigation of circulating molecules derived from the reactive stroma in AS setting. Indeed, patients eligible for AS are characterized by limited tumour burden and a very low-risk disease. This unique setting needs novel biomarkers characterized by a high specific potential to discriminate at the baseline between patients with indolent and insignificant disease patients from an occult aggressive disease.

However, the relevance of circulating periostin was confirmed in the plasma of patient with clinically significant PCa subjected to RT. Specifically, periostin circulating levels were found increased up to 20 compared to the levels observed in AS patients, suggesting that the use of more sensible detection methods could be relevant in the study of circulating biomarkers for cohort patients with apparently homogeneous characteristics, as are AS patients. In this regard, the concrete possibility to detect tumour related biomarkers in the urine sample of AS patients could overpass such limited conditions. It has been reported that urine samples from PCa patients were enriched with tumour components, as well as reactive stroma.

In this complex scenario, additional efforts are required to identify robust novel circulating biomarkers that, in combination with the currently used clinico-pathological parameters, could be particularly useful to guide decision-making for AS patients.

Bibliography

7. BIBLIOGRAPHY

1. Bray F, Ferlay J, Soerjomataram I, Siegel RL, Torre LA, Jemal A. Global cancer statistics 2018: GLOBOCAN estimates of incidence and mortality worldwide for 36 cancers in 185 countries. *CA Cancer J Clin*. 2018;68(6):394-424. doi:10.3322/caac.21492

2. Patel AR, Klein EA. Risk factors for prostate cancer. *Nat Clin Pract Urol*. 2009;6(2):87-95. doi:10.1038/ncpuro1290

3. Roussel B, Ouellet GM, Mohile SG, Dale W. Prostate Cancer in Elderly Men. Screening, Active Surveillance, and Definitive Therapy. *Clin Geriatr Med*. 2015;31(4):615-629. doi:10.1016/j.cger.2015.07.004

4. Bancroft EK, Page EC, Castro E, et al. Targeted prostate cancer screening in BRCA1 and BRCA2 mutation carriers: Results from the initial screening round of the IMPACT study. *Eur Urol*. 2014;66(3):489-499. doi:10.1016/j.eururo.2014.01.003

5. De Marzo AM, Platz EA, Sutcliffe S, et al. Inflammation in prostate carcinogenesis. *Nat Rev Cancer*. 2007;7(4):256-269. doi:10.1038/nrc2090

6. Stamey TA, Yang N, Hay AR, McNeal JE, Freiha FS, Redwine E. Prostate-Specific Antigen as a Serum Marker for Adenocarcinoma of the Prostate. *N Engl J Med*. 1987;317(15):909-916. doi:10.1056/nejm198710083171501

7. Cooner WH, Mosley BR, Rutherford CL, et al. Prostate cancer detection in a clinical urological practice by ultrasonography, digital rectal examination and

prostate specific antigen. *J Urol*. 1990;143(6):1146-1152. doi:10.1016/s0022-5347(17)40211-4

8. Thompson IM, Pauler DK, Goodman PJ, et al. Prevalence of Prostate Cancer among Men with a Prostate-Specific Antigen Level ≤4.0 ng per Milliliter. *N Engl J Med*. 2004;350(22):2239-2246. doi:10.1056/nejmoa031918

9. Carter HB, Albertsen PC, Barry MJ, et al. Early detection of prostate cancer: AUA guideline. *J Urol*. 2013;190(2):419-426. doi:10.1016/j.juro.2013.04.119

10. Wolf AMD, Wender RC, Etzioni RB, et al. American Cancer Society Guideline for the Early Detection of Prostate Cancer: Update 2010. *CA Cancer J Clin*. 2010;60(2):70-98. doi:10.3322/caac.20066

11. Barry MJ. Prostate-Specific–Antigen Testing for Early Diagnosis of Prostate Cancer. *N Engl J Med*. 2001;344(18):1373-1377. doi:10.1056/nejm200105033441806

12. Hodge KK, McNeal JE, Stamey TA. Ultrasound guided transrectal core biopsies of the palpably abnormal prostate. *J Urol*. 1989;142(1):66-70. doi:10.1016/S0022-5347(17)38663-9

13. Gleason DF. Classification of prostatic carcinomas. *Cancer Chemother Rep*. 1966;50(3):125-128.

14. Sathianathen NJ, Konety BR, Crook J, Saad F, Lawrentschuk N. Landmarks in prostate cancer. *Nat Rev Urol*. 2018;15(10):627-642. doi:10.1038/s41585-018-0060-7

15. Delahunt B, Miller RJ, Srigley JR, Evans AJ, Samaratunga H. Gleason grading:

Past, present and future. *Histopathology*. 2012. doi:10.1111/j.1365-2559.2011.04003.x

16. Billis A, Guimaraes MS, Freitas LLL, Meirelles L, Magna LA, Ferreira U. The Impact of the 2005 International Society of Urological Pathology Consensus Conference on Standard Gleason Grading of Prostatic Carcinoma in Needle Biopsies. *J Urol*. 2008;180(2):548-553. doi:10.1016/j.juro.2008.04.018

17. Epstein JI, Egevad L, Amin MB, Delahunt B, Srigley JR, Humphrey PA. The 2014 international society of urological pathology (ISUP) consensus conference on gleason grading of prostatic carcinoma definition of grading patterns and proposal for a new grading system. *Am J Surg Pathol*. 2016;40(2):244-252. doi:10.1097/PAS.0000000000000530

18. Newschaffer CJ, Otani K, McDonald K, Penberthy LT. Causes of death in elderly prostate cancer patients and in a comparison nonprostate cancer cohort. *J Natl Cancer Inst*. 2000;92(8):613-621. doi:10.1093/jnci/92.8.613

19. Tosoian JJ, Trock BJ, Landis P, et al. Active surveillance program for prostate cancer: An update of the Johns Hopkins experience. *J Clin Oncol*. 2011;29(16):2185-2190. doi:10.1200/JCO.2010.32.8112

20. Klotz L. Active surveillance: Patient selection. *Curr Opin Urol*. 2013;23(3):239-244. doi:10.1097/MOU.0b013e32835f8f6b

21. D'Amico A V., Whittington R, Bruce Malkowicz S, et al. Biochemical outcome after radical prostatectomy, external beam radiation therapy, or interstitial radiation therapy for clinically localized prostate cancer. *J Am Med Assoc*.

1998;280(11):969-974. doi:10.1001/jama.280.11.969

22. Epstein JI, Zelefsky MJ, Sjoberg DD, et al. A Contemporary Prostate Cancer Grading System: A Validated Alternative to the Gleason Score. *Eur Urol*. 2016;69(3):428-435. doi:10.1016/j.eururo.2015.06.046

23. Bastian PJ, Carter BH, Bjartell A, et al. Insignificant Prostate Cancer and Active Surveillance: From Definition to Clinical Implications. *Eur Urol*. 2009;55(6):1321-1332. doi:10.1016/j.eururo.2009.02.028

24. Tosoian JJ, Loeb S, Epstein JI, Turkbey B, Choyke PL, Schaeffer EM. Active Surveillance of Prostate Cancer: Use, Outcomes, Imaging, and Diagnostic Tools. *Am Soc Clin Oncol Educ B*. 2016;(36):e235-e245. doi:10.1200/edbk_159244

25. Brumm J. Brachytherapy as a Treatment Option for Prostate Cancer: Overview and Nursing Considerations. *Baylor Univ Med Cent Proc*. 2000;13(3):227-229. doi:10.1080/08998280.2000.11927679

26. Huggins C, Hodges C V. Studies on prostatic cancer i. the effect of castration, of estrogen and of androgen injection on serum phosphatases in metastatic carcinoma of the prostate. *Cancer Res*. 1941;1(4):293-297. doi:10.3322/canjclin.22.4.232

27. HUGGINS C. Studies on Prostatic Cancer. *Arch Surg*. 1941;43(2):209. doi:10.1001/archsurg.1941.01210140043004

28. Ryan CJ, Cheng ML. Abiraterone acetate for the treatment of prostate cancer. *Expert Opin Pharmacother*. 2013;14(1):91-96. doi:10.1517/14656566.2013.745852

29. Tannock IF, de Wit R, Berry WR, et al. Docetaxel plus Prednisone or Mitoxantrone plus Prednisone for Advanced Prostate Cancer. *N Engl J Med*. 2004;351(15):1502-1512. doi:10.1056/nejmoa040720

30. De Bono JS, Oudard S, Ozguroglu M, et al. Prednisone plus cabazitaxel or mitoxantrone for metastatic castration-resistant prostate cancer progressing after docetaxel treatment: A randomised open-label trial. *Lancet*. 2010;376(9747):1147-1154. doi:10.1016/S0140-6736(10)61389-X

31. Kantoff PW, Higano CS, Shore ND, et al. Sipuleucel-T Immunotherapy for Castration-Resistant Prostate Cancer. *N Engl J Med*. 2010;363(5):411-422. doi:10.1056/nejmoa1001294

32. Saini S. PSA and beyond: alternative prostate cancer biomarkers. *Cell Oncol*. 2016;39(2):97-106. doi:10.1007/s13402-016-0268-6

33. Schröder FH, Hugosson J, Roobol MJ, et al. Screening and prostate cancer mortality: Results of the European Randomised Study of Screening for Prostate Cancer (ERSPC) at 13 years of follow-up. *Lancet*. 2014;384(9959):2027-2035. doi:10.1016/S0140-6736(14)60525-0

34. Auvinen A, Moss SM, Tammela TLJ, et al. Absolute effect of prostate cancer screening: Balance of benefits and harms by center within the European Randomized Study of prostate cancer screening. *Clin Cancer Res*. 2016;22(1):243-249. doi:10.1158/1078-0432.CCR-15-0941

35. Catalona WJ, Partin AW, Slawin KM, et al. Use of the percentage of free prostate-specific antigen to enhance differentiation of prostate cancer from

benign prostatic disease: A prospective multicenter clinical trial. *J Am Med Assoc*. 1998;279(19):1542-1547. doi:10.1001/jama.279.19.1542

36. Partin AW, Brawer MK, Subong ENP, et al. Prospective evaluation of percent free-PSA and complexed-PSA for early detection of prostate cancer. *Prostate Cancer Prostatic Dis*. 1998;1(4):197-203. doi:10.1038/sj.pcan.4500232

37. Mikolajczyk SD, Millar LS, Wang TJ, et al. A precursor form of prostate-specific antigen is more highly elevated in prostate cancer compared with benign transition zone prostate tissue. *Cancer Res*. 2000;60(3):756-759.

38. Tosoian JJ, Druskin SC, Andreas D, et al. Prostate Health Index density improves detection of clinically significant prostate cancer. *BJU Int*. 2017;120(6):793-798. doi:10.1111/bju.13762

39. Catalona WJ, Partin AW, Sanda MG, et al. A multicenter study of [-2]pro-prostate specific antigen combined with prostate specific antigen and free prostate specific antigen for prostate cancer detection in the 2.0 to 10.0 ng/ml prostate specific antigen range. *J Urol*. 2011;185(5):1650-1655. doi:10.1016/j.juro.2010.12.032

40. Bussemakers MJG, Van Bokhoven A, Verhaegh GW, et al. DD3: A new prostate-specific gene, highly overexpressed in prostate cancer. *Cancer Res*. 1999;59(23):5975-5979.

41. Prensner JR, Rubin MA, Wei JT, Chinnaiyan AM. Beyond PSA: The next generation of prostate cancer biomarkers. *Sci Transl Med*. 2012;4(127). doi:10.1126/scitranslmed.3003180

42. Tosoian JJ, Loeb S, Kettermann A, et al. Accuracy of PCA3 Measurement in Predicting Short-Term Biopsy Progression in an Active Surveillance Program. *J Urol*. 2010;183(2):534-538. doi:10.1016/j.juro.2009.10.003

43. Hessels D, Van Gils MPMQ, Van Hooij O, et al. Predictive value of PCA3 in urinary sediments in determining clinico-pathological characteristics of prostate cancer. *Prostate*. 2010;70(1):10-16. doi:10.1002/pros.21032

44. Demichelis F, Fall K, Perner S, et al. TMPRSS2:ERG gene fusion associated with lethal prostate cancer in a watchful waiting cohort. *Oncogene*. 2007. doi:10.1038/sj.onc.1210237

45. Tomlins SA, Rhodes DR, Perner S, et al. Recurrent fusion of TMPRSS2 and ETS transcription factor genes in prostate cancer. *Science (80-)*. 2005;310(5748):644-648. doi:10.1126/science.1117679

46. Salami SS, Schmidt F, Laxman B, et al. Combining urinary detection of TMPRSS2: ERG and PCA3 with serum PSA to predict diagnosis of prostate cancer. *Urol Oncol Semin Orig Investig*. 2013;31(5):566-571. doi:10.1016/j.urolonc.2011.04.001

47. Barbieri CE, Baca SC, Lawrence MS, et al. Exome sequencing identifies recurrent SPOP, FOXA1 and MED12 mutations in prostate cancer. *Nat Genet*. 2012;44(6):685-689. doi:10.1038/ng.2279

48. Gandellini P, Casiraghi N, Rancati T, et al. Core Biopsies from Prostate Cancer Patients in Active Surveillance Protocols Harbor PTEN and MYC Alterations. *Eur Urol Oncol*. 2019;2(3):277-285. doi:10.1016/j.euo.2018.08.010

49. Stewart GD, Van Neste L, Delvenne P, et al. Clinical utility of an epigenetic assay to detect occult prostate cancer in histopathologically negative biopsies: Results of the MATLOC study. *J Urol*. 2013;189(3):1110-1116. doi:10.1016/j.juro.2012.08.219

50. Klein EA, Cooperberg MR, Magi-Galluzzi C, et al. A 17-gene assay to predict prostate cancer aggressiveness in the context of gleason grade heterogeneity, tumor multifocality, and biopsy undersampling. *Eur Urol*. 2014;66(3):550-560. doi:10.1016/j.eururo.2014.05.004

51. Erho N, Crisan A, Vergara IA, et al. Discovery and Validation of a Prostate Cancer Genomic Classifier that Predicts Early Metastasis Following Radical Prostatectomy. *PLoS One*. 2013;8(6). doi:10.1371/journal.pone.0066855

52. Blume-Jensen P, Berman DM, Rimm DL, et al. Biology of Human Tumors Development and clinical validation of an in situ biopsy-based multimarker assay for risk stratification in prostate cancer. *Clin Cancer Res*. 2015;21(11):2591-2600. doi:10.1158/1078-0432.CCR-14-2603

53. Mueller MM, Fusenig NE. Friends or foes - Bipolar effects of the tumour stroma in cancer. *Nat Rev Cancer*. 2004;4(11):839-849. doi:10.1038/nrc1477

54. Öhlund D, Elyada E, Tuveson D. Fibroblast heterogeneity in the cancer wound. *J Exp Med*. 2014;211(8):1503-1523. doi:10.1084/jem.20140692

55. De Wever O, Van Bockstal M, Mareel M, Hendrix A, Bracke M. Carcinoma-associated fibroblasts provide operational flexibility in metastasis. *Semin Cancer Biol*. 2014;25:33-46. doi:10.1016/j.semcancer.2013.12.009

56. Dumont N, Liu B, Defilippis RA, et al. Breast fibroblasts modulate early dissemination, tumorigenesis, and metastasis through alteration of extracellular matrix characteristics. *Neoplasia (United States)*. 2013;15(3):249-262. doi:10.1593/neo.121950

57. Parsonage G, Filer AD, Haworth O, et al. A stromal address code defined by fibroblasts. *Trends Immunol*. 2005;26(3):150-156. doi:10.1016/j.it.2004.11.014

58. Tomasek JJ, Gabbiani G, Hinz B, Chaponnier C, Brown RA. Myofibroblasts and mechano: Regulation of connective tissue remodelling. *Nat Rev Mol Cell Biol*. 2002;3(5):349-363. doi:10.1038/nrm809

59. Aoyagi Y, Oda T, Kinoshita T, et al. Overexpression of TGF-β by infiltrated granulocytes correlates with the expression of collagen mRNA in pancreatic cancer. *Br J Cancer*. 2004;91(7):1316-1326. doi:10.1038/sj.bjc.6602141

60. Löhr M, Schmidt C, Ringel J, et al. Transforming growth factor-β1 induces desmoplasia in an experimental model of human pancreatic carcinoma. *Cancer Res*. 2001;61(2):550-555.

61. Elenbaas B, Weinberg RA. Heterotypic signaling between epithelial tumor cells and fibroblasts in carcinoma formation. *Exp Cell Res*. 2001;264(1):169-184. doi:10.1006/excr.2000.5133

62. Kalluri R, Zeisberg M. Fibroblasts in cancer. *Nat Rev Cancer*. 2006;6(5):392-401. doi:10.1038/nrc1877

63. Lochter A, Galosy S, Muschler J, Freedman N, Werb Z, Bissell MJ. Matrix metalloproteinase stromelysin-1 triggers a cascade of molecular alterations that

leads to stable epithelial-to-mesenchymal conversion and a premalignant phenotype in mammary epithelial cells. *J Cell Biol*. 1997;139(7):1861-1872. doi:10.1083/jcb.139.7.1861

64. Malanchi I, Santamaria-Martínez A, Susanto E, et al. Interactions between cancer stem cells and their niche govern metastatic colonization. *Nature*. 2012;481(7379):85-91. doi:10.1038/nature10694

65. O'Connell JT, Sugimoto H, Cooke VG, et al. VEGF-A and Tenascin-C produced by S100A4 + stromal cells are important for metastatic colonization. *Proc Natl Acad Sci U S A*. 2011;108(38):16002-16007. doi:10.1073/pnas.1109493108

66. Calon A, Espinet E, Palomo-Ponce S, et al. Dependency of Colorectal Cancer on a TGF-β-Driven Program in Stromal Cells for Metastasis Initiation. *Cancer Cell*. 2012;22(5):571-584. doi:10.1016/j.ccr.2012.08.013

67. Pavlides S, Whitaker-Menezes D, Castello-Cros R, et al. The reverse Warburg effect: Aerobic glycolysis in cancer associated fibroblasts and the tumor stroma. *Cell Cycle*. 2009. doi:10.4161/cc.8.23.10238

68. Guido C, Whitaker-Menezes D, Capparelli C, et al. Metabolic reprogramming of cancer-associated fibroblasts by TGF-β drives tumor growth: Connecting TGF-β signaling with 'Warburg- like' cancer metabolism and L-lactate production. *Cell Cycle*. 2012;11(16):3019-3035. doi:10.4161/cc.21384

69. Fiaschi T, Marini A, Giannoni E, et al. Reciprocal metabolic reprogramming through lactate shuttle coordinately influences tumor-stroma interplay. *Cancer Res*. 2012;72(19):5130-5140. doi:10.1158/0008-5472.CAN-12-1949

70. Tuxhorn JA, Ayala GE, Rowley DR. Reactive stroma in prostate cancer progression. *J Urol*. 2001;166(6):2472-2483. doi:10.1016/S0022-5347(05)65620-0

71. Tomas D, Ulamec M, Hudolin T, Bulimbašić S, Belicza M, Krušlin B. Myofibroblastic stromal reaction and expression of tenascin-C and laminin in prostate adenocarcinoma. *Prostate Cancer Prostatic Dis*. 2006;9(4):414-419. doi:10.1038/sj.pcan.4500874

72. Tuxhorn JA, Ayala GE, Smith MJ, Smith VC, Dang TD, Rowley DR. Reactive stroma in human prostate cancer: Induction of myofibroblast phenotype and extracellular matrix remodeling. *Clin Cancer Res*. 2002;8(9):2912-2923.

73. Palumbo A, Ferreira LB, Reis de Souza PAV, et al. Extracellular matrix secreted by reactive stroma is a main inducer of pro-tumorigenic features on LNCaP prostate cancer cells. *Cancer Lett*. 2012;321(1):55-64. doi:10.1016/j.canlet.2012.02.026

74. Ayala G, Tuxhorn JA, Wheeler TM, et al. Reactive Stroma as a Predictor of Biochemical-Free Recurrence in Prostate Cancer. *Clin Cancer Res*. 2003;9(13):4792-4801.

75. Cirri P, Chiarugi P. Cancer-associated-fibroblasts and tumour cells: A diabolic liaison driving cancer progression. *Cancer Metastasis Rev*. 2012;31(1-2):195-208. doi:10.1007/s10555-011-9340-x

76. Zhang T, Lee WYW, Rui YF, Cheng TY, Jiang XH, Li G. Bone marrow-derived mesenchymal stem cells promote growth and angiogenesis of breast and prostate

tumors. *Stem Cell Res Ther*. 2013;4(3). doi:10.1186/scrt221

77. Zeisberg EM, Potenta S, Xie L, Zeisberg M, Kalluri R. Discovery of endothelial to mesenchymal transition as a source for carcinoma-associated fibroblasts. *Cancer Res*. 2007;67(21):10123-10128. doi:10.1158/0008-5472.CAN-07-3127

78. Taddei ML, Giannoni E, Comito G, Chiarugi P. Microenvironment and tumor cell plasticity: An easy way out. *Cancer Lett*. 2013;341(1):80-96. doi:10.1016/j.canlet.2013.01.042

79. Paland N, Kamer I, Kogan-Sakin I, Madar S, Goldfinger N, Rotter V. Differential influence of normal and cancer-associated fibroblasts on the growth of human epithelial cells in an in vitro cocultivation model of prostate cancer. *Mol Cancer Res*. 2009;7(8):1212-1223. doi:10.1158/1541-7786.MCR-09-0073

80. Giannoni E, Bianchini F, Masieri L, et al. Reciprocal activation of prostate cancer cells and cancer-associated fibroblasts stimulates epithelial-mesenchymal transition and cancer stemness. *Cancer Res*. 2010. doi:10.1158/0008-5472.CAN-10-0785

81. Olumi AF, Grossfeld GD, Hayward SW, Carroll PR, Tlsty TD, Cunha GR. Carcinoma-associated fibroblasts direct tumor progression of initiated human prostatic epithelium. *Cancer Res*. 1999;59(19):5002-5011.

82. Giannoni E, Bianchini F, Calorini L, Chiarugi P. Cancer associated fibroblasts exploit reactive oxygen species through a proinflammatory signature leading to epithelial mesenchymal transition and stemness. *Antioxidants Redox Signal*. 2011;14(12):2361-2371. doi:10.1089/ars.2010.3727

83. Gandellini P, Giannoni E, Casamichele A, et al. MiR-205 hinders the malignant interplay between prostate cancer cells and associated fibroblasts. *Antioxidants Redox Signal*. 2014;20(7):1045-1059. doi:10.1089/ars.2013.5292

84. Gandellini P, Folini M, Longoni N, et al. MiR-205 exerts tumor-suppressive functions in human prostate through down-regulation of protein kinase Cε. *Cancer Res*. 2009;69(6):2287-2295. doi:10.1158/0008-5472.CAN-08-2894

85. Dean JP, Nelson PS. Profiling influences of senescent and aged fibroblasts on prostate carcinogenesis. *Br J Cancer*. 2008;98(2):245-249. doi:10.1038/sj.bjc.6604087

86. Bavik C, Coleman I, Dean JP, Knudsen B, Plymate S, Nelson PS. The gene expression program of prostate fibroblast senescence modulates neoplastic epithelial cell proliferation through paracrine mechanisms. *Cancer Res*. 2006;66(2):794-802. doi:10.1158/0008-5472.CAN-05-1716

87. Yang G, Rosen DG, Zhang Z, et al. The chemokine growth-regulated oncogene 1 (Gro-1) links RAS signaling to the senescence of stromal fibroblasts and ovarian tumorigenesis. *Proc Natl Acad Sci U S A*. 2006;103(44):16472-16477. doi:10.1073/pnas.0605752103

88. Taddei ML, Cavallini L, Comito G, et al. Senescent stroma promotes prostate cancer progression: The role of miR-210. *Mol Oncol*. 2014;8(8):1729-1746. doi:10.1016/j.molonc.2014.07.009

89. Doldi V, Callari M, Giannoni E, et al. Integrated gene and miRNA expression analysis of prostate cancer associated fibroblasts supports a prominent role for

interleukin-6 in fibroblast activation. *Oncotarget*. 2015;6(31):31441-31460. doi:10.18632/oncotarget.5056

90. Broustas CG, Lieberman HB. RAD9 enhances radioresistance of human prostate cancer cells through regulation of ITGB1 protein levels. *Prostate*. 2014;74(14):1359-1370. doi:10.1002/pros.22842

91. Tuxhorn JA, McAlhany SJ, Dang TD, Ayala GE, Rowley DR. Stromal cells promote angiogenesis and growth of human prostate tumors in a differential reactive stroma (DRS) xenograft model. *Cancer Res*. 2002;62(11):3298-3307.

92. Hurle RA, Davies G, Parr C, et al. Hepatocyte growth factor/scatter factor and prostate cancer: A review. *Histol Histopathol*. 2005;20(4):1339-1349. doi:10.14670/HH-20.1339

93. Kwabi-Addo B, Ozen M, Ittmann M. The role of fibroblast growth factors and their receptors in prostate cancer. *Endocr Relat Cancer*. 2004;11(4):709-724. doi:10.1677/erc.1.00535

94. Santos AM, Jung J, Aziz N, Kissil JL, Puré E. Targeting fibroblast activation protein inhibits tumor stromagenesis and growth in mice. *J Clin Invest*. 2009;119(12):3613-3625. doi:10.1172/JCI38988

95. Fang J, Xiao L, Joo K Il, et al. A potent immunotoxin targeting fibroblast activation protein for treatment of breast cancer in mice. *Int J Cancer*. 2016;138(4):1013-1023. doi:10.1002/ijc.29831

96. Welt S, Divgi CR, Scott AM, et al. Antibody targeting in metastatic colon cancer: A phase I study of monoclonal antibody F19 against a cell-surface

protein of reactive tumor stromal fibroblasts. *J Clin Oncol*. 1994;12(6):1193-1203. doi:10.1200/JCO.1994.12.6.1193

97. Scott AM, Wiseman G, Welt S, et al. A phase I dose-escalation study of sibrotuzumab in patients with advanced or metastatic fibroblast activation protein-positive cancer. *Clin Cancer Res*. 2003;9(5):1639-1647.

98. Loeffler M, Krüger JA, Niethammer AG, Reisfeld RA. Targeting tumor-associated fibroblasts improves cancer chemotherapy by increasing intratumoral drug uptake. *J Clin Invest*. 2006;116(7):1955-1962. doi:10.1172/JCI26532

99. Kakarla S, Chow KKH, Mata M, et al. Antitumor effects of chimeric receptor engineered human T cells directed to tumor stroma. *Mol Ther*. 2013;21(8):1611-1620. doi:10.1038/mt.2013.110

100. Wang LCS, Lo A, Scholler J, et al. Targeting fibroblast activation protein in tumor stroma with chimeric antigen receptor T cells can inhibit tumor growth and augment host immunity without severe toxicity. *Cancer Immunol Res*. 2014;2(2):154-166. doi:10.1158/2326-6066.CIR-13-0027

101. Kraman M, Bambrough PJ, Arnold JN, et al. Suppression of antitumor immunity by stromal cells expressing fibroblast activation protein-α. *Science (80-)*. 2010;330(6005):827-830. doi:10.1126/science.1195300

102. Roberts EW, Deonarine A, Jones JO, et al. Depletion of stromal cells expressing fibroblast activation protein-α from skeletal muscle and bone marrow results in cachexia and anemia. *J Exp Med*. 2013;210(6):1137-1151. doi:10.1084/jem.20122344

103. Zalcman G, Mazieres J, Margery J, et al. Bevacizumab for newly diagnosed pleural mesothelioma in the Mesothelioma Avastin Cisplatin Pemetrexed Study (MAPS): A randomised, controlled, open-label, phase 3 trial. *Lancet*. 2016;387(10026):1405-1414. doi:10.1016/S0140-6736(15)01238-6

104. Ene-Obong A, Clear AJ, Watt J, et al. Activated pancreatic stellate cells sequester CD8+ T cells to reduce their infiltration of the juxtatumoral compartment of pancreatic ductal adenocarcinoma. *Gastroenterology*. 2013;145(5):1121-1132. doi:10.1053/j.gastro.2013.07.025

105. Froeling FEM, Feig C, Chelala C, et al. Retinoic acid-induced pancreatic stellate cell quiescence reduces paracrine Wntβ-catenin signaling to slow tumor progression. *Gastroenterology*. 2011;141(4). doi:10.1053/j.gastro.2011.06.047

106. Sherman MH, Yu RT, Engle DD, et al. Vitamin D receptor-mediated stromal reprogramming suppresses pancreatitis and enhances pancreatic cancer therapy. *Cell*. 2014;159(1):80-93. doi:10.1016/j.cell.2014.08.007

107. Albrengues J, Bertero T, Grasset E, et al. Epigenetic switch drives the conversion of fibroblasts into proinvasive cancer-associated fibroblasts. *Nat Commun*. 2015;6. doi:10.1038/ncomms10204

108. Johnson DE, O'Keefe RA, Grandis JR. Targeting the IL-6/JAK/STAT3 signalling axis in cancer. *Nat Rev Clin Oncol*. 2018;15(4):234-248. doi:10.1038/nrclinonc.2018.8

109. Hong D, Kurzrock R, Kim Y, et al. AZD9150, a next-generation antisense oligonucleotide inhibitor of STAT3 with early evidence of clinical activity in

lymphoma and lung cancer. *Sci Transl Med*. 2015;7(314). doi:10.1126/scitranslmed.aac5272

110. Pietras K, Pahler J, Bergers G, Hanahan D. Functions of paracrine PDGF signaling in the proangiogenic tumor stroma revealed by pharmacological targeting. *PLoS Med*. 2008;5(1):0123-0138. doi:10.1371/journal.pmed.0050019

111. Moatassim-Billah S, Duluc C, Samain R, et al. Anti-metastatic potential of somatostatin analog SOM230: Indirect pharmacological targeting of pancreatic cancerassociated fibroblasts. *Oncotarget*. 2016;7(27):41584-41598. doi:10.18632/oncotarget.9296

112. Chauhan VP, Martin JD, Liu H, et al. Angiotensin inhibition enhances drug delivery and potentiates chemotherapy by decompressing tumour blood vessels. *Nat Commun*. 2013;4. doi:10.1038/ncomms3516

113. Rhim AD, Oberstein PE, Thomas DH, et al. Stromal elements act to restrain, rather than support, pancreatic ductal adenocarcinoma. *Cancer Cell*. 2014;25(6):735-747. doi:10.1016/j.ccr.2014.04.021

114. Olive KP, Jacobetz MA, Davidson CJ, et al. Inhibition of Hedgehog signaling enhances delivery of chemotherapy in a mouse model of pancreatic cancer. *Science (80-).* 2009;324(5933):1457-1461. doi:10.1126/science.1171362

115. Hurwitz HI, Uppal N, Wagner SA, et al. Randomized, double-blind, phase II study of ruxolitinib or placebo in combination with capecitabine in patients with metastatic pancreatic cancer for whom therapy with gemcitabine has failed. *J Clin Oncol*. 2015;33(34):4039-4047. doi:10.1200/JCO.2015.61.4578

116. Liberzon A, Birger C, Thorvaldsdóttir H, Ghandi M, Mesirov JP, Tamayo P. The Molecular Signatures Database Hallmark Gene Set Collection. *Cell Syst*. 2015. doi:10.1016/j.cels.2015.12.004

117. Zimetbaum P. Antiarrhythmic drug therapy for atrial fibrillation. *Circulation*. 2012;125(2):381-389. doi:10.1161/CIRCULATIONAHA.111.019927

118. Liu T, Zhou L, Li D, Andl T, Zhang Y. Cancer-associated fibroblasts build and secure the tumor microenvironment. *Front Cell Dev Biol*. 2019;7(APR). doi:10.3389/fcell.2019.00060

119. Olumi A, Grossfeld G, Hayward S, et al. Carcinoma-associated fibroblasts stimulate tumor progression of initiated human epithelium. *Breast Cancer Res*. 2000;2(S1). doi:10.1186/bcr138

120. Giannoni E, Bianchini F, Masieri L, et al. Reciprocal activation of prostate cancer cells and cancer-associated fibroblasts stimulates epithelial-mesenchymal transition and cancer stemness. *Cancer Res*. 2010;70(17):6945-6956. doi:10.1158/0008-5472.CAN-10-0785

121. Gong Y, Chippada-Venkata UD, Oh WK. Roles of matrix metalloproteinases and their natural inhibitors in prostate cancer progression. *Cancers (Basel)*. 2014;6(3):1298-1327. doi:10.3390/cancers6031298

122. Dall'Era MA, Albertsen PC, Bangma C, et al. Active surveillance for prostate cancer: A systematic review of the literature. *Eur Urol*. 2012;62(6):976-983. doi:10.1016/j.eururo.2012.05.072

123. Bul M, Zhu X, Valdagni R, et al. Active surveillance for low-risk prostate cancer

worldwide: The PRIAS study. *Eur Urol*. 2013;63(4):597-603. doi:10.1016/j.eururo.2012.11.005

124. Tuxhorn JA, Ayala GE, Smith MJ, Smith VC, Dang TD, Rowley DR. Reactive stroma in human prostate cancer: Induction of myofibroblast phenotype and extracellular matrix remodeling. *Clin Cancer Res*. 2002.

125. Ruan K, Bao S, Ouyang G. The multifaceted role of periostin in tumorigenesis. *Cell Mol Life Sci*. 2009;66(14):2219-2230. doi:10.1007/s00018-009-0013-7

126. Taylor BS, Schultz N, Hieronymus H, et al. Integrative Genomic Profiling of Human Prostate Cancer. *Cancer Cell*. 2010;18(1):11-22. doi:10.1016/j.ccr.2010.05.026

127. Kweldam CF, Wildhagen MF, Steyerberg EW, Bangma CH, Van Der Kwast TH, Van Leenders GJLH. Cribriform growth is highly predictive for postoperative metastasis and disease-specific death in Gleason score 7 prostate cancer. *Mod Pathol*. 2015;28(3):457-464. doi:10.1038/modpathol.2014.116

128. Runa F, Hamalian S, Meade K, Shisgal P, Gray PC, Kelber JA. Tumor Microenvironment Heterogeneity: Challenges and Opportunities. *Curr Mol Biol Reports*. 2017;3(4):218-229. doi:10.1007/s40610-017-0073-7

129. Ribeiro Franco PI, Rodrigues AP, de Menezes LB, Pacheco Miguel M. Tumor microenvironment components: Allies of cancer progression. *Pathol Res Pract*. 2020;216(1). doi:10.1016/j.prp.2019.152729

130. Cortez E, Roswall P, Pietras K. Functional subsets of mesenchymal cell types in the tumor microenvironment. *Semin Cancer Biol*. 2014;25:3-9.

doi:10.1016/j.semcancer.2013.12.010

131. Kalluri R. The biology and function of fibroblasts in cancer. *Nat Rev Cancer*. 2016. doi:10.1038/nrc.2016.73

132. Sun Y, Campisi J, Higano C, et al. Treatment-induced damage to the tumor microenvironment promotes prostate cancer therapy resistance through WNT16B. *Nat Med*. 2012;18(9):1359-1368. doi:10.1038/nm.2890

133. Vancauwenberghe E, Noyer L, Derouiche S, et al. Activation of mutated TRPA1 ion channel by resveratrol in human prostate cancer associated fibroblasts (CAF). *Mol Carcinog*. 2017;56(8):1851-1867. doi:10.1002/mc.22642

134. Prevarskaya N, Skryma R, Shuba Y. Ion channels and the hallmarks of cancer. *Trends Mol Med*. 2010;16(3):107-121. doi:10.1016/j.molmed.2010.01.005

135. Kodama I, Kamiya K, Toyama J. Amiodarone: Ionic and cellular mechanisms of action of the most promising class III agent. In: *American Journal of Cardiology*. Vol 84. ; 1999:20-28. doi:10.1016/S0002-9149(99)00698-0

136. Lee KS, Tsien RW. Mechanism of calcium channel blockade by verapamil, D600, diltiazem and nitrendipine in single dialysed heart cells. *Nature*. 1983;302(5911):790-794. doi:10.1038/302790a0

137. Ranger S, Sheldon R, Fermini B, Nattel S. Modulation of flecainide's cardiac sodium channel blocking actions by extracellular sodium: A possible cellular mechanism for the action of sodium salts in flecainide cardiotoxicity. *J Pharmacol Exp Ther*. 1993;264(3):1160-1167.

138. Augsten M. Cancer-associated fibroblasts as another polarized cell type of the

tumor microenvironment. *Front Oncol*. 2014;4 MAR. doi:10.3389/fonc.2014.00062

139. Franco OE, Jiang M, Strand DW, et al. Altered TGF-β signaling in a subpopulation of human stromal cells promotes prostatic carcinogenesis. *Cancer Res*. 2011;71(4):1272-1281. doi:10.1158/0008-5472.CAN-10-3142

140. Zhang D, Wang Y, Shi Z, et al. Metabolic Reprogramming of Cancer-Associated Fibroblasts by IDH3α Downregulation. *Cell Rep*. 2015;10(8):1335-1348. doi:10.1016/j.celrep.2015.02.006

141. Mezawa Y, Orimo A. The roles of tumor- and metastasis-promoting carcinoma-associated fibroblasts in human carcinomas. *Cell Tissue Res*. 2016;365(3):675-689. doi:10.1007/s00441-016-2471-1

142. Romero-Otero J, García-Gómez B, Duarte-Ojeda JM, et al. Active surveillance for prostate cancer. *Int J Urol*. 2016;23(3):211-218. doi:10.1111/iju.13016

143. Suardi N, Capitanio U, Chun FKH, et al. Currently used criteria for active surveillance in men with low-risk prostate cancer: An analysis of pathologic features. *Cancer*. 2008;113(8):2068-2072. doi:10.1002/cncr.23827

144. Garisto JD, Klotz L. Active Surveillance for Prostate Cancer: How to Do It Right. *Oncology (Williston Park)*. 2017;31(5).

145. Mo F, Lin D, Takhar M, et al. Stromal Gene Expression is Predictive for Metastatic Primary Prostate Cancer. *Eur Urol*. 2018;73(4):524-532. doi:10.1016/j.eururo.2017.02.038

146. Planche A, Bacac M, Provero P, et al. Identification of prognostic molecular

features in the reactive stroma of human breast and prostate cancer. *PLoS One*. 2011;6(5). doi:10.1371/journal.pone.0018640

147. Morra L, Moch H. Periostin expression and epithelial-mesenchymal transition in cancer: A review and an update. *Virchows Arch*. 2011;459(5):465-475. doi:10.1007/s00428-011-1151-5

148. Tischler V, Fritzsche FR, Wild PJ, et al. Periostin is up-regulated in high grade and high stage prostate cancer. *BMC Cancer*. 2010;10. doi:10.1186/1471-2407-10-273

149. Tsunoda T, Furusato B, Takashima Y, et al. The increased expression of periostin during early stages of prostate cancer and advanced stages of cancer stroma. *Prostate*. 2009;69(13):1398-1403. doi:10.1002/pros.20988

150. Cattrini C, Rubagotti A, Nuzzo PV, et al. Overexpression of periostin in tumor biopsies is associated with aggressive prostate cancer phenotype and poor clinical outcome. *Eur Urol Suppl*. 2017;16(10):e2735-e2736. doi:10.1016/s1569-9056(17)31871-7

151. Wright JL, Salinas CA, Lin DW, et al. Prostate Cancer Specific Mortality and Gleason 7 Disease Differences in Prostate Cancer Outcomes Between Cases With Gleason 4 + 3 and Gleason 3 + 4 Tumors in a Population Based Cohort. *J Urol*. 2009;182(6):2702-2707. doi:10.1016/j.juro.2009.08.026

152. Kretschmer A, Tilki D. Biomarkers in prostate cancer – Current clinical utility and future perspectives. *Crit Rev Oncol Hematol*. 2017;120:180-193. doi:10.1016/j.critrevonc.2017.11.007

153. McDaniel AS, Ferraldeschi R, Krupa R, et al. Phenotypic diversity of circulating tumour cells in patients with metastatic castration-resistant prostate cancer. *BJU Int*. 2017;120(5):E30-E44. doi:10.1111/bju.13631

154. Wang F Bin, Yang XQ, Yang S, Wang BC, Feng MH, Tu JC. A higher number of circulating tumor cells (CTC) in peripheral blood indicates poor prognosis in prostate cancer patients - A meta-analysis. *Asian Pacific J Cancer Prev*. 2011;12(10):2629-2635.

155. Srivastava A, Suy S, Collins SP, Kumar D. Circulating microRNA as Biomarkers: An update in prostate cancer. *Mol Cell Pharmacol*. 2011;3(3):115-124. doi:10.4255/mcpharmacol.11.16

156. C S, H C, S C. Expression Profiles and Mechanisms of microRNAs in Prostate Cancer. *Biomarkers J*. 2018;01(09). doi:10.21767/2472-1646.100051

157. Mitchell PS, Parkin RK, Kroh EM, et al. Circulating microRNAs as stable blood-based markers for cancer detection. *Proc Natl Acad Sci U S A*. 2008;105(30):10513-10518. doi:10.1073/pnas.0804549105

158. Vlaeminck-Guillem V. Extracellular vesicles in prostate cancer carcinogenesis, diagnosis, and management. *Front Oncol*. 2018;8(JUN). doi:10.3389/fonc.2018.00222

159. Li Z, Ma YY, Wang J, et al. Exosomal microRNA-141 is upregulated in the serum of prostate cancer patients. *Onco Targets Ther*. 2015;9:139-148. doi:10.2147/OTT.S95565

160. Nguyen HCN, Xie W, Yang M, et al. Expression differences of circulating

microRNAs in metastatic castration resistant prostate cancer and low-risk, localized prostate cancer. *Prostate*. 2013;73(4):346-354. doi:10.1002/pros.22572

161. Khan S, Jutzy JMS, Valenzuela MMA, et al. Plasma-Derived Exosomal Survivin, a Plausible Biomarker for Early Detection of Prostate Cancer. *PLoS One*. 2012;7(10). doi:10.1371/journal.pone.0046737

Declaration of Authorship

I declare that I was actively engaged in the realization of the project, including participation in the concept and design of the study, acquisition and analysis of the data.

In particular, I was first hand involved in the execution of all experiments included in the project, except for:

- *In vivo* experiments (animal manipulation): performed by Monica Tortoreto
- Profiling analyses: carried out by the institutional genomics core facility
- Immunohistochemical analysis: carried out by the institutional anatomic pathology unit, under the supervision of Dr. Maurizio Colecchia
- Bioinformatic analysis: carried out by Dr. Stefano Percio
- Biostatistics analysis: carried out by institutional Biostatistics Unit

The concept/design of the study was carried out under the supervision and with the intellectual contribution of my supervisors Dr. Nadia Zaffaroni and Dr. Paolo Gandellini.